



INDC International Nuclear Data Committee

Nuclear Reaction Data and Uncertainties for Radiation Damage

Summary Report of the Technical Meeting

IAEA Headquarters, Vienna, Austria

13 – 16 June 2016

prepared by

P.J. Griffin, Sandia National Laboratories, Albuquerque, NM, USA

H. Sjöstrand, Uppsala University, Uppsala, Sweden

S.P. Simakov, Karlsruhe Institute of Technology, Karlsruhe, Germany

August 2016

IAEA Nuclear Data Section
Vienna International Centre, P.O. Box 100, 1400 Vienna, Austria

Selected INDC documents may be downloaded in electronic form from

<http://www-nds.iaea.org/publications>

or sent as an e-mail attachment.

Requests for hardcopy or e-mail transmittal should be directed to

NDS.Contact-Point@iaea.org

or to:

Nuclear Data Section

International Atomic Energy Agency

Vienna International Centre

PO Box 100

1400 Vienna

Austria

Printed by the IAEA in Austria

August 2016

Summary Report
of the Technical Meeting
**Nuclear Reaction Data and Uncertainties
for Radiation Damage**

IAEA Headquarters, Vienna, Austria

13 - 16 June 2016

prepared by

P.J. Griffin, Sandia National Laboratories, Albuquerque, NM, USA

H. Sjöstrand, Uppsala University, Uppsala, Sweden

S.P. Simakov, Karlsruhe Institute of Technology, Karlsruhe, Germany

Abstract

This Meeting was organized to implement the recommendation of the second Research Coordinated Meeting (RCM) of the International Atomic Energy Agency (IAEA) Coordinated Research Project (CRP) "Primary Radiation Damage Cross Sections" to analyse the accuracy and consistency of the radiation damage-relevant nuclear data in the major nuclear data evaluations with the eventual goal of identifying the most reliable data and providing quantitative uncertainty estimates. Participants have considered the status of the primary nuclear data, such as reaction recoils spectra in the latest releases of ENDF, JEFF, JENDL, FENDL, ROSFOND and TENDL nuclear data libraries, and the ways of deriving the damage quantities KERMA, NRT- or arc-dpa and gas production cross sections as well as the recipes for an assessment of their uncertainties. This report contains the contemporary view of the Meeting participants on these issues in the form of a consolidated set of statements, recommendations and individual summaries.

August 2016

Table of Contents

I. Objectives of Meeting, Participants and Report structure	6
II. Highlighted Statements and Recommendations of Meeting.....	7
III. Individual Summaries of the TM participants.....	11
TENDL-TMC for Δdpa and Δpka , D. Rochman ^a , H. Ferroukhi ^a , A.J. Koning ^{b,c} , M. Gilbert ^d , J.C. Sublet ^d , H. Sjostrand ^c and P. Helgesson ^c	11
Uncertainties and correlations for the ⁵⁶ Fe damage cross sections and spectra averaged quantities based on TENDL-TMC, S.P. Simakov ¹ , A. Koning ² , A.Yu. Konobeyev ¹	12
Estimation of uncertainties of displacement cross-sections for iron and tungsten at neutron irradiation energies above 0.1 MeV, A.Yu. Konobeyev, U. Fischer, S.P. Simakov	19
Estimation of bias and uncertainties for radiation damage calculation (Fission Reactors), D. Bernard	25
Justified and complete gas-production cross sections with uncertainties for ⁵⁹ Ni and consequences for stainless steel in LWR spectra, P. Helgesson and H. Sjöstrand.....	28
A rigorous treatment of uncertainty quantification for Silicon damage metrics, P. Griffin.....	32
Comparative study of Monte Carlo particle transport code PHITS and nuclear data processing code NJOY for PKA energy spectra and heating number under neutron irradiation, Y. Iwamoto, T. Ogawa	43
Scoping of material damage with FISPACT-II and different nuclear data libraries: transmutation, activation, and PKAs, M.R. Gilbert and J.-Ch. Sublet.....	52
Differences among KERMA or DPA data calculated from JENDL-4.0, ENDF/B-VII.1, JEFF-3.2 and FENDL-3.1b with NJOY, C. Konno	57
ROSFOND based heating-damage cross sections sub-library: preliminary uncertainty assessment, V.V. Sinitza	62
Some experiences of dpa assessments using MCNP and SPECTER codes, C.S. Gil, W. Park, J. Kwon.....	67
Damage clustering in metals: importance, advances and challenges, K. Nordlund, A.E. Sand, F. Granberg, E. Levo, and F. Djurabekova	69
A methodology to assess dpa uncertainties from nuclear data covariances, L. Fiorito.....	73
Links with NEA activities: Nuclear Data services and WPs, O. Cabellos.....	78
Preliminary study on DPA cross-section of ¹⁸⁴ W in JEFF-3.2, C. Konno	79
Appendix I: Agenda	82
Appendix II: List of Participants	84

I. Objectives of Meeting, Participants and Report structure

The Nuclear Data Section of the IAEA currently manages the Coordinated Research Project (CRP) No. F44003 commenced in 2013. The main outputs of CRP are expected to be the recommended damage response functions such as: *NRT-*, *arc-* (athermal recombination-corrected) displacements per atom (dpa), replacements per atom (*rpa*), *KERMA* and *gas*-production cross sections, and should include a quantitative expression of their uncertainties. The final documents of the CRP will make recommendations for the source of the numerical data and for a methodology to be used in processing this nuclear data. Further information, collected up to now, is available on the CRP web-page: <https://www-nds.iaea.org/CRPdpa/>.

The CRP was initiated by the Technical Meeting (TM) convened 1 - 4 Oct 2012, Summary Report [INDC\(NDS\)-0624](#) [1]. Then two Research Coordination Meetings (RCM) have been held: RCM-1 (4 to 8 Nov 2013, Summary Report [INDC\(NDS\)-0648](#) [2]) and RCM-2 (29 June to 2 July 2015, Summary Report [INDC\(NDS\) 0691](#) [3]).

The latest RCM made the recommendation (see Section III in [Section III in INDC\(NDS\) 0691](#)):

"4. We need to improve the accuracy and consistency of PKA spectra, including recoils from the neutron absorption reactions. Differences are seen currently between different evaluations. We need to try to establish the most reliable data, and this would be recommended by CRP, and provide a quantitative uncertainty estimate.

Uncertainties are needed for the PKA spectra, KERMA, gas production and damage energy. PKA spectra are derived from all nuclear reactions, so their uncertainties are affected by the accuracy of the neutron cross section total and spectral data. Methods for their estimation should be established.

The IAEA NDS should organize a meeting to address these issues."

Following this recommendation, the Nuclear Data Section organised the dedicated Technical Meeting (TM) which was held from 13 to 16 June 2016 at IAEA Headquarters, Vienna, Austria. The Nuclear Data experts already participating in the IAEA CRP F44003 and specialists additionally recommended by National Nuclear Data Centres were invited to participate in this TM. The TM was attended by: D. Bernard, O. Cabellos, L. Fiorito, M.R. Gilbert, C.S. Gill, P. Griffin, P. Helgesson, Y. Iwamoto, A. Konobeev, K. Nordlund, D. Rochman, S.P. Simakov, H. Sjöstrand and J.-C. Sublet. The Nuclear Data Section of IAEA was represented by A. Koning (Scientific Officer of TM), B. Braams, V. Dimitriou, N. Otuka, V. Semkova and A. Trkov; the Physics Section of IAEA - by I. Swainson.

The Meeting was opened by A. Koning, Head of the IAEA Nuclear Data Section, who welcomed the participants and underlined the importance of this TM for establishing well defined nuclear data as a baseline for the analysis of radiation damage in the materials. He also outlined the expertise and capabilities accumulated by the NDS to model and process the nuclear data relevant to the topic of Meeting.

A. Öchs, as responsible for the Meeting preparation issues, made several announcements. It was followed by the self-introduction of participants, election of P. Griffin as the Chairman, M. Gilbert and H. Sjöstrand as the Rapporteurs of this Meeting and approval of Agenda (Appendix I).

The list of participants and their affiliations are filed in Appendix II.

During Meeting the participants presented 17 technical talks (available on the [TM web page](#)) and reported their own studies relevant to the context of this meeting.

The set of consolidated statements and recommendations for the further actions, as a result of the TM discussions, are summarized in Section II.

The individual summaries of the TM participants which detail the information presented at this meeting are collected in Section III.

The Nuclear Data Section acknowledged participants for their cooperation and contributions to this Technical Meeting.

II. Highlighted Statements and Recommendations of Meeting

During joint discussion, the Meeting participants came to the following consolidated statements about the current status of damage data and provided recommendations for further steps to improve their status in the future.

1. A set of damage metrics is needed to support radiation damage studies. This Technical Meeting recommends that the following damage metrics, with uncertainties, be provided through the work conducted under the Primary Radiation Damage CRP:
 - Gas production for ^4He , ^3He , ^3H , ^2H , and ^1H ;
 - Cross sections;
 - PKA spectra and light recoil ion spectra, as a function of incident neutron energy, emission energy and angle, and reaction channel;
 - Total KERMA;
 - NRT damage energy;
 - arc-dpa damage energy.
2. The covariance matrix, with sufficient resolution, needs to be provided for each of the damage metrics. The TM recommends that the neutron group structure at which the covariance is reported for the KERMA, gas production, and damage energy metrics include, at least, 89 groups in the 0-20 MeV neutron energy range and that the neutron energy structure in the 20-200 MeV range have energy increments not less than 10 MeV and be matched to points selected from the group structure presented by J.-C. Sublet. J.-C. Sublet has an action to contribute the details of his reported group structure.

The PKA spectra should be reported on a reaction/channel basis and will have a 2D representation since they will be presented as a function of incident neutron energy and will provide a full recoil ion energy distribution.
3. Relevant integral metrics represent a folding over incident neutron spectra, outgoing reaction channels and isotopes within the target material. Hence, uncertainties in all these quantities are important, i.e. neutron spectra, material composition, and the reaction channels considered. It was observed that the uncertainty in the characterization of both the incident neutron spectra and the channel-dependent recoil spectra may be important in an integral material damage metric.
4. The elastic channel can be the dominant contributor to the PKA. The uncertainties of the angular distributions for the elastic channel are used to derive the uncertainties in the elastic recoil spectra. Because of this, the characterization of the uncertainties in the elastic angular distribution needs to be given extra attention by the nuclear data community.
5. For the 22 elements identified as important in the Minutes from the Primary Damage CRP [3], checks were performed on the cumulative (integrated over reaction channel) energy-dependent PKA spectra. These checks indicated that there was good agreement for the PKA spectra computed from different nuclear data libraries for most of the elements. The exceptions noted were for Ge, Mn, Zr and W. These consistency checks were performed at neutron energies of 5 MeV and 14.5 MeV.
6. A sufficient amount of nuclear data needs to be included in recommended evaluated nuclear data files (ENDFs) to permit the calculation of KERMA. Thus, at a minimum, the following quantities need to be included for each open reaction channel:
 - cross-section;
 - angular distribution;
 - emitted recoil spectrum for the PKA and any emitted alpha particle.

No current ENDF6-format library satisfies the community's needs for the full set of requirements stated above and for a sufficiently wide range of isotopes. However, a careful expert-based

selection of data from the available libraries may be sufficient to derive a neutron energy-dependent KERMA representation for selected isotopes of current interest.

7. The TM observed that, due to technical deficiencies, the JEFF 3.2 Tungsten evaluations, above 20 MeV, should be corrected before being used for damage calculations in this energy range. ENDF/B-VII.1 and TENDL-2015 are good candidate libraries to support the determination of damage metrics in this material if care is taken in how the data are processed.
8. The TM recommends that, when deciding upon a recommended library for damage calculations, the recommendations should be accompanied by the input deck that supports the processing of the nuclear data as well as information on the name and version of the recommended processing code.
9. Notable discrepancies in the damage cross-section for W-184 were observed between the TENDL-2015, ENDF/B-VII.1 and JEFF-3.2 evaluations in the energy range 0-5 keV (differences ~ 100%) and 2 to 20 MeV (differences ~30%). It was thought that the most likely explanation for this difference in the range 0-5 keV is related to the issue addressed in item 12. The discrepancy in the 2 to 20 MeV range needs to be investigated further by the Primary Damage CRP.
10. In order to support the rapid and efficient convergence on recommended cross sections, specific members of the Primary Damage CRP and this TM should be tasked to identify nuclear data evaluations with the required high quality for supporting the derivation of the identified set of relevant damage metrics for the following important elements identified by the Primary Damage CRP: Fe, Ni, Al, Ti, Si, Cr, Cu, W, Zr, Be. The criteria for a good evaluation include: agreement with experimental data; and the fulfilment, as far as possible, of the criteria listed in points 1 - 3 above. The following individuals/ institutions accepted this tasking for the indicated elements:
 - Si: P. Griffin, Sandia National Lab, USA;
 - Be: A. Konobeev and S. Simakov, KIT, German;
 - Fe, Ni, Al, Ti, Cr, Cu, W, Zr: Y. Iwamoto, JAEA, Japan;
 - Fe, Cu: S. Simakov, KIT, Germany;
 - Ni, Al, Ti, Si, Cr, Cu, W and Zr, UKAEA, UK;
 - Fe: O. Cabellos, OECD, NEA.
11. ^4He gas production, and its associated uncertainty, in ^{56}Fe , need to be further investigated since large discrepancies were observed between ENDF/B-VII.1, TENDL-2015 and JEFF-3.2 evaluations.
12. It became clear from discussion at this TM that the way that data is expressed in the ENDF-6 formatted file affects the manner in which the available processing codes derive a KERMA value, e.g., the KERMA from a capture reaction is treated differently in the NJOY processing code depending on if it is stored in MF 6 MT 102 or MF 12-15 MT 102 format. The compliant ENDF-6 formats for MF 6 allows for a very complex specification of the energy/angle representation of recoil spectra and the results may not be properly interpreted by the current version of the NJOY processing code for all permitted data formats.
13. It is clear from discussions at the TM that the only widely used processing code to calculate KERMA is the NJOY/HEATR module. The radiation damage community is dependent on the NJOY/HEATR module to provide derived KERMA values. This lack of diversity / redundancy / independency in calculation tools is seen as a serious limitation for the radiation damage community. This TM recommends that the IAEA/NDS address this deficiency, and notes that this role falls within the current objective of the NDS to develop an open source, general purpose, processing code. The PHITS (JAEA) code new independent capabilities (e.g. the event generator mode) are a useful verification path for KERMA values. The TRIPOLI 4.9 (CEA) code has recently gained a similar event generator capability and should soon be utilized by a broader audience. The maturing capabilities within the GRUCON (Kurchatov Institute) code should also be capable of addressing this observed lack of diversity in processing tools.

14. For ^{56}Fe in the 0-1 keV energy interval, the (n, γ) capture gammas are well represented by the prompt-gamma activation analysis (PGAA) library that is implemented within the JEFF-3.2 evaluation. This approach, i.e. use of the PGAA detailed line representation, is the recommended treatment of low energy gammas from this capture reaction.
15. Kai Nordlund, University of Helsinki, Finland, accepted tasking to provide the recommended “replacement per atom” (*rpa*) and athermal recombination-corrected dpa (*arc-dpa*) parameters for the Fe, Ni, Cu, Pd, Pt, Ag, W and Au elements where material response metrics have been analyzed by the material damage community. In addition to the identification of the *rpa*- and *arc-dpa* parameters, K. Nordlund will provide an estimate of the variance in the damage efficiency, as represented by the parametric fit, and the maximum recoil ion energy for which the parameter derivation is supported by the available data.
16. The TM recommends that the IAEA/NDS serve as the repository for the various sets of random evaluation files that have been used to support the determination of the uncertainty in damage metrics and have been presented during this meeting.
17. Presentations at this TM showed that there are multiple ways to perform random sampling of nuclear data and to produce uncertainties in derived damage metrics such as KERMA. This use of a Monte Carlo-based random sampling is the recommended path for obtaining uncertainties in derived damage metrics.
18. In all uncertainty quantification analyses related to calculated damage metrics, care should be taken to address potential model defects in the computational formalism.
19. Presentations at this TM showed that a proper treatment of energy correlations is critical in generating spectrum-averaged uncertainties for integral radiation damage metrics - and that differences as large as a factor of two or three can be observed when contrasted with a treatment that assumes no energy correlation. Negligible correlations were observed between the integral damage metrics of gas production and damage energy in ^{56}Fe .
20. It is recommended that the Primary Damage CRP open communication channels with the Organization for Economic Co-operation and Development (OECD) Working Party on International Nuclear Data Evaluation Co-operations (WPEC) Subgroup 38: Designing a New Format for Storing Nuclear Data (SG38) so that they can collaborate in establishing the details for how the next generation of nuclear data structure files will capture details relevant to the representation of radiation damage metrics.

The TM recommends that the methodology used to specify KERMA, NRT-dpa, arc-dpa and gas production should: a) include a representation of the energy-dependent covariance; b) support multiple different forms of a given damage metric that are derived using different auxiliary parameters and c) explicitly capture documentation of the auxiliary parameters used in the derivation of the damage metric. This is a complex issue and planning for its implementation methodology should be discussed further between the groups before the final format decisions are made.

21. This TM considers the experimental validation of the damage metrics to be of paramount importance. Regrettably, at present, the EXFOR database does not include the majority of the KERMA factor data that has been reported in the literature. The Technical Meeting participants encourage the International Network of Nuclear Data Centres (NRDC) to compile this data and to monitor the status of other important experimental damage data such as gas production.

Actions undertaken after this TM before the issue of this Report

- Item 16: The TENDL-2015 random ENDF files library was made available for the nuclei of the CRP and TM interest in the form of one archive file for each isotope for easier downloading: see [TENDL-2015 random files](#) (D. Rochman). This hyperlink was also inserted on the [CRP web-page](#).
- Item 20: SG38 of NEA is developing the next-generation nuclear data formats and supporting tools, see [SG38 web-page](#) and links there. As part of this effort, SG38 aims to support radiation damage data and uncertainties. Communication between the NEA SG38 and this IAEA CRP has begun with an exchange of emails and test data (D. Brown, O. Cabellos, C. Mattoon, S. Simakov). In the next year or so SG38 should have draft format specifications and a sample I/O implementation in one or more processing codes.
- Item 21: The list of the published measured KERMA data still missing in the EXFOR database was submitted to the NDS of IAEA inviting the NRDC network to start compilation, see NRDC Memo [CP-N/132](#) (O. Cabellos, S. Simakov, N. Otsuka).

References to Sections I-II

1. R.E. Stoller, K. Nordlund and S.P. Simakov, Summary Report of the Technical Meeting “Primary Radiation Damage: from nuclear reaction to point defects”, [INDC\(NDS\)-0624](#), IAEA, Nov 2012
2. R.E. Stoller, L.R. Greenwood and S.P. Simakov, Summary Report of the First Research Coordination Meeting on Primary Radiation Damage Cross Sections, [INDC\(NDS\)-0648](#), IAEA, Dec 2013
3. R.E. Stoller, L.R. Greenwood and S.P. Simakov, Summary Report of the Second Research Coordination Meeting, [INDC\(NDS\)-0691](#), IAEA, Dec 2015

III. Individual Summaries of the TM participants

This section contains summaries of the researches carried out and presented by participants during Technical Meeting (the order of summaries follows the Agenda of TM, Appendix I).

TENDL-TMC for Δ dpa and Δ pka, D. Rochman^a, H. Ferroukhi^a, A.J. Koning^{b,c}, M. Gilbert^d, J.C. Sublet^d, H. Sjostrand^c and P. Helgesson^c

^a Reactor Physics and Systems Behaviour Laboratory, Paul Scherrer Institut, Villigen, Switzerland

^b Nuclear Data Sections, IAEA, Vienna, Austria

^c University of Uppsala, Sweden

^d Culham Centre for Fusion Energy, Abingdon, UK

The TENDL library (Talys Evaluated Nuclear Data Library) [1] contains the necessary information (e.g. recoil spectra, double differential data) to calculate quantities of interest for the material damage. Additionally, it is one of the most complete libraries in terms of number of isotopes and format-wise: 2800 isotopes (ground states and isomers) and all ENDF-6 sections from MF1 to MF40. It can then be naturally used for the estimation of “DPA” and “PKA”, given the correct NJOY processing. Details of the library, its production, formatting and processing are given during the technical meeting.

Comparison with other libraries indicated the importance of including all the “MT” sections for the correct processing with NJOY, but also it showed the difference obtained depending of the format chosen to store the decay data.

Regarding the uncertainties on DPA and PKA, the TMC method seems to be one of the most convenient methods [2]. As presented during the meeting, the uncertainty propagation using random ENDF-6 files produced from variations of model parameters leads to non-Gaussian distributions for the damage quantities. As a function of the incident neutron energy, the skewness of such distributions can strongly vary and be far from 0. This indicates that the standard deviation alone cannot represent, well enough, the dispersion of the calculated data.

A viable alternative is the production of so-called random ENDF-6 files based on given covariance information. This method is limited by the available information given in the covariance files, but can help to capture part of the uncertainties for the DPA and PKA quantities. For TENDL-2016, the covariance format MF32 will be less used and efforts will be devoted to produce MF33, which will facilitate the production of random ENDF-6 files with SCK codes such as SANDY.

A PSI internal project to link the nuclear data with the atomistic simulation of damage formation and microstructure evolution was also presented. Cross sections and spectra for DPA and PKA can be produced based on nuclear data files and be used by atomistic simulations. Results can be evaluated in terms of C/E, and provide a feedback to the evaluation of basic nuclear data. Such a project is under development, with possible applications using NJOY, SPECTER or SPECTRA-PKA based on the “NRT-DPA” or “arc-DPA” calculation methods.

In conclusion, some information was provided about another CRP on fuel modelling and radiation effects (SMORE) and its follow-up (SMORE-2) which will also consider the results of this current CRP.

[1] A.J. Koning and D. Rochman, Nuclear Data Sheets 113 (2012) 2841.

[2] A.J. Koning and D. Rochman, Annals of Nuclear Energy 35 (2008) 2024.

Uncertainties and correlations for the ^{56}Fe damage cross sections and spectra averaged quantities based on TENDL-TMC, S.P. Simakov¹, A. Koning², A.Yu. Konobeyev¹

¹ Karlsruhe Institute of Technology
Karlsruhe, Germany

² Nuclear Data Section, IAEA,
Vienna, Austria

Introduction

The goal of this work is a calculation of the covariance matrices for the physical quantities used to characterize the neutron induced radiation damage in the materials. Such quantities usually encompass: the charged particles kinetic energy deposition KERMA (locally deposited nuclear heating), damage energy (to calculate then the number of displaced atoms) and gas production cross sections [(n,x α), (n,xt), (n,xp) ... to calculate then transmuting of target nuclei to gases].

The uncertainties and energy-energy or reaction-reaction correlations for such quantities were not assessed so far, whereas the covariances for many underlying cross sections are often presented in the evaluated data libraries.

Due to the dependence of damage quantities on many reactions channels, on both total and differential cross sections, and in particular on the energy distribution of reaction recoils, the evaluation of uncertainty is not straightforward. To reach a goal, we used the method based on idea of Total Monte Carlo application to the Nuclear Data [1].

This report summarises the current results for evaluation, validation and representation in the ENDF-6 format of the radiation damage covariances for n + ^{56}Fe from thermal energy up to 20 MeV. This study was motivated by the IAEA Coordinated Research Project "Primary Radiation Damage Cross Sections" [2] and by present dedicated Technical Meeting "Nuclear Reaction Data and Uncertainties for Radiation Damage".

1. Method of evaluation of Energy-Energy and Reaction-Reaction Covariances

As a starting point in our study we used one unperturbed and five hundred perturbed evaluated files for n + ^{56}Fe reaction from TENDL-2013 evaluations [3]. These files were generated during the modelling of nuclear reaction cross sections by sampling the input underlying parameters within their uncertainties, which reflect the spread of known experimental cross section data.

All 501 files were processed by the NJOY-2012.50+ code [4] to calculate the damage quantities of interest in the ENDF-6 format. For this, the HEATR and GASPR modules were used to calculate KERMA (energy balanced designed by MT =301), Damage Energy (MT = 444) and gas production cross sections (n,x ^4He) (MT = 207), (n,x ^3He) (MT = 206), (n,xt) (MT = 205), (n,xd) (MT = 204) and (n,xp) (MT = 203). The modules RECONR and BROADR were used before to reconstruct the cross sections at room temperature 293 $^{\circ}\text{K}$. At the end, the GROUPE module was used to generate the desired data in the grouped-wise format *gendf* to reduce the number of points, but, at the same time, to retain the characteristic structure in the cross sections. We have selected the VITAMIN-J group presentation, which has 175 groups between 10 $^{-5}$ eV and 19.64 MeV.

The Fortran-90 code was written to read the NJOY output *gendf* files and to calculate the mean (i.e., averaged over 500 random evaluations) quantities, energy-energy (E-E) and reaction-reaction (MT-MT) correlations matrices.

The first order covariance matrix for values of function y_i from the N_{random} random set is calculated following the general definitions [5]:

$$cov(y_i, y_j) = \langle (y_i - \bar{y}_i)(y_j - \bar{y}_j) \rangle = \langle y_i y_j \rangle - \bar{y}_i \bar{y}_j = \sum_{N_{random}} \frac{(y_i - \bar{y}_i)(y_j - \bar{y}_j)}{N_{random}},$$

where \bar{y}_i is a mean.

The diagonal elements ($i = j$) of covariance matrix deliver a variance or square of the standard deviation σ_i :

$$\sigma_i^2 = cov(y_i, y_i)$$

The correlation matrix was then calculated as:

$$cor(y_i, y_j) = \frac{cov(y_i, y_j)}{\sigma_i \sigma_j} , \quad \text{diagonal elements } cor(y_i, y_i) = 1$$

In the above notation, indices i or j refer to the quantities values corresponding the specific energy group or reaction MT.

2. Derived Covariance Matrices

The results of calculation of the uncertainties and energy-energy correlation matrices for Damage Energy, KERMA, ^4He and ^1H production cross sections are shown in Figs. 1 to 3.

We observed for:

- Damage Energy (MT=444) – 1 to 40% uncertainties and strong positive (corr. coefficient ≤ 1) energy-energy correlations within 2 - 3 large regions not correlating each other;
- KERMA (MT = 301) – similar to Damage Energy but 2 to 20% uncertainties;
- He-4 production (MT = 207) - $\approx 30\%$ uncertainties and positive energy-energy correlations within a whole energy range where the correlation strength decreases from 1 to 0.

The covariance matrices were checked for statistical significance: it was shown that the correlation coefficients even in the energy domains, where they are close to zero, do converge on the ensemble of 200-300 random files.

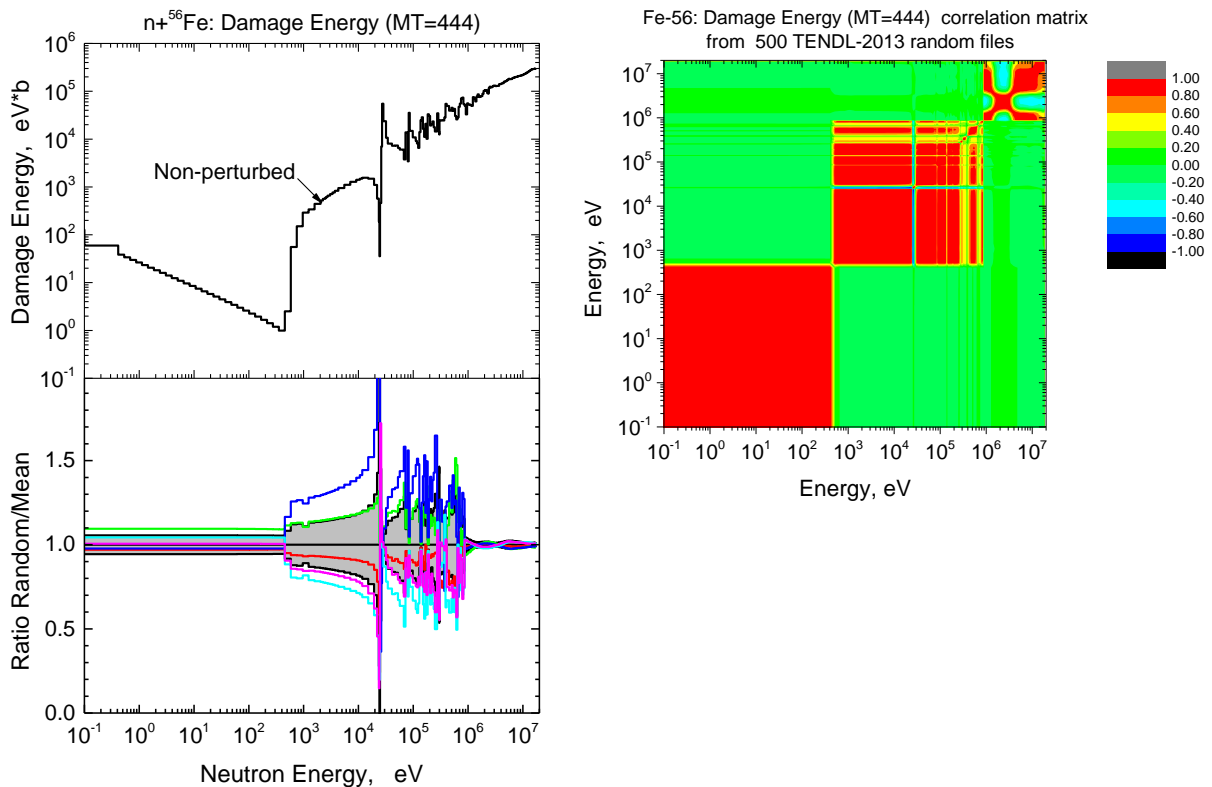


Fig. 1. Damage Energy: (left-top) non-perturbed TENDL-2013 evaluation; (left-bottom) ratio of 5 random files (colour curves) to mean over 500 and standard deviation (grey zone); (right) energy-energy correlation matrix calculated from 500 TENDL-2013 random files.

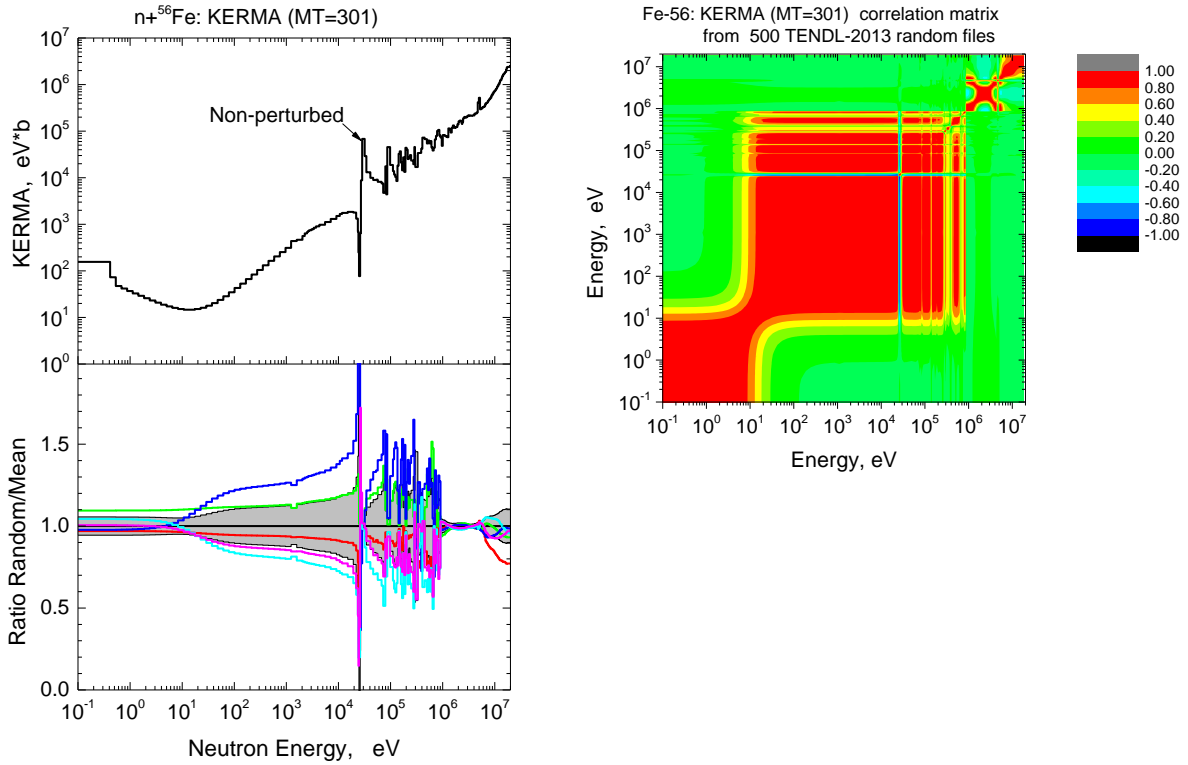


Fig. 2. KERMA: (left-top) non-perturbed TENDL-2013 evaluation; (left-bottom) ratio of 5 random files (colour curves) to mean over 500 and standard deviation (grey zone); (right) energy-energy correlation matrix calculated from 500 perturbed TENDL-2013 files.

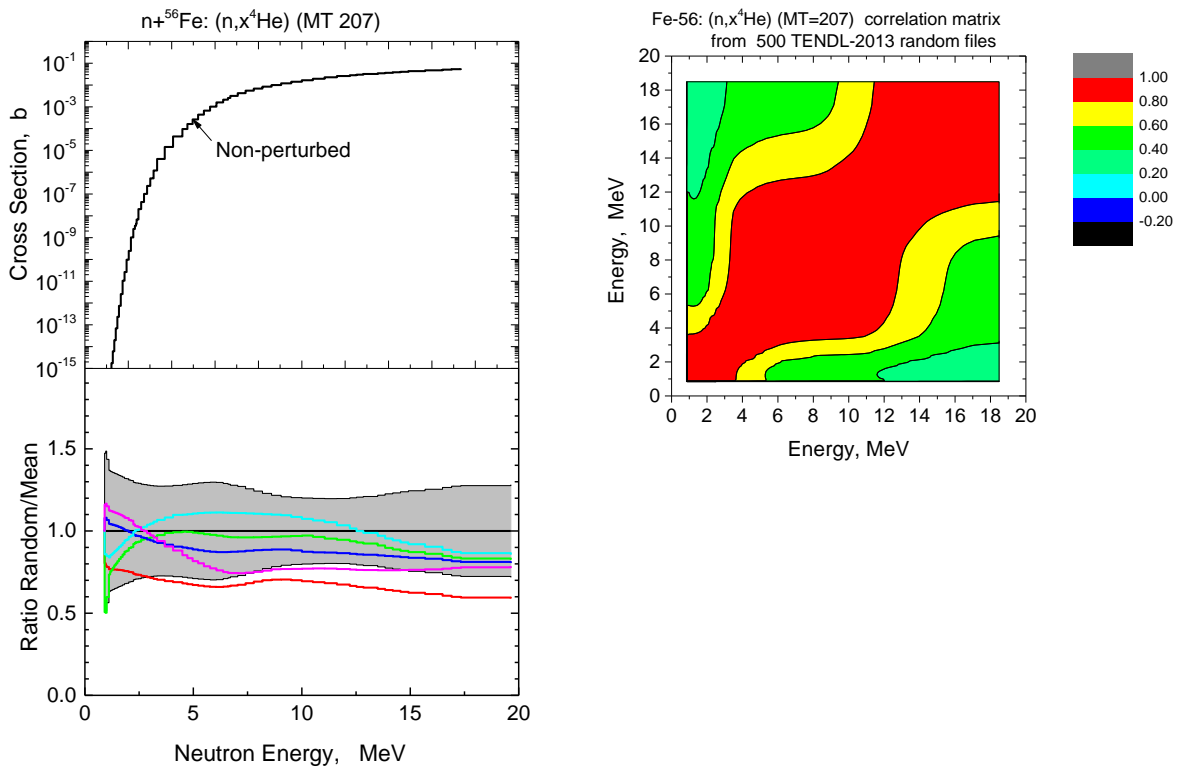


Fig. 3. ^4He production: (left-top) non-perturbed TENDL-2013 evaluation; (left-bottom) ratio of 5 random files (colour curves) to mean over 500 and standard deviation (grey zone); (right) energy-energy correlation matrix calculated from 500 perturbed TENDL-2013 files.

The statistical significance of the covariance matrix elements was checked. As an example, Fig. 4 shows the mean value of damage energy (MT444) for energy group #100 (497.8 - 523.4 keV), its uncertainty and correlation coefficient between this groups and one #15 (8.32 - 10.7 eV) as a function of the number of the random files N_{random} used for calculation of these values. It is seen that the mean and its uncertainty are stabilized already at the ensemble of 50-100 sampled files whereas correlation coefficient converges after usage of more than 200-300 files.

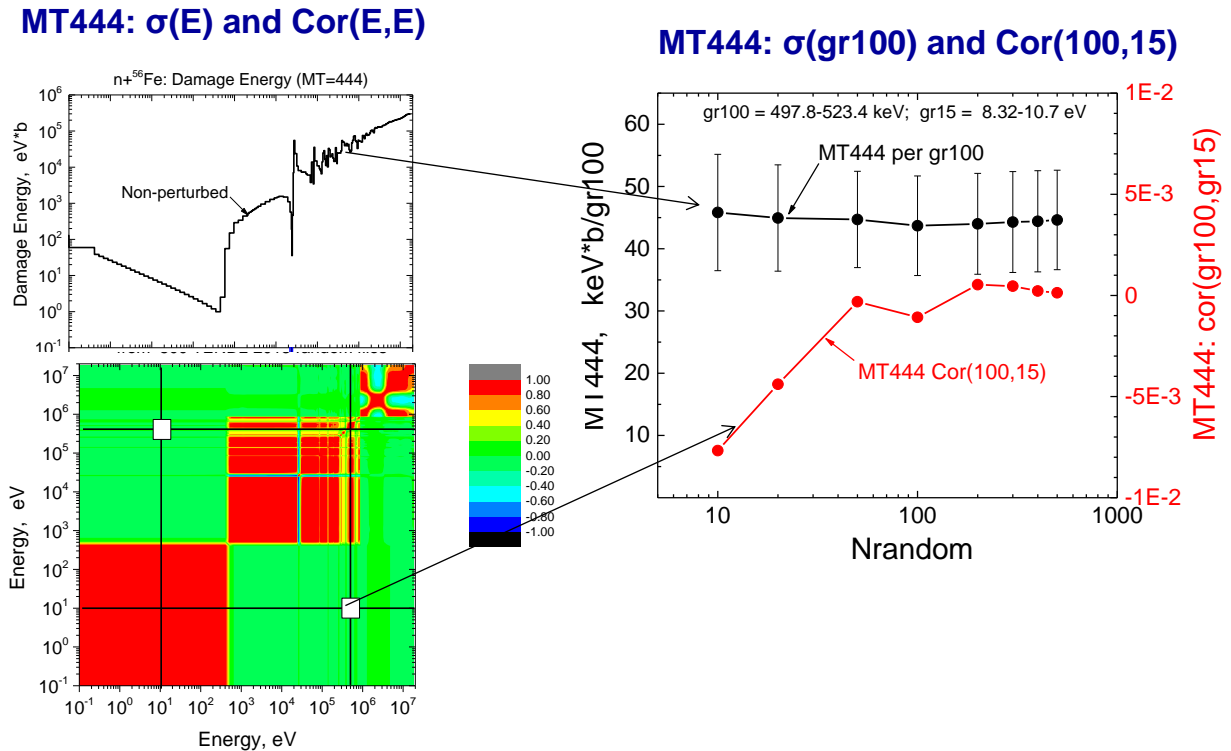


Fig. 4. The Damage Energy and Energy-Energy correlation matrix (left); the dependence of element values for the selected groups on the number of sampled files used for their calculations.

3. Comparison of the evaluated Uncertainties with Experiment

The evaluated uncertainties are compared with [known measured KERMA factors](#) (most of them are not compiled in EXFOR yet) and (n,α) cross sections in Fig. 5. It is seen that energy dependant standard deviations, which varies from 5 to 20%, are close to the experimental ones.

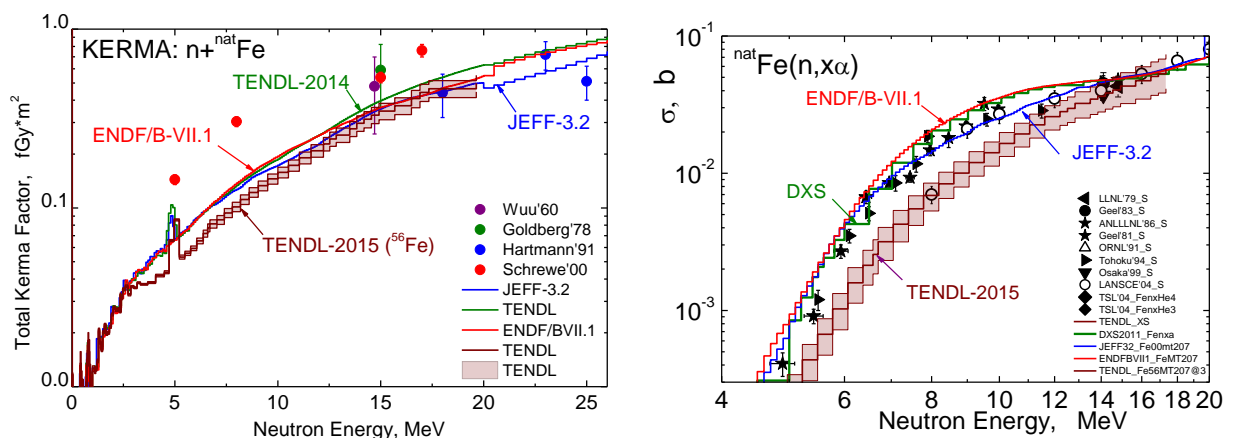


Fig. 5. The KERMA factor and ^4He production cross section for Iron: comparison of TENDL-2015 evaluation and Uncertainties, obtained from analysis of the TENDL-2013 random files, with measured data and their uncertainties.

4. Energy Spectrum Averaged Damage Quantities.

To demonstrate the practical importance of obtained covariance data we calculated the energy averaged damage quantities for ^{56}Fe inside the **representative fission, fusion and spallation nuclear facilities**. The [energy spectra collected by the IAEA CRP participants](#) are displayed in Fig. 6. For the actual calculations we selected:

- thermalized spectrum in centre of the irradiation channel C5 inside the High Flux Isotope Reactor HFIR (HFIR/C5);
- fast spectrum with 14-MeV peak in the First Wall of ITER (ITER/FW);
- spectrum with high cut-off energy 55 MeV averaged over the High Flux Test Module volume of the projected accelerator driven fusion material test facility IFIMF (IFIMF/HFTM).

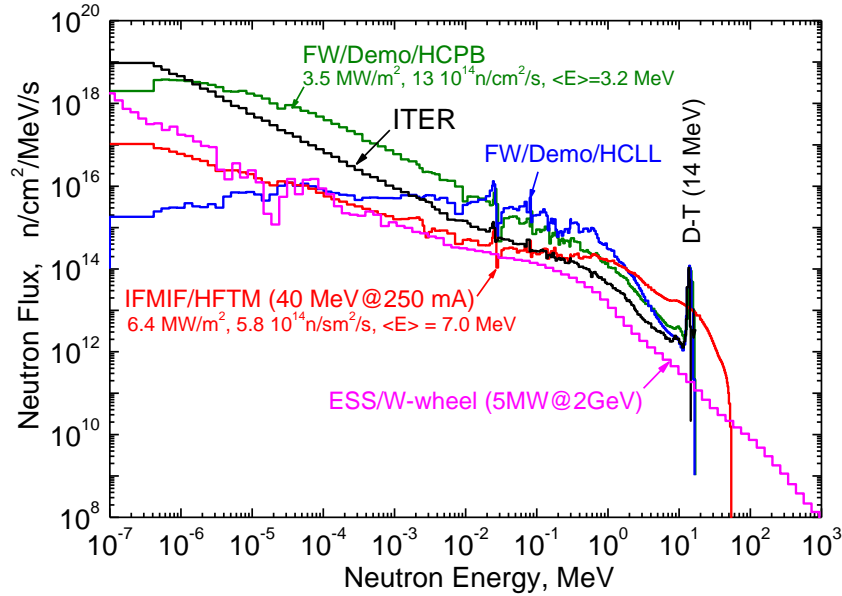


Fig. 6. Neutron Energy spectrum in ITER and other fast neutron facilities.

The neutron fluxes during full operation and estimated damage quantities with **uncertainties** for ^{56}Fe in HFIR/C5, ITER/FW and IFMIF/ITER are summarised in Table 1. The uncertainties were calculated with full energy-energy covariance matrices and, for the purpose of comparison, only with diagonal elements. It is seen that ignoring of the off-diagonal correlation coefficients result to the underestimation of uncertainties by factor 2-3.

Table 1. The Spectrum Averaged Damage Quantities and their Uncertainties assessed for ^{56}Fe under irradiation in the HFIR/C5, ITER/FW and IFMIF/HFTM (*italic font indicates the uncertainties calculated when off-diagonal elements of covariance matrices are ignored*).

Facility/Location	HFIR/C5	ITER/FW	IFMIF/HFTM
Neutron Flux [$\text{n}/\text{cm}^2/\text{s}$]	5.10E+15	3.90E+14	7.32E+14
Displacements [dpa/fpy]	30.5 ± 0.95 (3.1%)	10.4 ± 0.16 (1.5%)	25.1 ± 0.36 (1.4%)
	<i>30.5 ± 0.24 (0.8%)</i>	<i>10.4 ± 0.05 (0.5%)</i>	<i>25.1 ± 0.09 (0.4%)</i>
KERMA [W/Kg]	277 ± 7 (2.7%)	246 ± 21 (8.7%)	469 ± 31 (6.7%)
	<i>277 ± 2 (0.7%)</i>	<i>246 ± 12 (4.9%)</i>	<i>469 ± 10 (2.2%)</i>
$(\text{n},\text{x}^4\text{He})$ [appm/fpy]	5.7 ± 1.3 (23%)	92 ± 21 (23%)	136 ± 31 (23%)
	<i>5.7 ± 0.3 (6%)</i>	<i>92 ± 12 (13%)</i>	<i>136 ± 11 (7.8%)</i>
$(\text{n},\text{x}^1\text{H})$ [appm/fpy]	37 ± 6.3 (16.9%)	410 ± 72 (17%)	642 ± 102 (16%)
	<i>37 ± 1.6 (4.4%)</i>	<i>410 ± 41 (10%)</i>	<i>642 ± 31 (4.9%)</i>
MT-MT correlation: max. between $(\text{n},\text{x}^4\text{He})$ & (dpa)	204-206 = + 1.05%	205-206 = + 1.07%	204-206 = + 0.66%
	207-444 = - 5.9E-5	207-444 = + 1.8E-4	207-444 = + 1.4E-4

Table 1 also lists the reaction-reaction (MT-MT) correlations. One notices that they are very small. Thus for the practically important correlation between NRT-dpa and He-production (444-207), which is used for characterization of potential damage in Fusion materials, the correlation coefficient is less than 2×10^{-4} . The correlation between gas production rates, such as (n,xp), (n,xa), (n,xt), is below 10^{-2} .

We additionally compared the contributions of the **Nuclear Data** and **Material Physics** to the **total uncertainties** for nuclear heating, dpa and gas production in the representative nuclear facilities, Table 2. The Nuclear Data are the sole source for the Damage Energy and gas production, on the other hand, the Material Physics contributes to the NRT-dpa, e.g. through the uncertainty of Lattice Threshold E_d . For the iron crystalline lattice, an averaged E_d was estimated as 40 ± 2 eV or $\pm 5\%$ [7]. The arc-dpa additionally depends on a simulation of the primary defects surviving function by Molecular Dynamics (MD) or Binary Collision Approximation (BCA). The ‘‘OECD fit’’ to the surviving efficiency estimates this uncertainty as $\pm 2\%$ [8]. However the visible spread of the MD results is essentially larger and should be increased up to about $\pm 20\%$.

Table 2. The contribution of Nuclear Data and Material Physics to the Spectrum Averaged Damage Quantities **Uncertainties** assessed for ^{56}Fe under irradiation in the facilities HFIR/C5, ITER/FW and IFMIF/HFTM.

Source of Uncertainty	Nuclear Data	Material Physics
Damage Energy DE (MT=444) Lattice Threshold $E_d = 40 \pm 2$ eV [7]	$\pm (1.4 - 3.1)\%$ do not contribute	do not contribute $\pm 5.0\%$
Total Uncertainty for NRT-dpa = $0.8 \cdot \text{DE} / 2E_d$	$\pm (5.2 - 5.9)\%$	
Primary Defects Surviving Efficiency	do not contribute	from OECD fit $\approx \pm 2\%$ [8] spread of MD res. $\sim \pm 20\%$ [8]
Total Uncertainty for arc-dpa \sim NRT-dpa * Efficiency	$\pm (5.2 - 5.9)\%$ plus $\pm 20\%$	
KERMA or Nuclear Heating from charged reaction products	$\pm (2.7 - 8.7)\%$	do not contribute
Gas production: (n,xα) or (n,xH)	$\pm 23\%$ or $\pm 17\%$	do not contribute

5. Presentation of Covariance Matrices in the ENDF-6 format

The derived covariance matrices for damage quantities MT 203-444 were converted in the ENDF-6 formatted file MF33 using dedicated subroutines [9]. Then the formatted covariance matrices were checked for: (i) positive definiteness by calculating the eigenvalues using code COVEIG [10] and (ii) compliance with ENDF-6 format using on-line utilities on *myENDF web tools* [11].

Finally and solely for the testing purpose, the MF33/MT203-444 file was added to the complete TENDL-2013 evaluation for ^{56}Fe . It was then successfully processed by NJOY-2012.50 using the covariance relevant modules ERROR and COVARR. As an example of processing, the NJOY’ plots for added damage energy covariance MF33/MT444 is depicted in Fig. 7.

Conclusions

The Total Monte Carlo method and 500 random evaluated files for the $n+^{56}\text{Fe}$ reaction were used to qualify the energy-energy and reaction-reaction covariance matrices for the radiation damage cross sections up to 20 MeV such as nuclear heating due to the charged particles KERMA, Damage Energy, atom displacement and gas production cross sections.

The obtained covariance matrices were recorded as ENDF-6 formatted MF33 file and tested for their positive definiteness, on the ENDF-6 format compliance using standard checkers and whether NJOY will process the complete evaluated file with added covariance for damage quantities.

For the practical applications, the uncertainties of the energy weighted quantities inside the representative fission, fusion or spallation nuclear facilities were calculated: (1.3 - 3.0)% for NRT-dpa, (3 - 9)% for KERMA, (17 - 23)% for gas production. These uncertainties were shown will be 2-3 times smaller if the diagonal-off elements of the corresponding energy-energy correlation matrices will be omitted.

The uncertainty for NRT- and arc-dpa, estimated from underlying nuclear data, have to be additionally increased by (5-20)%. The latter addition stems from the uncertainties of the involved Material Physics parameters such as lattice threshold and primary defects surviving efficiency.

Reaction-Reaction correlations were found to be negligible small: between He and dpa $< 2 \cdot 10^{-4}$, between any gas (^4He , ^3He , t, d, H) production rates $< 10^{-2}$.

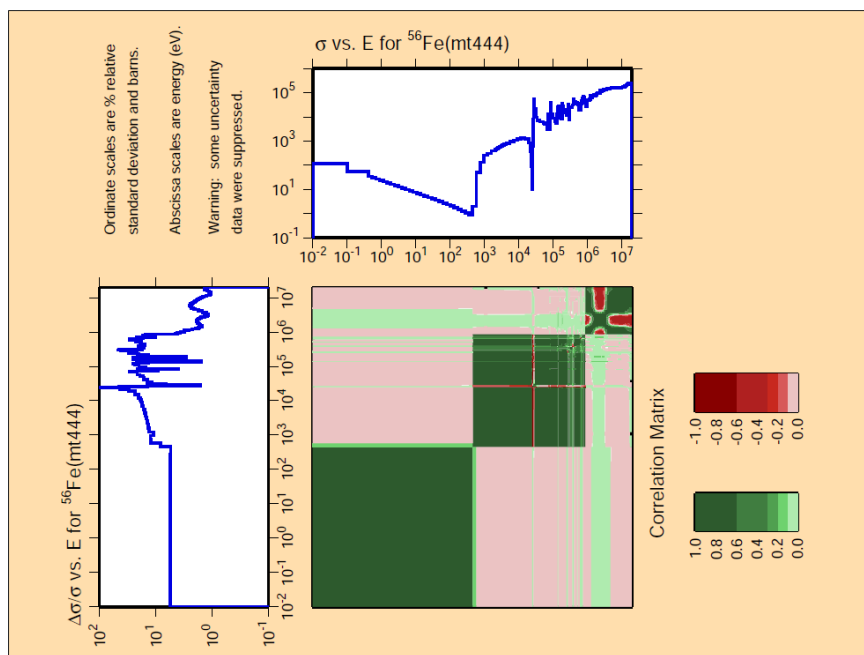


Fig. 7. Damage Energy, relative uncertainty and correlation matrix for Fe-56 proceed and plotted by NJOY-2012.50.

References

1. A.J. Koning, D. Rochman, Nuclear Data Sheets 113(2012) 2841
2. IAEA CRP "Primary Radiation Damage Cross Sections", <https://www-nds.iaea.org/CRPdpa/>
3. A.J. Koning and D. Rochman, Random nuclear data files TENDL-2013: <ftp://ftp.nrg.eu/pub/www/talys/tendl2013/random.html>
4. "The NJOY Nuclear Data Processing System, Version 2012", Report LA-UR-12-27079, Ed. A.C. Kahler, Los Alamos National Lab, 2015
5. Wolfram MathWorld, the web mathematics resource: <http://mathworld.wolfram.com/Covariance.html>
6. Nuclear Data Processing System NJOY-2012, <http://t2.lanl.gov/nis/codes/NJOY12/index.html>
7. K. Nordlund et al., Nucl. Instr. Meth. B246(2005)32
8. "Primary Radiation Damage in Materials", Report NEA/NSC/DOC(2015)9, OECD 20105
9. A. Konobeyev, private communication
10. COVEIG code, available on <https://www-nds.iaea.org/IRDF/>
11. Web tools for ENDF evaluators <https://www-nds.iaea.org/exfor/myendf.htm>

Estimation of uncertainties of displacement cross-sections for iron and tungsten at neutron irradiation energies above 0.1 MeV, A.Yu. Konobeyev, U. Fischer, S.P. Simakov

Karlsruhe Institute of Technology
Karlsruhe, Germany

1. Introduction

The goal of this work is the evaluation of uncertainties of calculated atomic displacement cross-sections for iron and tungsten irradiated with neutrons. Uncertainties were analysed for neutron incident energies above 0.1 MeV, which make the main contribution to the value of radiation damage rate for different types of nuclear or fusion reactors and neutron sources [1].

Covariance matrices for displacement cross-sections, σ_d were obtained using the Monte Carlo method described in Ref. [2]. The procedure consists of: a) the choice of the “best” set of model parameters, b) the estimation of uncertainties of model parameters, c) the Monte Carlo sampling of N number of input data sets for the code used, d) the execution of calculations for obtained N input data files, and e) the computation of covariance matrices for particular reactions:

$$V_{ij} = N^{-1} \sum_{k=1}^N (\sigma_{d,ik} - \sigma_{d,i0})(\sigma_{d,jk} - \sigma_{d,j0}) , \quad (1)$$

where $\sigma_{d,ik}$ is the displacement cross-section corresponding to the “i”-th primary neutron energy in the “k”-th Monte Carlo event, $\sigma_{d,i0}$ is the cross-section calculated using set of unchanged model parameters. The standard deviation of displacement cross-section is equal to

$$\Delta\sigma_{d,ii} = \sqrt{V_{ii}} \quad (2)$$

Recoil energy distributions were calculated for different input data sets using the TALYS-1.8 code [3] at incident neutron energies below 150 MeV and the CASCADE-2014 code [4,5] at energies above 100 MeV.

The uncertainties of displacement cross-section, σ_d were estimated using both the NRT model [6] and the arc-dpa approach [7,8].

When using the NRT model four parameters, α_i were varied. Three parameters $\alpha_1 - \alpha_3$ concern the numerical coefficients in $g(\varepsilon)$ formula [6] obtained in Ref. [9] by approximating the Lindhard’s function:

$$g(\varepsilon) = 3.4008\varepsilon^{1/6} + 0.40244\varepsilon^{3/4} + \varepsilon , \quad (3)$$

The fourth parameter α_4 is the effective threshold displacement energy E_d .

Two parameters b_{arcdpa} and c_{arcdpa} [8] were varied when using the arc-dpa approach for iron and tungsten. In this case the parameters of the NRT formula applied [7,8] and E_d remained unchanged.

The variation of parameters of nuclear models and defect production models was done using a normal distribution. The Δp -value shown in figures and discussed below is the relative standard deviation (RSD) or the coefficient of variation concerning the σ/μ ratio of the distribution. The criticism of the MC variation of NRT model parameters and the arguments for the variation are discussed in [10,11].

2. Incident neutron energies below 150 MeV

Energy and angular particle distributions, and recoil spectra were calculated using the TALYS-1.8 code. Optical model calculations were performed with the Koning-Delaroche potential [12].

The calculations for iron were made using TALYS with 6,700 MC-generated input data files, for tungsten with 3,200 input data files. The recoil spectra for neutron elastic and inelastic discrete-level scattering (n,n') were obtained using calculated neutron angular distribution. A special procedure was applied to get recoil spectra for neutron inelastic continuum scattering using results of TALYS-1.8 calculations. The contribution of shape elastic scattering in displacement cross-section calculated

using the ECIS code [13] with a large number of MC-generated input data files is discussed in Refs. [10, 11].

2.1 Iron

Fig. 1 shows an example of the number of defects and defect production efficiency calculated with varied NRT and arc-dpa parameters with the RSD value equal to 20%. The effective threshold displacement energy E_d is equal to 40 eV.

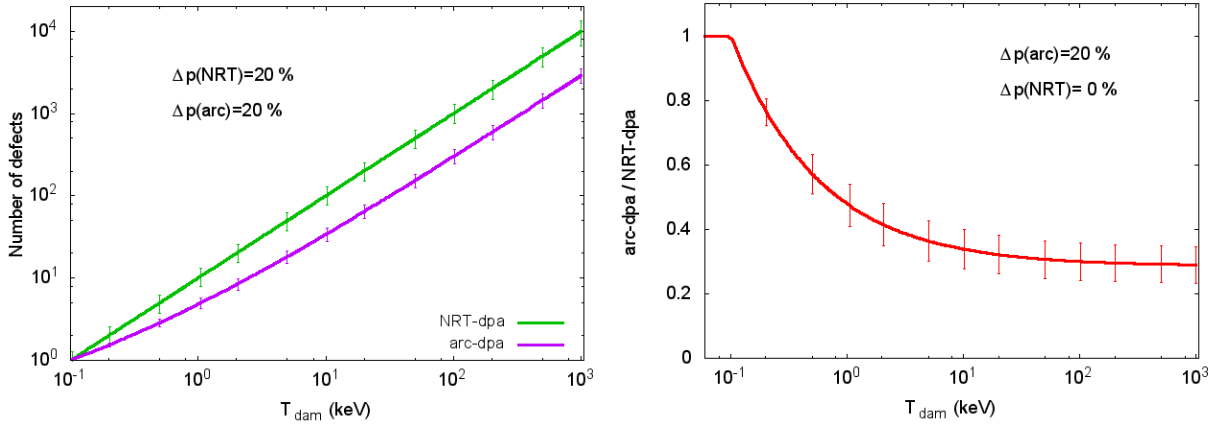


Fig. 1. The number of defects calculated using the NRT model and the arc-dpa approach (left) and the efficiency of defect generation (right) calculated for iron with the coefficient of variation of NRT and arc-dpa parameters equal to 20%.

Fig. 2 shows the RSD of the number of defects depending on different parameter variation.

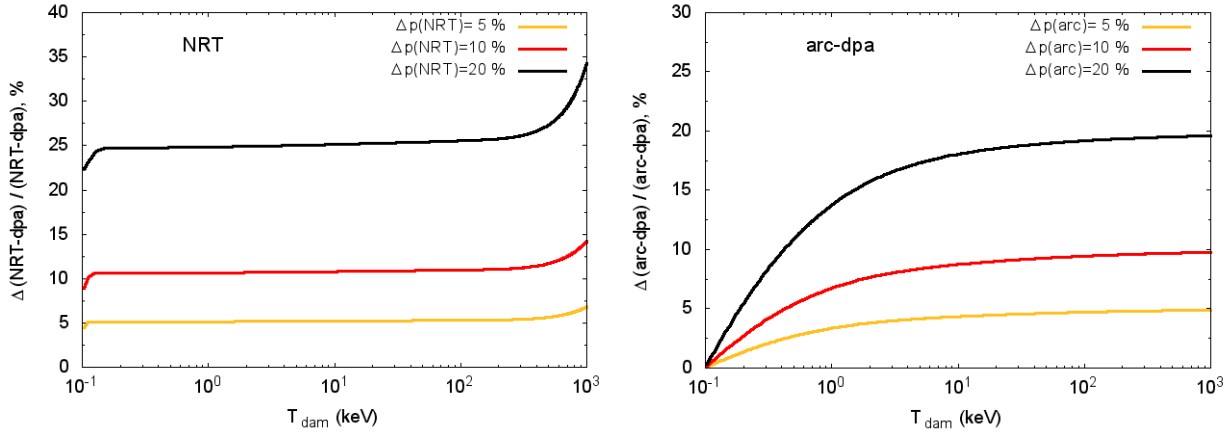


Fig. 2. The RSD values for number of defects calculated using the NRT model and the arc-dpa approach for iron.

2.1.1 Components of displacement cross-section

Figs. 3 and 4 show examples of calculated RSD of components of displacement cross-section obtained with the coefficient of variation of optical model parameters $\Delta p(\text{opt})$ equal to 5% and with the same coefficient for nuclear level density parameters $\Delta p(\text{levd})$ equal to ten percent. The resulting values $\Delta\sigma_{d,el}/\sigma_{d,el}$ are shown in Fig. 3 for neutron elastic scattering and in Fig. 4 for (n,2n) reaction.

The $\Delta\sigma_d/\sigma_d$ values for other reactions and results obtained with different variation of optical model parameters can be found in Refs. [10,11]. The influence of the adopted $\Delta p(\text{opt})$ value on the scatter of “common” cross-sections and the comparison with TENDL-2015 is also discussed in Refs. [10, 11].

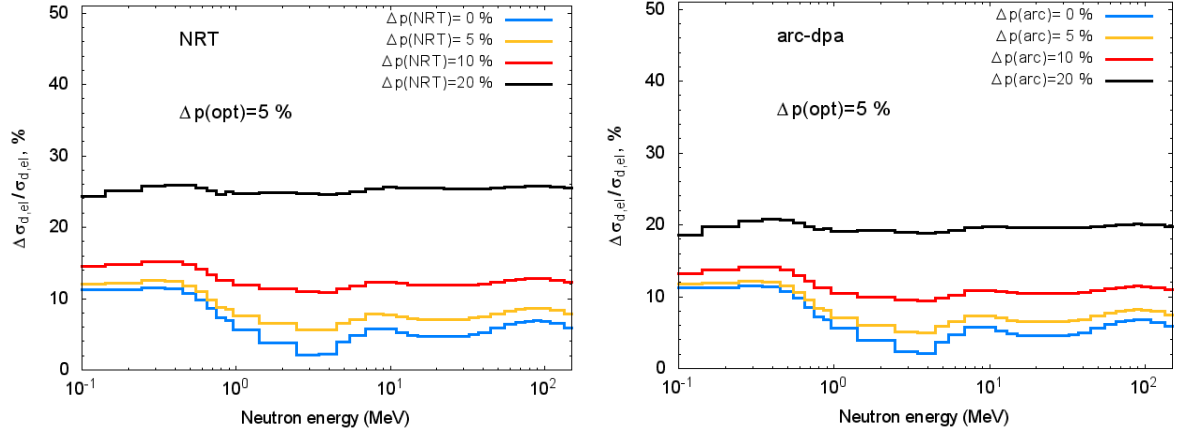


Fig. 3. RSD of displacement cross-sections for neutron elastic scattering calculated using the NRT model and the arc-dpa approach for iron.

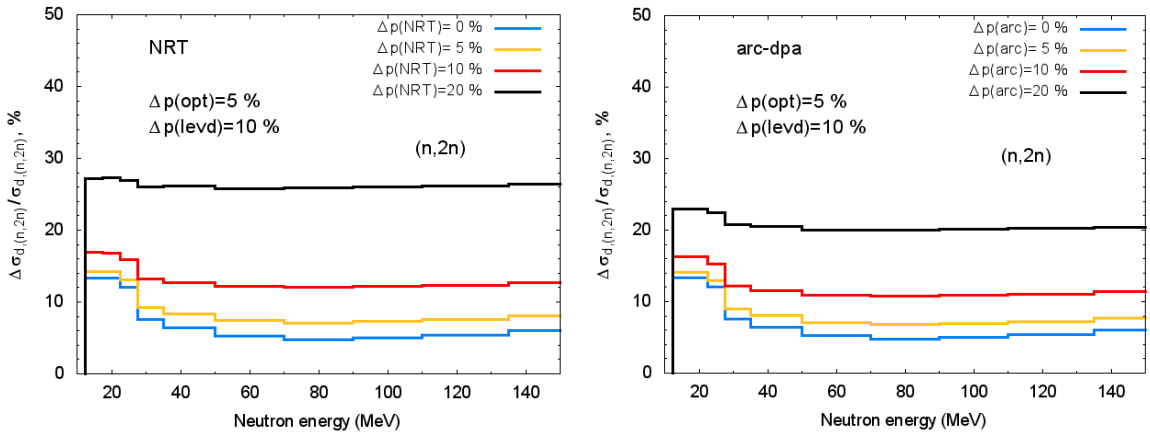


Fig. 4. RSD of displacement cross-sections for the (n,2n) reaction for iron. See details in the text.

2.1.2 Total cross-section

Fig. 5 shows RSD of the total displacement cross-section calculated with different coefficients of variation of NRT, $\Delta p(\text{NRT})$ and arc-dpa, $\Delta p(\text{arc})$ parameters. The $\Delta p(\text{opt})$ and $\Delta p(\text{levd})$ values are equal to 5% and 10% respectively. The results obtained with $\Delta p(\text{NRT})$ and $\Delta p(\text{arc})$ equal to zero illustrate the impact of the change of nuclear model parameters on the σ_d value. The variation of NRT and arc-dpa parameters results to similar $\Delta\sigma_d/\sigma_d$ values.

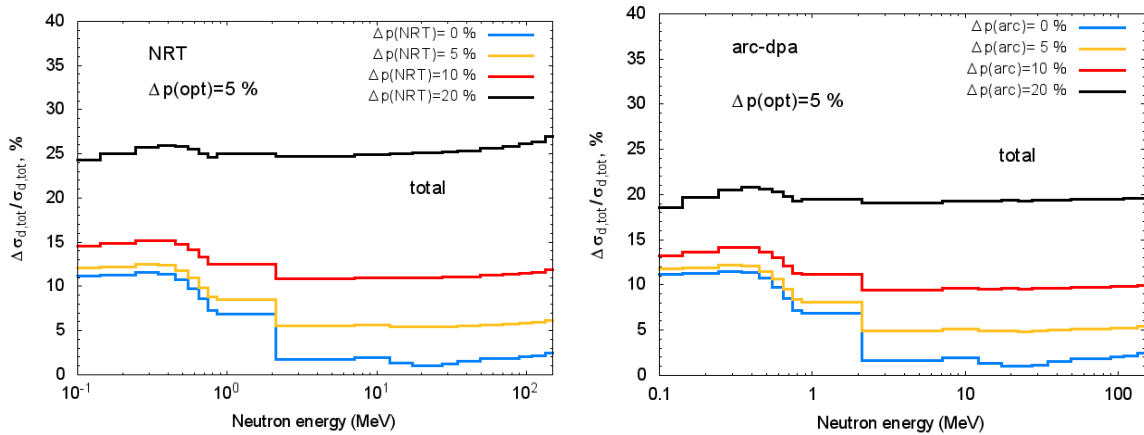


Fig. 5. RSD of total displacement cross-sections for iron calculated using the NRT model and the arc-dpa approach.

The example of calculated displacement cross-sections with errors is shown in Fig. 6. The additional information can be found in Refs. [10,11].

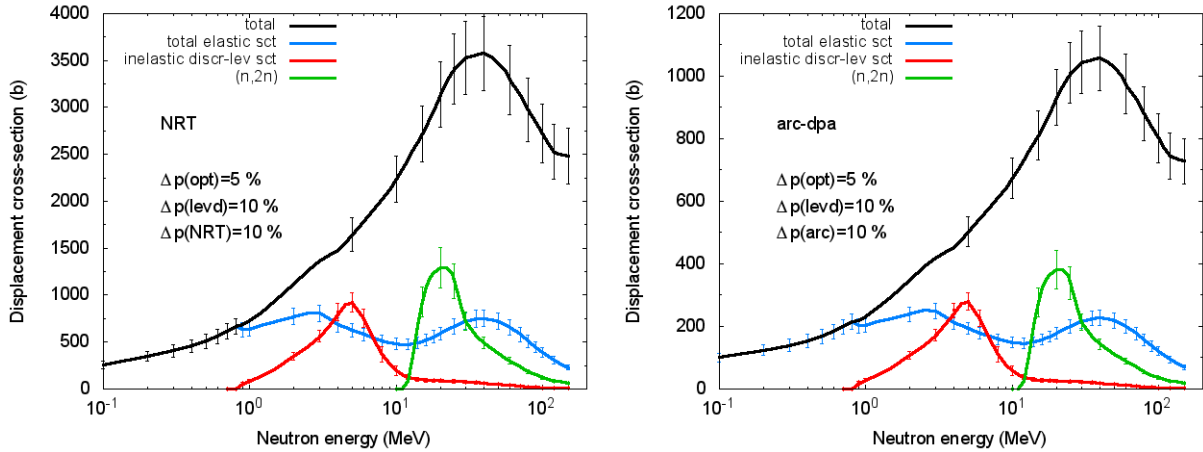


Fig. 6. Example of total displacement cross-sections with errors calculated for iron using the NRT model and the arc-dpa approach. See explanations in the text.

2.2 Tungsten

Fig. 7 shows the $\Delta\sigma_d/\sigma_d$ values for total displacement cross-section calculated for tungsten. The $\Delta p(\text{opt})$ value is equal to 5% and $\Delta p(\text{levd})$ is equal to 10%. As in the case of iron the results of calculations using the NRT model and the arc-dpa approach are similar.

Fig. 8 shows the example of calculated total displacement cross-sections with errors. The effective threshold displacement energy E_d for tungsten is taken equal to 70 eV [8]. More information about $\Delta\sigma_d/\sigma_d$ for tungsten can be found in Refs. [10,11].

3. Incident neutron energies up to 3 GeV

Fig. 9 shows the example of RSD-value and displacement cross-sections calculated for neutron nonelastic interactions with iron using the CASCADE code. The following values concerning simulations with the intranuclear cascade evaporation model were varied, the corresponding RSD values are given in brackets: nuclear level density parameters (a : 10%, δ : 20%), nucleus radius (4%), nucleon-nucleon and nucleon-pion cross-sections (10%), total reaction cross-section used for the normalization of results (10%), and the NRT model parameters including E_d (from 0 to 20%).

The results (Fig. 9) seem to be close to values obtained using the TALYS code (Fig. 5 left). The scatter of displacement cross-sections calculated using different codes implementing intranuclear cascade evaporation model is discussed briefly in Refs. [10,11].

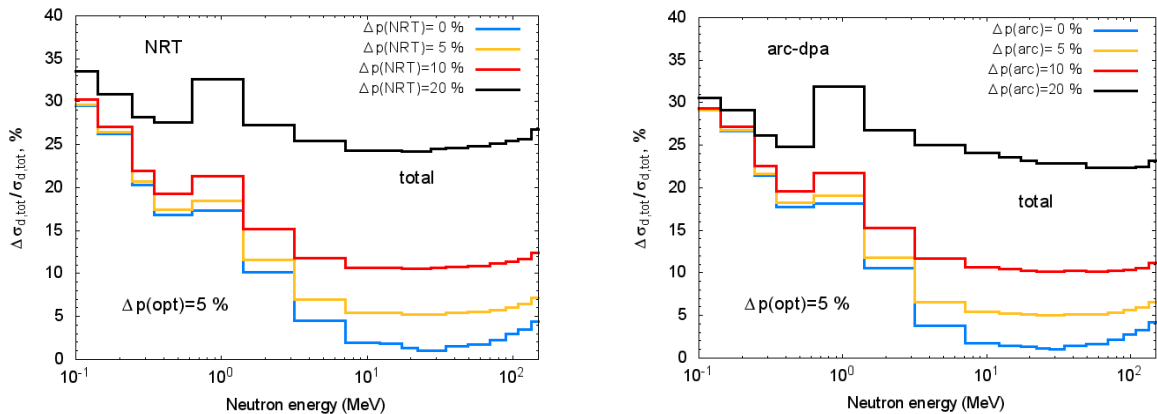


Fig. 7. RSD of total displacement cross-sections for tungsten calculated using the NRT model and the arc-dpa approach.

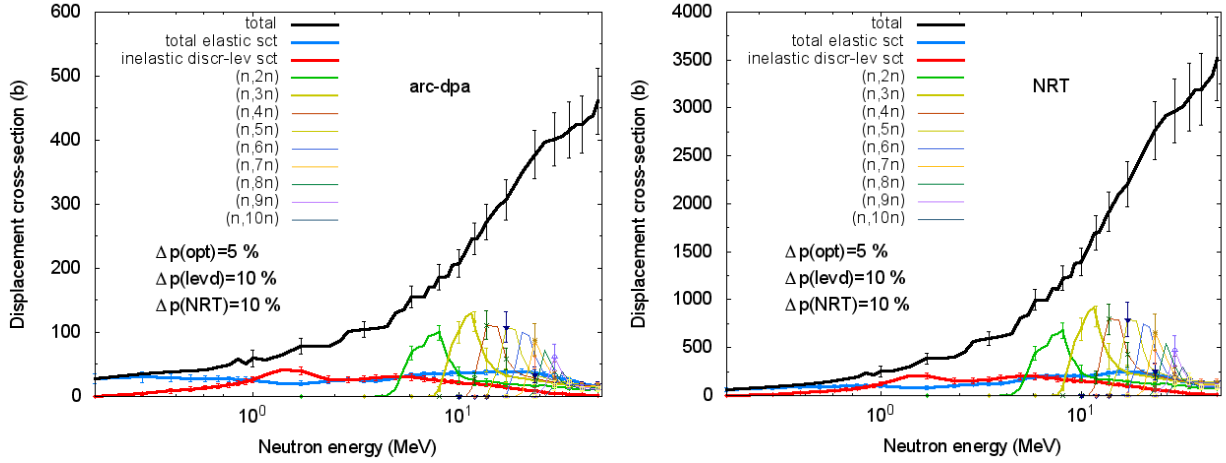


Fig. 8. Example of total displacement cross-sections for iron calculated using NRT model and arc-dpa approach. The E_d value is equal to 70 eV.

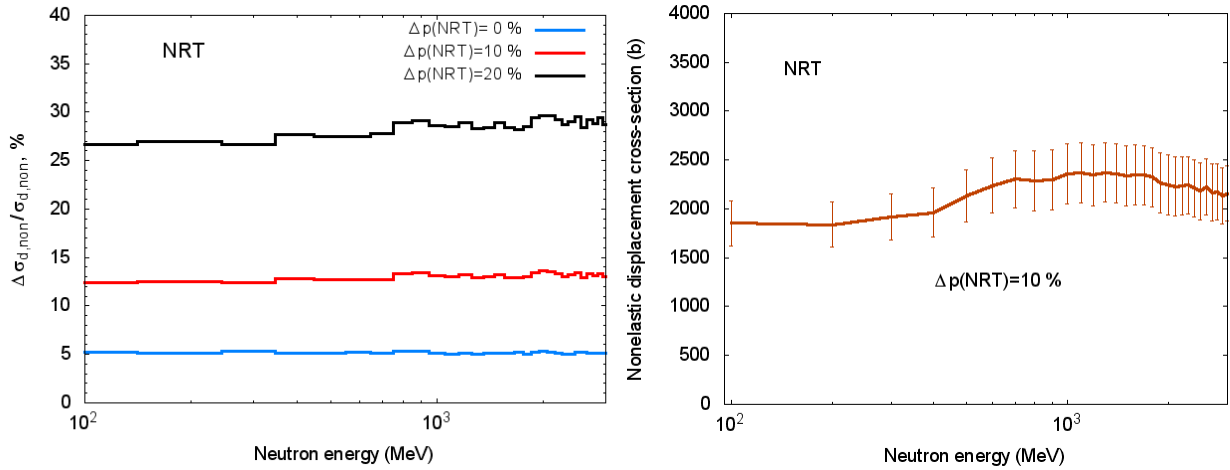


Fig. 9. Example of $\Delta\sigma_d/\sigma_d$ values (left) and displacement cross-sections (right) for neutron nonelastic interactions with iron calculated using the CASCADE code at neutron incident energies from 100 MeV to 3 GeV. See details in the text.

4. Conclusion

Uncertainty of displacement cross-sections σ_d was evaluated for iron and tungsten irradiated with neutrons with energies from 0.1 MeV to 3 GeV. The TALYS [3] and ECIS [13] codes were applied for recoil energy distribution calculations in the energy range 0.1 to 150 MeV; the CASCADE code [4,5] implementing the intranuclear cascade evaporation model was used at the higher energies.

The NRT model [6] and the arc-dpa approach [7,8] were utilized to calculate the number of stable defects.

The RSD-values and correlation matrices, for σ_d , were obtained for different variation of optical model parameters, nuclear level density parameters, and parameters of models used for estimation of the number of defects produced under irradiation.

An additional study is needed to define the optimal range for possible variation of NRT and arc-dpa parameters.

References

- [1] A.Yu. Konobeyev, U. Fischer, P.E. Pereslavitsev, S.P. Simakov, Uncertainties in the Displacement Cross-Sections of Fe and W, EFFDOC-1180; https://www.oecd-neo.org/dbdata/nds_effdoc/effdoc-1180.pdf
- [2] D.L. Smith, Covariance Matrices for Nuclear Cross Sections Derived from Nuclear Model Calculations, ANL/NDM-159, Argonne National Laboratory, 2004
- [3] A.J. Koning, S. Hilaire, and M.C. Duijvestijn, TALYS, Proc. Int. Conf. on Nuclear Data for Science and Technology, April 22-27, 2007, Nice, France, 2008, p. 211; TALYS-1.8, <http://www.talys.eu/>
- [4] V.S. Barashenkov, Monte Carlo simulation of ionization and nuclear processes initiated by hadron and ion beams in media, *Comp. Phys. Comm.* **126** (2000) 28
- [5] A.Yu. Konobeyev, U. Fischer, Simulation of heavy cluster emission in nucleon induced reactions on targets from C to Bi at intermediate energies, KIT Scientific Reports 7684 (2014); <http://digbib.ubka.uni-karlsruhe.de/volltexte/1000043611>
- [6] M.J. Norgett, M.T. Robinson, I.M. Torrens, A proposed method of calculating displacement dose rates, *Nucl. Eng. Des.* **33** (1975) 50
- [7] K. Nordlund, A.E. Sand, F. Granberg, S.J. Zinkle, R. Stoller, R.S. Averback, T. Suzudo, L. Malerba, F. Banhart, W.J. Weber, F. Willaime, S. Dudarev, D. Simeone, Primary radiation damage in materials, NEA/NSC/DOC(2015)9, OECD 2015
- [8] K. Nordlund, Summary of the 2nd RCM of CRP on Primary Radiation Damage Cross-Section, Primary Radiation Damage Cross Sections. Summary Report of the Second Research Coordination Meeting, 29 June - 2 July 2015, IAEA Headquarters, Vienna, Austria, INDC(NDS)-0691, December 2015, p.19; <https://www-nds.iaea.org/publications/indc/indc-nds-0691.pdf>
- [9] M.T. Robinson, The energy dependence of neutron radiation damage in solids, Proc. Conf. on Nuclear Fusion Reactors, UKAEA Culham Lab. 17-19 Sept. 1969, eds. J.L. Hall and J.H.C. Maples (British Nuclear Energy Society, London, 1970) p. 364
- [10] A.Yu. Konobeyev, U. Fischer, Slides of presentation, this meeting
- [11] A.Yu. Konobeyev, U. Fischer, Uncertainties of atomic displacement cross-sections for iron and tungsten irradiated with neutrons of intermediate energy, KIT Scientific Working Papers, to be published
- [12] A.J. Koning, J.P. Delaroche, Local and global nucleon optical models from 1 keV to 200 MeV, *Nucl. Phys.* **A713** (2003) 231
- [13] J. Raynal, ECIS96, Proc. Specialists' Meeting on the Nucleon Nucleus Optical Model up to 200 MeV, Bruyères-le-Chatel, France, Nov. 13-15, 1996, <http://www.nea.fr/html/science/om200/raynal.pdf>

Estimation of bias and uncertainties for radiation damage calculation (Fission Reactors), D. Bernard

CEA/DEN/CAD/DER/SPRC/LEPh
Cadarache, France

The first part of this presentation was dedicated to the review of DPA metrics, starting from the original KP (Kinchin-Pease [1]) for which the damage estimation is a Heaviside function (0 below the effective displacement energy E_d and 1 above), while the available energy is below $2E_d$. Above this latter value, damage factor (or the surviving number of Frenkel Pairs) is then proportional to the available energy over $2E_d$ (the supposed energy to displace 2 atoms). A second simpler model, thanks to Norgett, Robinson and Torrens [2], proposes one formula equation linking real damages in material to the available energy: $NRT-DPA=0.8E_a/(2E_d)$, but accounting for an efficiency factor estimated to be $\zeta=0.8$.

At final, nowadays, a more reliable model (arc-DPA: Athermal Recombination Corrected) is proposed by OECD [3] to account for thermal recombination in materials, leading to a new efficiency factor depending on the available energy. This model has 2 new parameters ‘b’ and ‘c’ which are fitted on atom cascade results performed by Molecular Dynamics. arc-DPA values is approximately one third of NRT-DPA values for reactor applications and does not depend that much on E_d values as the NRT-DPA metric does.

The limitations of such models are listed such as, their domain of applicability (crystalline material only, the treatment of polyatomic material is not yet done and no temperature dependence is accounted for recombination for instance ...).

The second part of the presentation was dedicated to the detailed calculation of so-called damage cross sections by the NJOY [4] processing code. For the time being, NJOY/HEATR treats only proportional DPA metrics such as NRT or KP. NJOY users are waiting for the development of the more realistic arc-DPA kernel for coming versions. NJOY calculates DPA partial cross section per channel and one has to be aware that the ‘self-shielding’ correction has to be accounted in transport codes. That’s why the use of reduced (and partial) DPA cross section is recommended:

$$E_{a,iso,react}(E_n) = \frac{\sigma_{dpa,iso,react}^{\infty \text{ diluted}}(E_n)}{\sigma_{iso,react}^{\infty \text{ diluted}}(E_n)}$$

For all reaction channels, DPA cross section calculation were reviewed. The specific radiative capture (MT102 in ENDF sense) lead to many discussions during the meeting (even if this partial DPA is not important in the total displacement rates). Indeed from one evaluation to another, we can see high discrepancies. We have to keep in mind that the following formula as used in NJOY proposed the upper value for the recoil energy of nucleus accounting for the actual neutron kick and an approximate value for the recoil during the γ emission. The latter is calculated by using the averaged value of the square γ spectrum: $\overline{E_\gamma^2}$ (see Fig. 1). The displacement cross section due to capture processes is then very sensitive to the high energy part of the γ spectrum (stored in MF6 or MF12+13+15 for the MT102 channel depending of evaluations) especially when high energy γ peaks are not accounted for in evaluations.

An important point is that partial damage cross sections are not that much sensitive to the displacement energy value (used in partition functions to account for the electronic screening) because it concerns only low cross section values and at ‘low’ neutron energies (see Fig. 2).

A comment for the Monte Carlo TRIPOLI4 code is that the partial cross section computation is now including in version 9.

To conclude this part of the description of the DPA processing, the energy shape of cross sections is not very sensitive to Doppler broadening. The temperature dependence has, nevertheless, to be accounted for thermal recombination.

Once folded over a real neutron spectrum (see Fig. 3), one can deduce the median neutron energy in NRT-DPA metric (GEN-III and GEN-IV): half of DPA is induced by neutrons with kinetic energy more than 1 MeV. The > 1 MeV neutron fluence indicator (easy to measure with dosimetric threshold reactions) is then incomplete for real radiation damage estimation.

The third part is divided in two subsections. One deals with model defects and one deals with ‘statistical’ uncertainties in DPA calculations.

Phenomenological metrics for DPA (KP, NRT or arc) constitute a first model defect for the damage estimation. The choice of the partition function is another one (historical Robinson as programmed in NJOY or the new Akkerman one for instance as used for silicon). The kernel in NJOY for calculating available energy cross sections uses crude approximations such as classical kinematics for only 2 body scattering and looks like it does not accurately account for (n,np) channel kinematics. Integration is first done over angular variable and then over the energy variable where a double integration should be needed.

The second subsection lists the overall sources of ‘statistical’ uncertainties to be propagated to DPA rates calculations: the uncertainties associated to Prompt Fission Neutron Spectrum or more general high energy neutron spectra, scattering and disappearance cross section, secondary angular and energetic distributions is part of the ‘nuclear part’ of the uncertainty. The COMAC (Covariance Matrix from Cadarache) is proposed [5]. Molecular Dynamics part of the uncertainty is vectored by E_d (for NRT-DPA) or ‘b’ and ‘c’ fitted parameters (for arc-DPA model).

The method proposed is to use the sandwich formula with sensitivities previously calculated by Generalized Perturbation Theory applied to the Boltzmann transport equation.

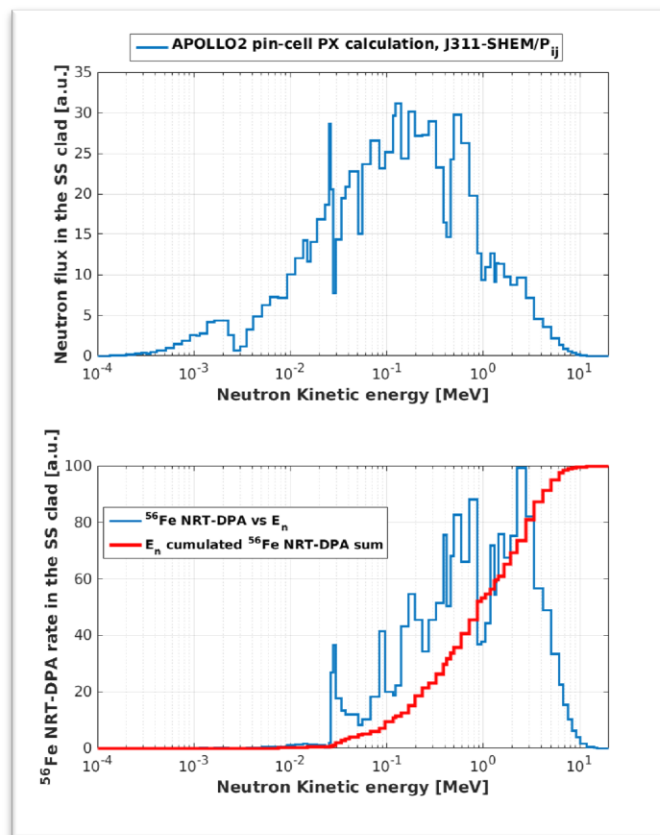


Fig. 3. FBR neutron flux, and NRT-DPA rate as a function of neutron kinetic energy.

An attempt for Molecular Dynamic uncertainties through arc-DPA model is proposed by analytical differentiation with respect to ‘b’ and ‘c’ parameters:

$$S_b^{[arc]} = \frac{b(1-c)}{arc} \int \left\{ \left[\frac{0.8E_a(E_n)}{2E_d} \right]^b \times \ln \left[\frac{0.8E_a(E_n)}{2E_d} \right] \right\} \times \sigma_{NRT-dpa}(E_n) \cdot \phi(E_n) dE_n \sim -0.15 \frac{NRT}{arc} < -0.6$$

$$S_c^{[arc]} = \left(\frac{1}{1-1/c} \right) \left[c - \frac{NRT}{arc} \right] \sim \frac{1}{3} \frac{NRT}{arc} \sim 1.2$$

To conclude, nuclear data and molecular dynamics uncertainties have to be propagated to DPA rates but one has to keep in mind that γ -DPA for specific applications and gas production could be important as well.

References

- [1] G. H. Kinchin and R. S. Pease, 1955 Rep. Prog. Phys. 18 1.
- [2] M. Norgett et al., Nucl. Eng. and Des. 33 (1975) 50-34.
- [3] OECD/NEA/NSC/DOC(2015)9.
- [4] R.E. MacFarlane and A.C. Kahler, Nucl. Data Sheets, 111 (2010) 2739-2890.
- [5] C. De Saint Jean, P. Archier, G. Noguere, O. Litaize, C. Vaglio, D. Bernard, O. Leray, “Estimation of multi-group cross section covariances of $^{238,235}\text{U}$, ^{239}Pu , ^{241}Am , ^{56}Fe and ^{23}Na ”, Proc. Int. Conf. PHYSOR 2012, Knoxville, USA, April 15-20 (2012).

Justified and complete gas-production cross sections with uncertainties for ^{59}Ni and consequences for stainless steel in LWR spectra, P. Helgesson and H. Sjöstrand

Department of Physics and Astronomy, Uppsala University
Uppsala, Sweden

Background

In the work for this TM, we have produced justified and complete gas-production cross sections with uncertainties for ^{59}Ni and investigated its consequences for stainless steel in LWR spectra, in part using the nuclear model code TALYS and the Total Monte Carlo Method (TMC) / TENDL method [Kon12].

In order to obtain justified best estimates and uncertainties in gas production data derived from nuclear modelling, a proper calibration of the nuclear data with respect to experimental data is necessary. A rigorous treatment of experimental uncertainties can improve the predictive power of damage modelling.

For this TM, we have investigated the gas production in ^{59}Ni , since the two-step thermal neutron reaction sequence, $^{58}\text{Ni}(n,\gamma)^{59}\text{Ni}(n,\alpha)^{56}\text{Fe}$, ($Q_{\text{value}} = 5.1$ MeV) results in non-linear He production rates and is an important contribution to the He production in steel in thermal spectrum. The reaction sequence is also an important contribution to the damage energy. We have also investigated the hydrogen producing reaction sequence $^{58}\text{Ni}(n,\gamma)^{59}\text{Ni}(n,p)^{59}\text{Co}$, ($Q_{\text{value}} = 1.9$ MeV) and all other important reaction channels. Currently, the existing evaluated data have no uncertainty information, neither for $^{59}\text{Ni}(n,\alpha)^{56}\text{Fe}$, nor for $^{59}\text{Ni}(n,p)^{58}\text{Co}$ reactions, in the thermal region. Furthermore, the TENDL evaluation does not seem to treat the resonances in a consistent way for these reactions in the thermal region.

Results

Largely motivated by improving the He production prediction and the uncertainty estimate of it, a new evaluation of ^{59}Ni cross section data has been developed, and is under consideration for inclusion in the next JEFF3.2T2 release. The evaluation is based on three main components:

1. An analysis of available thermal cross section experiments;
2. Resonance parameters (including alpha and proton widths) provided by J.A. Harvey (EXFOR entry 10680);
3. TENDL-2015 and URR parameter distribution resulting from the same parameter distribution as in TENDL-2015 [Kon15b].

For the thermal cross section experiments, included uncertainty components are identified, and seemingly missing uncertainty components are given default values based on the other analyzed experiments. The different experimental uncertainty components are then sampled based on a normal distribution, and components that are identified to be common for different experimental points (even in different experiments) are ensured to be the same for each particular observation in the sample. For each of (n,tot), (n,gamma), (n,alpha) and (n,p), generalized least squares is used to obtain one value (out of the different experiments) *for each observation in the sample*. This procedure gives a sample from the full multivariate distribution of the thermal cross sections. Also, Bayes' theorem is used to include physical constraints, for example that $(n,el) > 0$, by rejecting samples which do not fulfil physical constraints.

The resonance parameters are sampled using Harvey's central values and standard deviations, but also adding error components to the gamma, alpha and proton widths that approximate the systematic errors for underlying (n,gamma), (n,alpha) and (n,p) cross section measurements (correlated to Harvey's thermal cross section experiments used above).

For non-cross section data and cross sections above the URR, TENDL-2015 is used. TALYS is also used to give URR parameters, with the TALYS parameter distribution [Kon15b] used for the TENDL-2015 random files. The mean values are used for the URR parameters in MF2 and the covariances are given in MF32.

The different components are combined in a novel fashion. For each random nuclear data file:

- i) TALYS 1.8 [kon15a] is run with random parameters as in TENDL 2015 [Kon15b];
- ii) Thermal cross sections are sampled as outlined above;
- iii) Harvey's resonance parameters are sampled as outlined above;
- iv) Bound resonances (at negative energies) and resonances in the URR below 3.89e4 eV are sampled using the Wigner distribution for the energies (for each $(J,1)$) and chi-squared distributions (different number of degrees of freedom motivated by the physics) for the widths. The expected values (which determines the full distributions) of these respectively distributions are taken as the average level spacings and widths produced by TALYS with the same TALYS parameters as in the TENDL-2105 random files;
- v) The widths of the bound resonances are adjusted to match the thermal cross sections obtained in (ii), using a numerical root finding; if impossible, the combination obtained in (i)-(iv) is deemed unphysical, and the procedure is redone from step (ii), as an application of Bayes' theorem (as mentioned above). This has a small effect on the distribution of the thermal cross section.

The resulting cross sections are illustrated in Figure 1, and the energy-energy covariance of the (n, α) cross section is illustrated in Figure 2. In particular, the thermal (n, α) cross section obtained in this work is $12.68(4) \pm 0.67(4)$ b, which can be compared to the value in the Atlas of neutron resonances by Mughabghab [Mug06], 12.3 ± 0.6 b, and to what is found in JEFF 3.2 (which is copied to ENDF/B-VII.1), 13.5 b. The value of this work is different from both Mughabghab and JEFF 3.2, but still consistent with it.

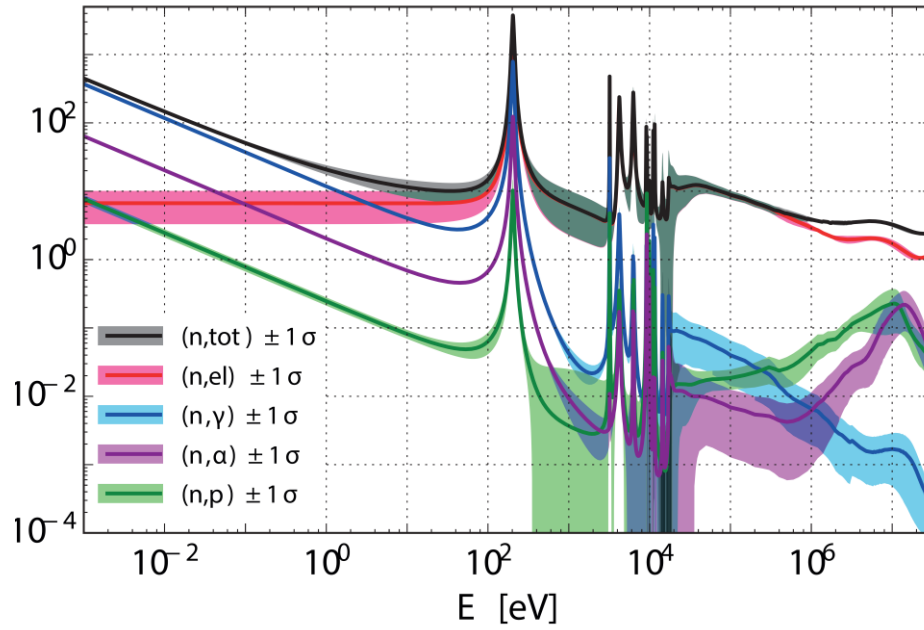


Fig. 1. The distribution of the random files of the new Ni-59 evaluation at 0 K, as functions of energy.

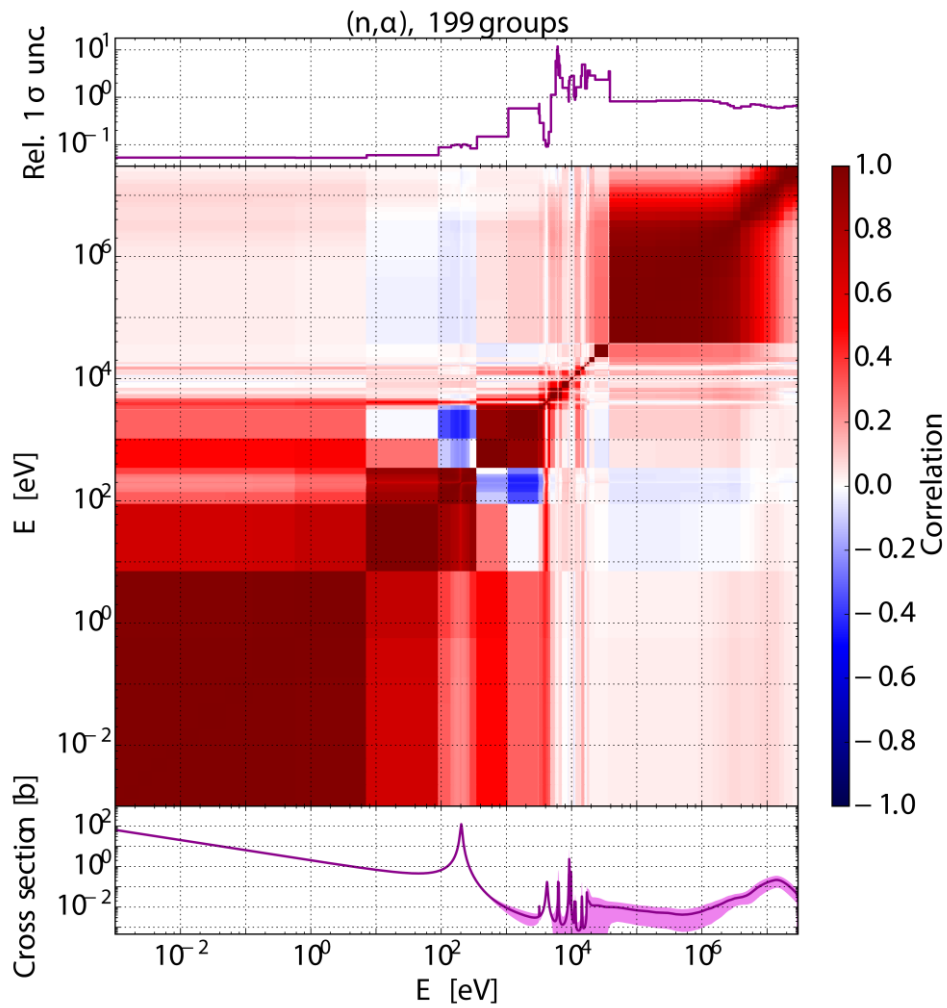


Fig. 2. Energy-energy correlation matrix and uncertainties as function of energy for the (n,α) cross section in the new Ni-59 evaluation. The cross section is also given.

In order to check the performance of the random files and get a first indication of their impact on applications, they have been tested on an MCNP 6 model, after processing using NJOY 99. The model consisted of an SS 304 cylinder ($r = 100$ cm, $h = 1$ cm). The composition of the steel was 69.5% Fe, 19% Cr, 9.5% Ni, and 2% Mn. A ‘typical’ LWR spectrum was used [Pes11]. The ^{59}Ni and ^{58}Ni content was modified to the values in the ^{59}Ni peak in Ref. [Gri13]. The results were compared to the (n,α) reaction rate in a reference case with only natural Ni. It was found that ^{59}Ni increased the (n,α) reaction rate with a factor of $5.16(1) \pm 0.26(1)$, i.e., with a ^{59}Ni uncertainty of 5.1(2)%. The corresponding ratio using JEFF 3.2 (or ENDF/B-VII.1) is 5.77, which can partly be understood from the larger thermal (n,α) cross section given in this evaluation.

Discussion

During the TM it was brought up by P. Griffin that it could have been better, in step (v), to return to step (iii) instead of step (ii) if the sampled combination was deemed unphysical. This would have kept the experimental thermal distribution unchanged by the Bayesian updating procedure. This would bias the results towards the evaluation of the thermal cross sections; this could however be justified if there is reason to believe that this part of the distribution is better estimated than, e.g., the distribution of Harvey’s resonance parameters (with the added approximate uncertainty components). In practice, for this particular application, the choice had only limited impact on the results. The suggestion will be reconsidered for future work.

In this work, the Multi-Level Breit Wigner (MLBW) distribution was used for the resonance parameters. Also the Reich Moore formalism using the LRF7 format was considered, but the MLBW was chosen for two main reasons:

- 1) our understanding is that Harvey used the Breit Wigner formalism when the resonance parameters were fitted to experimental data, and since the original data is not available, it would have been necessary to translate the parameters to the alternative formalism;
- 2) in LRF7, all different channels need to be provided with their particular widths. For (n,α) , this means that the widths need to be split up between all possible excited states of the daughter nucleus. Experimental information for how this would be done is not available, and simply choosing the ground state would be poorly motivated and lead to missing resonances because of incompatible quantum numbers.

Conclusions

In this work we have seen that methods based on the TENDL and the TMC method have a great potential to address damage relevant macroscopic quantities.

The two-step thermal neutron reaction sequence $^{58}\text{Ni}(n,\gamma)^{59}\text{Ni}(n,\alpha)^{56}\text{Fe}$ results in an important contribution to the He production in steel in thermal spectrum and is an important contribution to the damage energy. We have evaluated the ^{59}Ni cross sections using a novel approach including the sampling of individual error components of thermal cross section experiments.

The $^{59}\text{Ni}(n,\alpha)$ reaction rate in stainless steel in a thermal spectrum has been determined using MCNP, resulting in a five-fold increase of the (n,α) reaction rate with an uncertainty of 5%.

The TM highlighted the importance of covariance data for damage metrics. We believe that the proposed method, based on the TENDL/TMC method, which includes justified covariance data for all important channels, including cross-channel correlations, as well as for angular distributions in the high energy range, can serve as an example for the continued nuclear data evaluation work for the damage community.

Acknowledgment

The performed work is part of a research project (MÅBiL) in collaboration with the main stakeholders in the Swedish nuclear sector with the aim to improve nuclear materials for LWR. We greatly acknowledge the funding from Ringhals AB, Forsmark AB, OKG AB and Westinghouse.

A special thanks to the participants in the TENDL team, Arjan Koning, Dimitri Rochman and Jean-Christophe Sublet, whose input to the project has been paramount.

References

- [Kon12] A. Koning and D. Rochman, Nucl. Data Sheets 113,2841 (2012)
- [Pes11] M. Pescarini et al., *ENEA-Bologna Multi-Group Cross Section Libraries for LWR Shielding and Pressure Vessel Dosimetry Applications*, Tech. rep., ENEA (2011)
- [Gri13] M. Griffiths, *The Effect of Irradiation on Ni-containing Components in CANDU Reactor Cores: A Review*, AECL Nuclear Review 2 (2013)
- [Kon15a] A. Koning, et al., *TALYS-1.8, User Manual*, Nuclear Research and Consultancy Group NRG (December 2015)
- [Kon15b] A. Koning, et al., *Bayesian Monte Carlo method for nuclear data evaluation*, Eur. Phys. J. A (2015) 51: 184
- [Mug06] S. Mughabghab, *Atlas of Neutron Resonances*, Elsevier Science (2006)

A rigorous treatment of uncertainty quantification for Silicon damage metrics, P. Griffin

SAND2016-6542 O

Sandia National Laboratories, Radiation and Electrical Sciences Center
Albuquerque, NM, USA

Abstract. These report summaries the contributions made by Sandia National Laboratories in support of the International Atomic Energy Agency (IAEA) Nuclear Data Section (NDS) Technical Meeting (TM) on Nuclear Reaction Data and Uncertainties for Radiation Damage. This work focused on a rigorous treatment of the uncertainties affecting the characterization of the displacement damage seen in silicon semiconductors.

1 Purpose

This is the report from Sandia National Laboratories (SNL) presented at the Nuclear Reaction Data and Uncertainties for Radiation Damage, Technical Meeting (F4-TM-52919), held at IAEA Headquarters, Vienna, Austria in support of the Cooperative Research Project (CRP) on Primary Radiation Damage Cross Sections. The focus of our work was on a rigorous quantification of the uncertainty in the silicon displacement damage metric used in the assessment of the damage to the minority carrier lifetime in silicon bipolar junction transistors (BJTs). Once a consistent and complete uncertainty quantification methodology is worked out for one material/damage mode, it should be easy to replicate the analysis for metrics that describe other material damage modes.

We elected to examine the bipolar gain change in silicon devices as the important damage metric in a neutron field because of: 1) the availability and high quality of the important supporting nuclear data; 2) the existence of a radiation effects community endorsed standard that addresses the proper calculated metric to use for correlating radiation damage in different neutron fields, i.e. the ASTM E722 Standard Practice for Characterizing Neutron Fluence Spectra in Terms of an Equivalent Monoenergetic Neutron Fluence for Radiation-Hardness Testing of Electronics [1]. This response function is also recommended as a direct dosimetry metric in ASTM E1855-15 Standard Test Method for Use of 2N2222A Silicon Bipolar Transistors as Neutron Spectrum Sensors and Displacement Damage Monitors [2]. This ASTM standard supports the use of this response function, in conjunction with a silicon bipolar transistor, for both the direct characterization of the damage metric for silicon electronics in neutron fields and as a sensor appropriate for use in spectrum adjustments/unfolds in order to cover an energy region in research reactors that is not easily covered by non-fission based dosimetry sensors.

The following sections of this report address: a) the definition of the calculated radiation exposure metric that is correlated with the observed damage mechanism; b) the sources of uncertainty in the calculated metric; and c) approaches to obtain for this metric a rigorous quantification of the neutron energy-dependent uncertainty in the form of a covariance matrix.

2 Definitions

The fundamental calculated displacement damage metric is the microscopic displacement kerma factor, κ^{dpa} , see ASTM E722-14 [1], which can be written as:

$$\kappa^{dpa}(E) = \sum_{i,j_i} \sigma_{i,j_i}(E) \int_0^\infty dT_{R,j_i} \int_{-1}^1 d\mu \cdot f_{i,j_i}(E, \mu, T_{R,j_i}) \cdot {}^{ion}T_{dam}(T_{R,j_i}) \quad (1)$$

where:

- the summation is over all open neutron-induced reaction channels, i , and emitted particles j_i
- $\sigma_{i,j_i}(E)$ is the cross section for the j_i particle in the i^{th} reaction channel
- $f_{i,j_i}(E, \mu, T_{R,j_i})$ is the energy distribution for resulting charged particles which are emitted with:
 - an energy T_{R,j_i} and at an angle characterized by μ and resulting from the j_i particle in the i^{th} channel,
 - induced by the incident neutron energy with energy E .
- ${}^{ion}T_{dam}(T_{R,j_i})$ is the displacement energy partition function for the emitted ion j_i in the i^{th} open channel with energy T_{R,j_i} .

The displacement kerma, K , is equal to the microscopic kerma factor multiplied by the number of atoms per unit mass in the target material and the incident particle fluence. The ionizing kerma can be obtained by subtracting the displacement kerma from the total material kerma.

A related, but very important, damage metric used by the radiation effects community is the neutron damage energy, ${}^nT_{dam}$, however, the definition of damage energy is not entirely consistent throughout the literature [3]. The variation in the use of the term involves the: 1) selection of the lower energy bound for the integration over recoil ion energies that are to represent interactions where a subsequent lattice atom displacement can occur; 2) selection of the displacement model, which involves identifying a transfer energy associated with the generation of a Frenkel pair; and 3) treatment of the effective deposited energy for ion recoil energies near the threshold displacement energy. The concept of a "damage energy" is intended to capture the energy imparted by secondary charged particles, integrated over a defined portion of the slowing down process, and going into the creation of Frenkel pairs.

The most commonly used form of the neutron damage energy has a lower recoil integration bound, a bound for the integral over the recoil ion energy, set to the threshold displacement energy, E_d , and uses a sharp threshold Kinchin-Pease displacement model [4] with the Robinson damage partition function [5]. E_d is intended to represent an emission angle-integrated average recoil ion energy below which the recoiling atom can no longer result in a displacement of any additional lattice atoms. This selection is labelled here as the "threshold-based damage energy", will be notated as ${}^n_{KP}T_{dam}^{Rob}(E)$, and is written as:

$${}^n_{KP}T_{dam}^{Rob}(E) = \sum_{i,j_i} \sigma_{i,j_i}(E) \int_{E_d}^\infty dT_{R,j_i} \int_{-1}^1 d\mu \cdot K_{i,j_i}^{recoil}(E \rightarrow T_{j_i}) \cdot {}^{ion}T_{dam}^{Rob}(T_{R,j_i}) \quad (2)$$

Here the ${}^n_{KP}K_{i,j_i}^{recoil}(E \rightarrow T_{j_i})$ factor includes the identification of the reaction channel-dependent recoil energies, similar to the $f_{i,j_i}(E, \mu, T_{R,j_i})$ term in Equation 1, as well as a term that includes the efficiency of the ion-based damage energies from the ${}^{ion}T_{dam}^{Rob}(T_{R,j_i})$ term for ion contributions in the threshold displacement region.

For neutrons, a code such as NJOY-2012 [6] is often used in conjunction with a nuclear data evaluation to find the microscopic displacement kerma factor, κ^{dpa} . NJOY first calculates the reaction-specific total kerma induced by neutron interactions and then identifies the recoil energy distribution for all of the reaction products. The recoil atom energy distribution for each reaction channel is then partitioned into a displacement energy component using a damage partition function. The NJOY-2012

code implements the Robinson fit [5] to the LSS theory [7] for the energy partition and applies a displacement threshold energy, E_d , as the lower integration limit over recoil ion energy. NJOY-2012, in normal operational mode, calculates this sharp threshold Kinchin-Pease neutron damage energy [3]. The neutron damage energy is equal to the displacement kerma only when a displacement threshold energy of zero is used.

Another related and commonly used neutron damage metric is the non-ionizing energy loss (NIEL), which is equal to the threshold-based damage energy multiplied by the factor N_A/A_L where N_A is Avogadro's number and A_L is the atomic mass of the lattice atom. While a kerma is only defined for uncharged particles, the damage energy and the NIEL are defined for both charged and uncharged particles.

A displacement model is used in conjunction with the damage energy to produce a quantity that can be related to the number of displaced atoms, v_d , due to the lattice damage introduced by the recoiling atoms from a neutron interaction. The non-ionizing damage from a recoiling ion is characterized by the ion damage energy, $^{ion}T_{dam}$. Several displacement models are used by the community. In order to differentiate these models we adopt the notation of $^{type}v_d$ to distinguish the various Frenkel pair production models. In order to support a discussion of various damage metrics and, in particular, to provide a clear consistent definition of the damage energy, we elect to break up the displacement model into three parts:

- a threshold function, $^{type-A}\Lambda(E_d, ^{ion}T_{dam})$;
- a Frenkel pair generation efficiency component, $^{type-B}\zeta_d(E_d, ^{ion}T_{dam})$; and
- a residual defect efficiency survival term, $^{type-C}\xi(^{ion}T_{dam})$.

Thus the number of induced Frenkel pairs can be written as:

$$^{type}v_d(E_d, ^{ion}T_{dam}) = ^{type-A}\Lambda(E_d, ^{ion}T_{dam}) \square ^{type-B}\zeta_d(E_d, ^{ion}T_{dam}) \square ^{type-C}\xi(^{ion}T_{dam}) \quad (3)$$

The original Kinchin-Pease model [4,5] relates the number of defects, $^{orig_K\&P}v_d(E_d, E_I, T_R)$, to the primary recoil atom energy:

$$^{orig_K\&P}v_d(E_d, E_I, T_R) = \begin{pmatrix} 0 & 0 \leq T_R < E_d \\ 1 & E_d \leq T_R < 2E_d \\ T_R / (2E_d) & 2E_d \leq T_R < E_I \\ E_I / (2E_d) & E_I \leq T_R < \infty \end{pmatrix} \quad (4)$$

where E_I is the energy above which ions lose their energy only through ionization and below which energy loss could be modelled with an elastic hard sphere scattering model; E_d is the displacement threshold energy; and T_R is the recoil atom energy. When this expression is coupled with the LSS model for the energy partition function, there was no longer a need to introduce the E_I energy and the equation could be rewritten as a function of $^{ion}T_{dam}$. The most commonly seen version of the Kinchin-Pease model uses this LSS energy partition function to define $^{K\&P}v_d(E_d, ^{ion}T_{dam})$. The Kinchin-Pease model is sometimes quoted as using a sharp transition to define $^{sp_K\&P}v_d(E_d, ^{ion}T_{dam})$, the transition being modelled as occurring at E_d . This is the formalism for the damage energy that is built into codes such as NJOY-2012.

The community has examined various forms for the number of Frenkel pairs resulting from different analytic forms of the differential elastic scattering cross section between atoms, represented by a screened Coulomb interaction. The Robinson-Sigmund modification [8], while imposing a consistency condition on the average number of Frenkel pairs produced in a random cascade, calculated an asymptotic solution for $E > 2E_d$ that led to the introduction of a factor of $\beta = (12/\pi^2)/\ln(2) = 0.84$ in the Kinchin-Pease expression for the breakpoint energy of the transition region.

A group of experts at an IAEA Specialist's meeting [5] on radiation damage units adopted a modified formulation for the number of displacements. This approach used the Robinson-Sigmund modification of the hard-sphere scattering energy loss model. This model is called the Norgett, Robinson, and Torrens (NRT) Frenkel pair model, or the modified Kinchin-Pease model, and is the most commonly

used displacement model. This expression is given by:

$${}^{NRT}v_d(E_d, {}^{ion}T_{dam}) = \begin{pmatrix} 0 & 0 \leq {}^{ion}T_{dam} < E_d \\ 1 & E_d \leq {}^{ion}T_{dam} < 2 \cdot E_d / \beta \\ \beta \cdot {}^{ion}T_{dam} / (2 \cdot E_d) & 2 \cdot E_d / \beta \leq {}^{ion}T_{dam} < \infty \end{pmatrix} \quad (5)$$

where β is an atomic scattering correction and is taken to be 0.8. This adopted value of 0.8 is close to the analytically derived asymptotic value used in the Robinson-Sigmund analysis.

The spirit of including a lower integration bound for neutron damage energy in Equation 2, but not for the definition of the ion damage energy, is based on a desire for the “damage energy” metric to be proportional to experimentally observed damage metrics related to Frenkel pair creation. Consistent with this theme of considering the Frenkel pair production to be the primary metric of interest, the damage energy should treat the threshold in the same way that it is treated in the NRT displacement cross section metric. Using the notation incorporated into the threshold treatment of the NRT displacement cross section, the “dpa-equivalent damage energy” can be written as:

$${}^n_{NRT=E_d} T_{dam}(E) = \sum_{i,j_i} \int_0^\infty \sigma_{i,j_i}(E) K_{i,j_i}^{recoil}(E \rightarrow T_{j_i}) \Lambda_d^{NRT}[E_d, {}^{ion}T_{dam}(T_{j_i})] \cdot dT_{j_i} \quad (6)$$

Here the explicit lower integration bound is zero but the threshold function, ${}^{type-A}A(E_d, {}^{ion}T_{dam})$, is used to produce an quantity where the effective lower integration bound corresponds to the energy at which the recoil ion energy is capable of producing an ion damage energy equal to the displacement threshold energy, that is, it is the ion damage energy is equal to E_d and mimics the Kinchin-Pease displacement model formalism.

3 Uncertainty Components

The determination of the uncertainty in the calculated damage energy requires that we look at the energy-dependent uncertainty in the various quantities in Equation 2. This energy-dependent uncertainty is best captured as a covariance function, which is equivalent to providing an energy-dependent standard deviation and a correlation matrix. The major components within the integrand of Equation 2 are: 1) the reaction cross section and resulting recoil ion spectra; 2) the partition function that divides the recoil energy into an ionizing component and a non-ionizing component; and 3) a threshold treatment. The following sections capture some of the primary observations on how to characterize the uncertainty in each of these three separate quantities. Since these components are uncorrelated, the uncertainty in the damage energy can be expressed as the sum of the component covariance matrices.

a) Nuclear Data

The investigation of uncertainties in the damage energy starts with a consideration of the uncertainty due to the underlying nuclear data. Our approach to this is to use the NJOY-2012 code to calculate the damage energy for a sharp threshold Kinchin-Pease model that uses the Robinson fit to the LSS damage partition function. NJOY cannot only produce the total damage energy, but it can separately output the various components of the damage energy. The distributed version of the NJOY code supports output of the total, elastic [ENDF-6 MT=2], inelastic [ENDF-6 MT=51 - 91], and disappearance [ENDF-6 MT=102-120] damage energy components. There is another component, one obtained by subtracting the elastic, inelastic and disappearance component from the total damage energy, that, for the ${}^{28}\text{Si}$ isotope, includes ENDF-6 MT=16, 22, 24, 28, and 29 channels, i.e. the (n,2n), (n, α), (n,2 α), (n,np) and (n,n2 α) channels. Figure 1 shows the energy-dependent fractional contribution from each of these channels.

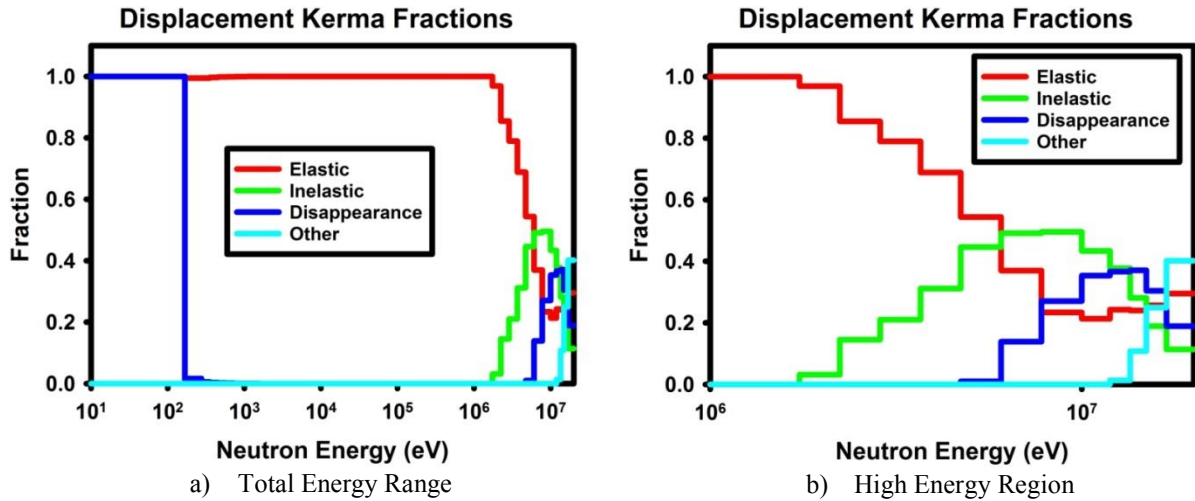


Fig. 1. Fractional Contributions of the Various ^{28}Si Cross Damage Energy Components

The damage energy depends not just on the cross section, but also on the resulting recoil ion spectra. These recoil spectra are quite complex, varying with the incident neutron energy and the reaction channel. Figure 2a shows some representative recoil energy spectra for a 15-MeV neutron on ^{28}Si . Figure 2b shows a representative comparison of the agreement of the recoil spectrum between different evaluated nuclear data files for the (n,n α) reaction with an incident neutron energy of 20 MeV. From the broad study, the agreement is seen to be very good in the elastic channel, but there can be significant differences for some of the disappearance channels for neutron energies near the reaction threshold energy.

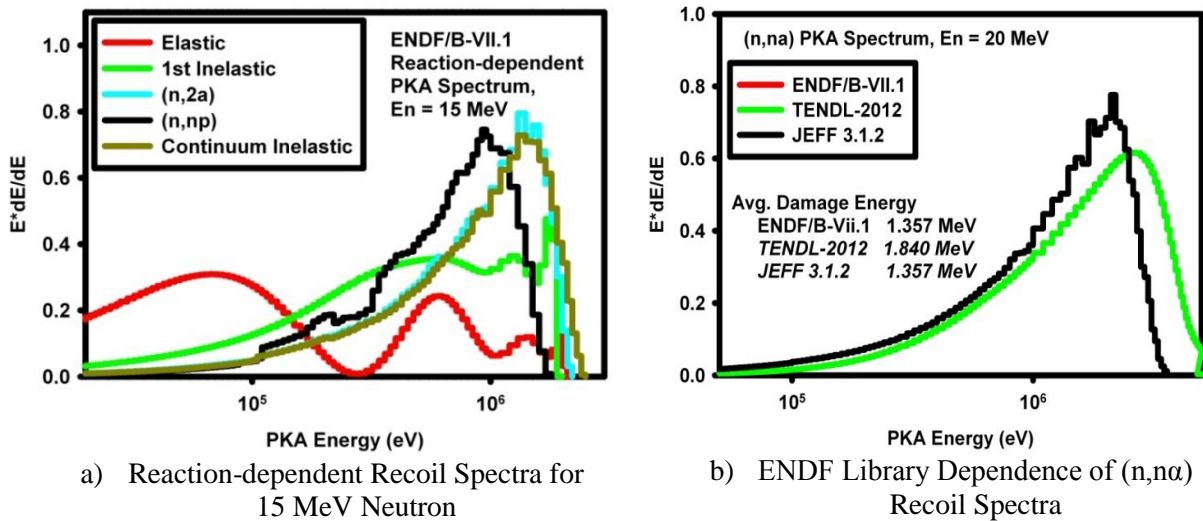


Fig. 2. Fractional Contributions of the Various ^{28}Si Cross Damage Energy Components

A. Koning and D. Rochman provided the author with a set of random cross section libraries generated with the TALYS system of codes and made available as part of the TENDL-2015 release [9]. The 297 element random samplings for the nuclear data for the ^{28}Si isotope permits us to use a Total Monte Carlo (TMC) [10] approach to treat the nonlinear propagation of uncertainty through the equation that defines the damage energy. We used an 89-group structure in the NJOY-2012 code to generate a 297-element set of damage energies and then computed the covariance matrix for the threshold-based damage energy. Figure 3 shows the standard deviation and correlation matrix that provide the uncertainty characterization due to this variation in nuclear data. The analysis was carried out for each of the previously defined damage energy components. Figure 4 shows the energy-dependence of the

standard deviation for the various damage energy components. One immediately notes that, while the total damage energy is the sum of the various component damage energies, at high energy the uncertainty in the total damage energy is significantly smaller than the uncertainty for any of the individual components. This indicates that there is a strong correlation between the various damage energy components, a correlation that cannot be neglected in characterizing the uncertainty in the total damage energy. This study clearly shows that a sample-based, i.e. Monte Carlo, nonlinear propagation of uncertainty that fully incorporates the underlying physics-based correlations between the different reaction channels, like that provided by the TMC approach, is required for this analysis.

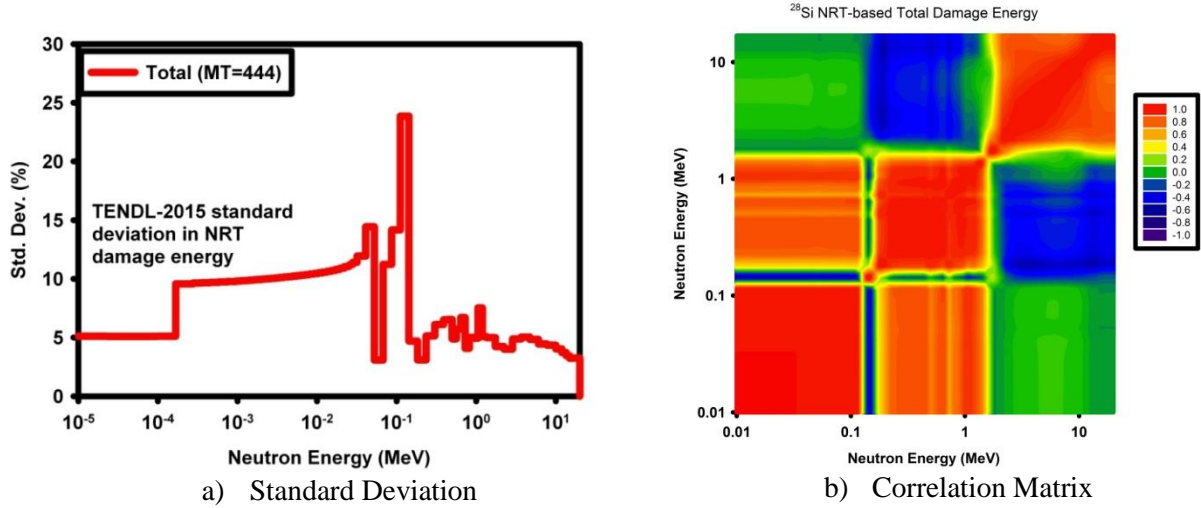


Fig. 3. Uncertainty Characterization for Effect of Nuclear Data on the ^{28}Si Threshold-based Damage Energy.

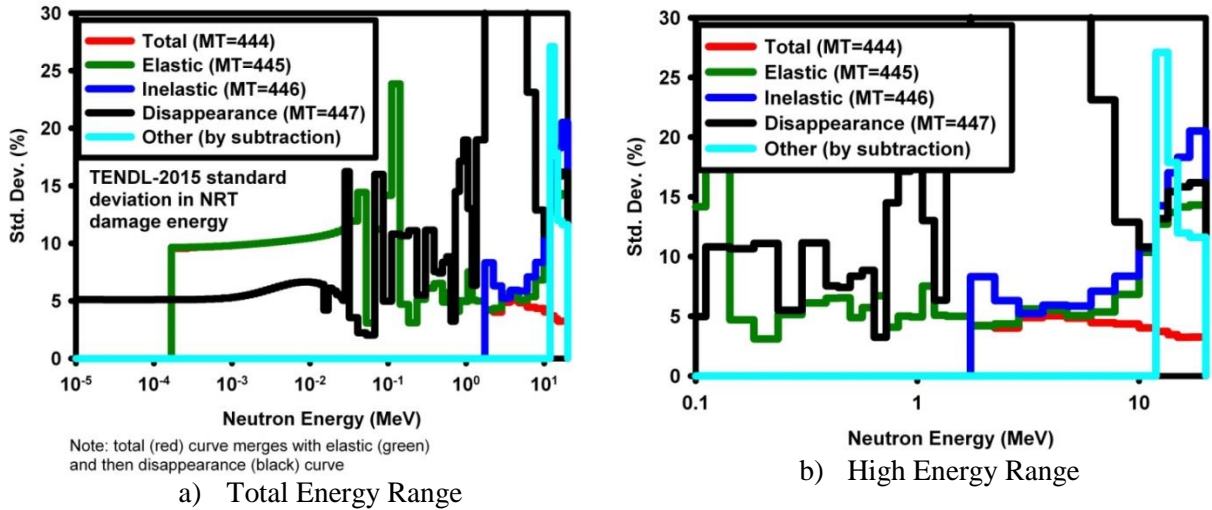


Fig. 4. Standard Deviation for Effect of Nuclear Data on the ^{28}Si Threshold-based Damage Energy Components.

b) Partition Function

The second major source of uncertainty in Equation 2 is from the damage partition function. This is the function $^{ion}T_{dam}(T_r)$ in Equation 2 that converts the recoil ion energy, T_r , into a non-ionizing component that can be correlated with the production of Frenkel pairs. The most widely used energy partition model is the Robinson fit to the Lindhard, Scharff, and Schiott (LSS) energy partition [7]. The LSS approach assumes the local density approximation (LDA) and uses a Thomas-Fermi

screening function over the Coulomb potential to model the elastic interactions and a non-local free uniform electron gas model for the inelastic electronic scattering. Robinson and Torrens fit [11] the LSS energy partition with an analytic representation based upon the atomic mass, A , and atomic number, Z , for the incident ion and the lattice ion. This formulation is valid for all monoatomic crystalline materials at energies less than $\sim 25 * Z^{4/3} * A$ (keV) and when the ratio of the atomic numbers for the incident and lattice atoms do not differ significantly from unity [5].

Work by Akkerman [12] used updated Ziegler, Biersack, and Littmark (ZBL) [13] potentials for silicon to derive a new partition function that is valid only for silicon and at ion energies less than ~ 500 keV. The Akkerman partition model uses the same functional representation as was adopted by the Robinson methodology, but used different coefficients in the functional form. Figure 5a shows the ion energy-dependent damage partition functions for silicon. In order to better highlight the difference in the high ion energy region between the two damage partition models, Figure 5b shows the ratio of the two damage partition functions.

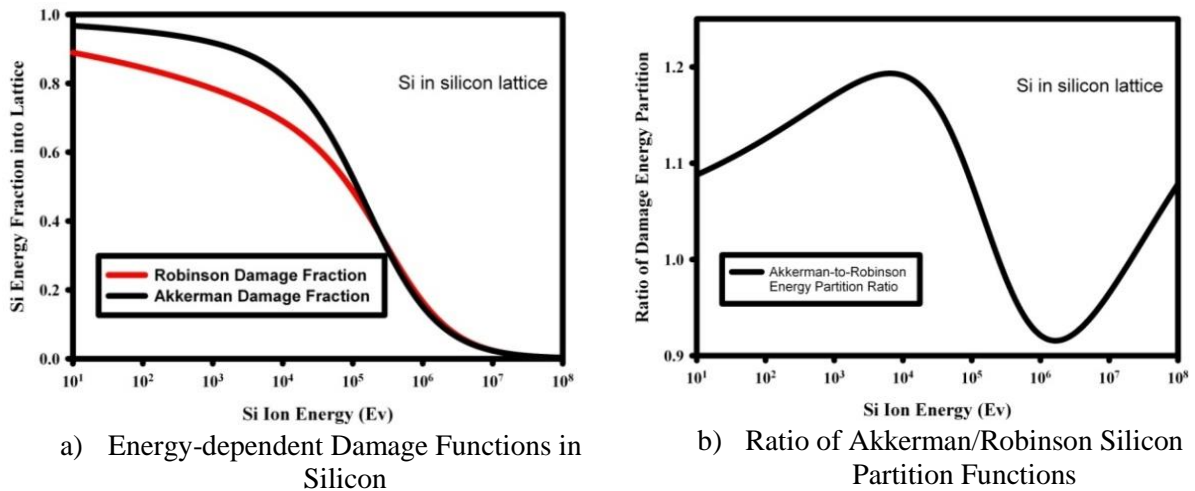
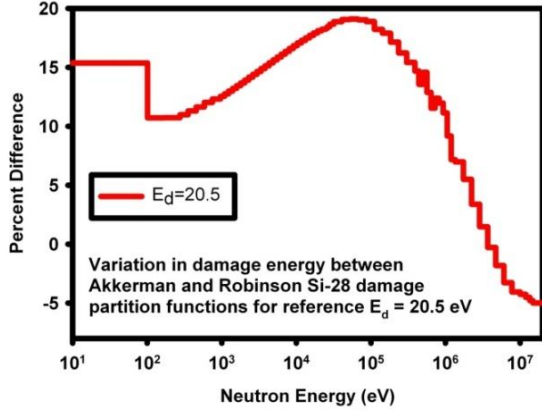
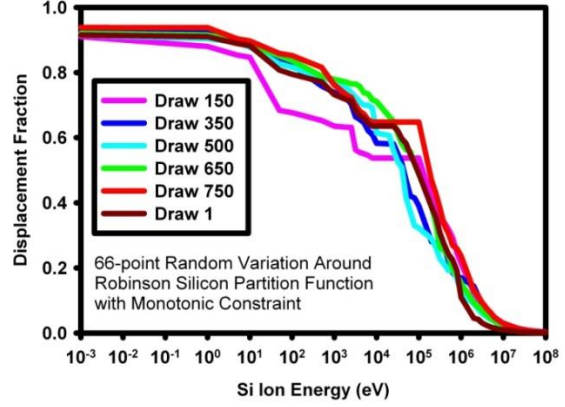


Fig. 5. Commonly Used Partition Functions in Silicon.

Figure 6a shows how this difference in partition function affects the neutron damage energy in silicon. Since the effect can be important, work was undertaken to more rigorously characterizing the uncertainty. In order to more completely explore this sensitivity, we used the binary collision approximation (BCA) code, MARLOWE [14], to calculate the ion energy-dependent partition function for a range of ion interaction potentials that have been used by the ion modeling community. There are two types of potentials: those that describe the electronic interaction and those that describe the ion interaction with the lattice atoms. The former is called the electronic potential and is typically described by the LSS or ZBL potential. The latter is called the nuclear potential - even though it has nothing to do with nuclear interactions - and the MARLOWE BCA code has implemented models with the Moliere, exponential, and Lenz-Jensen potential. After generating a range of possible partition functions, a statistical sampling process was again used to propagate this variation into a good characterization of the uncertainty in the neutron damage energy. Figure 6b shows a random sampling of the partition functions that arose from one approach that utilized Cholesky decomposition [15]. Figure 7 shows the result of one of several approaches to composing a covariance matrix for the partition function, sampling, and generating a covariance matrix for the neutron damage energy.

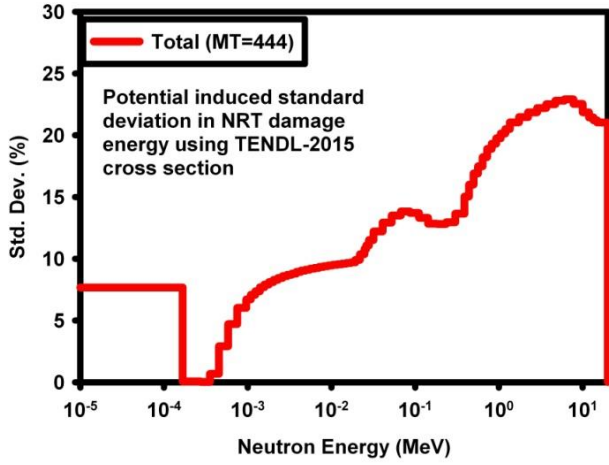


a) Influence of Partition Function on Damage Energy

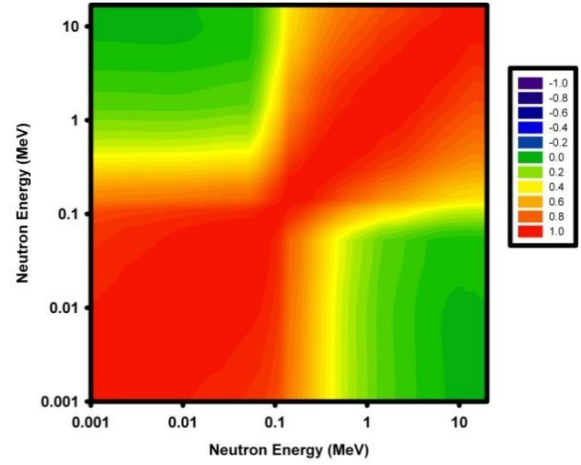


b) Random Samples of Partition Function

Fig. 6. Uncertainty Contributions from the Damage Partition Function.



c) Standard Deviation



d) Correlation Matrix

Fig. 7. Effect of the Partition Function on the Uncertainty in the Damage Energy.

c) Displacement Threshold Methodology

The next contribution to the uncertainty to consider is the treatment of the displacement threshold region. While the displacement kerma is basically the damage energy with a zero eV lower integration bound and a zero displacement threshold energy, the damage energy can be strongly affected by the choice of the displacement threshold energy and by the formalism for treating the effective damage near the threshold where actual displaced lattice atoms can be generated. The nominal/recommended displacement threshold energy in silicon is 20.5 eV [16]. However, there is significant uncertainty in the value for the displacement threshold energy. For silicon, the range found in both experimental investigation and in model-based calculation is between 10 eV and 30 eV [16].

Figure 8a shows that the difference between the various displacement model metrics is negligible except in a narrow neutron energy range between 100 eV and 1 keV. However, the effect can be large in this region, $\pm 50\%$. The difference between these damage energy metrics based on the displacement model in this neutron energy region is due to the fact that elastic scattering is the dominant reaction in this region and conservation of momentum and energy for each elastic interaction results in a maximum energy transfer to a lattice atom given by:

$$E_{recoil} = \frac{4 \cdot A \cdot E_n}{(A+1)^2} \quad , \quad (7)$$

where E_n is the energy of the incident neutron and A is the atomic weight of the lattice atom. The case where the lattice recoil energy in silicon from elastic scattering is equal to a displacement threshold energy of 20.5 eV corresponds to an incident neutron energy of ~ 153 eV. For lower neutron energies, the deviations are very small since the displacement kerma is dominated by the contributions from the (n,γ) reaction, which kinematically permits a larger recoil energy for the residual ion, so that the lower integration bound for the displacement threshold energy no longer plays an important role in the damage energy calculation.

Figure 8b shows the variation in the threshold-based damage energy, i.e. with E_d as the lower integration bound that can result from this range of possible values for the displacement threshold energy in silicon. This figure shows the percent difference relative to the nominal/recommended displacement threshold energy of 20.5 eV. The maximum deviation seen in Figure 8b between damage energies with different E_d values [relative to $E_d = 20.5$ eV] is seen to be about $\pm 80\%$ - but this is only significant over a small energy region.

In our work we have quantified the change in the damage energy when the displacement threshold energy is varied using a Total Monte Carlo approach to capture the nonlinear change in the damage energy. The energy-dependent standard deviation in the magnitude of the response is shown in Figure 9a. The energy-dependent correlation matrix is shown in Figure 9b.

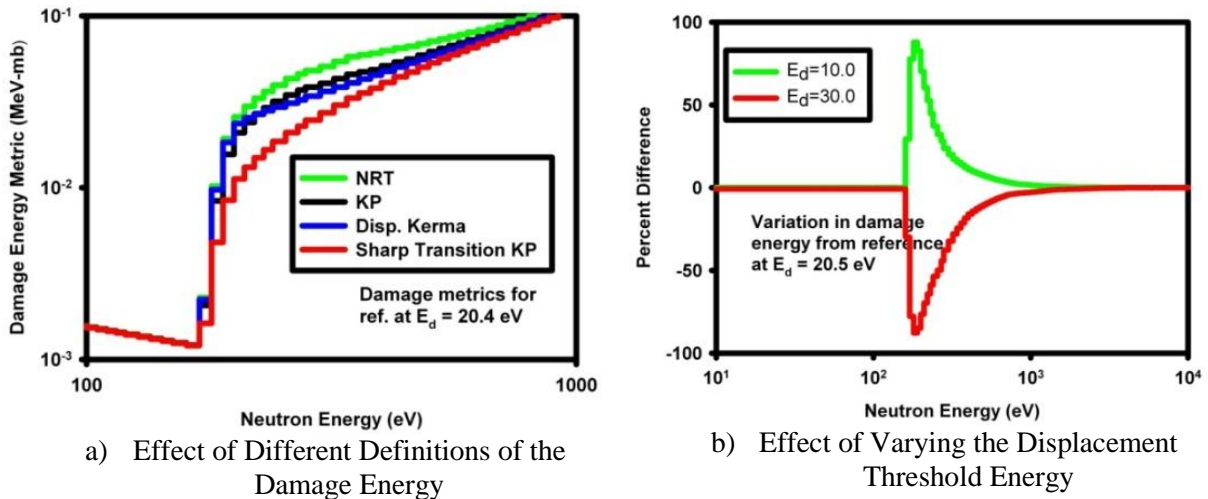


Fig. 8. Effect of the Treatment of the Threshold on the Damage Energy.

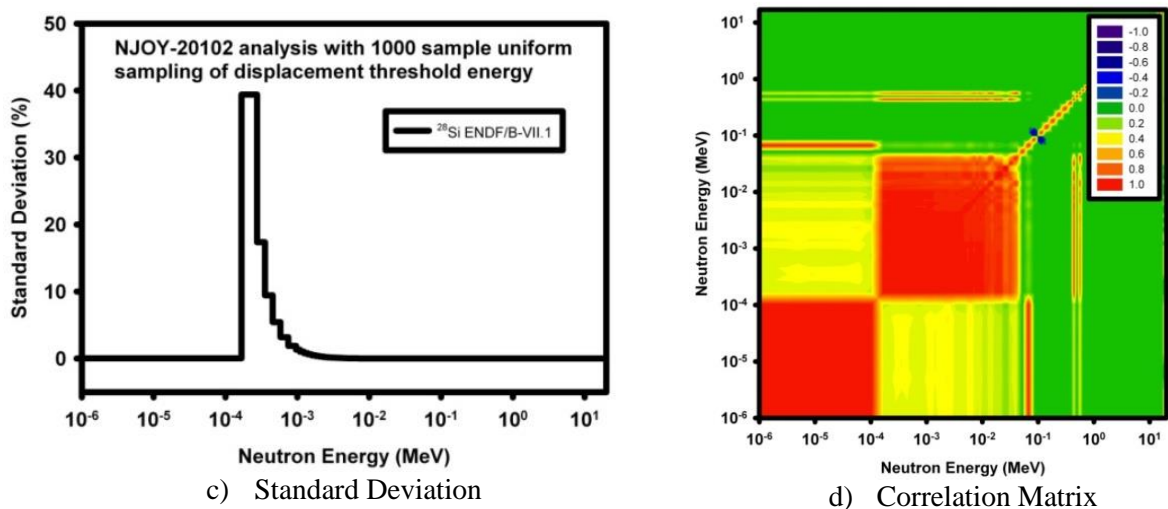


Fig. 9. Effect of the Threshold Function on the Uncertainty in the Damage Energy

d) Model Defect

The above sections dealt with all of the obvious contributions to the uncertainty in the damage energy. The purpose of “model defect” category is to address any uncertainty aspects that were not captured in the normal accessible parameter variation, i.e. a model attribute that did not have a user-accessible parameterized form. While we may not be able to statistically vary the “model defect” uncertainty contributions in order to characterize them, we should be able to use “subject matter expertise” to recognize the uncertainty contributions and propose, based on expert judgement, an energy-dependent term that provides for a conservative treatment of this potential uncertainty contribution.

The treatment of “model defect” is still a work in progress and will be addressed within the context of next year’s contributions to the CRP. Uncertainty contributions to “model defect” that should be considered for this application to gain degradation in silicon bipolar devices include:

- 1) Potential uncertainty in the underlying nuclear reaction models that cannot be captured with accessible nuclear reaction model parameter variation. A comparison of the TENDL-2015 random nuclear data files with other nuclear data files provides some indication that, while the variation in the elastic channel is adequately represented, the magnitude of the expected variation in recoil energy spectra from some of the non-threshold reaction contributions to damage energy may not be completely captured.
- 2) The may be differences in the energy-dependence of the calculated damage metric and the phenomena with which it is intended to be correlated. In particular, for silicon displacement damage, there is some experimental data that suggests that low energy neutron damage is much less than predicted with the calculated damage energy. This may be related to the fact that this damage metric was developed to correlate with the formation of primary Frenkel pair, whereas the actual change in minority carrier lifetime in silicon devices is caused by the more complex defect, i.e. divacancies and vacancy-phosphorous defects rather than the vacancy-oxygen defects that predominate from low damage energy induced point defects. The modelling of the efficiency with which Frenkel pair defects migrate and form complex defect with impurities and dopants is not captured in the currently modelled physics.
- 3) Experimental data in silicon indicate a good match between observed gain degradation and the displacement kerma for neutron energies between 100 keV and 14 MeV [17]. There is insufficient validation evidence for higher neutron energies. Since some other semiconductors, e.g. GaAs, indicate a thermal spike phenomenon at higher neutron energies [18], this thermal spike effect may exist in silicon at neutron energies above 20 MeV. An arc-dpa formalism [19] has a functional behaviour that could capture the recoil energy dependence of this effect if experimental evidence is gathered.

4 Conclusions

The above discussion has captured the recent work performed at Sandia National Laboratories in support of a better understanding of the uncertainties in radiation damage metrics. The work reported here focused on an examination of primary radiation damage in silicon semiconductor materials that affects the change in minority carrier lifetime, and, in particular, on properly expressing the relevant damage metric and then on quantifying the energy-dependent uncertainty of this metric in the form of a covariance matrix. Future work in this area will proceed under the auspices of the Primary Damage CRP. Work also needs to be done to expand this uncertainty analysis to address the uncertainty in the displacement damage in GaAs semiconductors, a case where there is a recoil energy dependence similar to what is captured in the arc-dpa metric, and to material embrittlement in iron used in light water reactor (LWR) pressure vessels.

References

1. ASTM E722-14, Standard Practice for Characterizing Neutron Fluence Spectra in Terms of an Equivalent Monoenergetic Neutron Fluence for Radiation-Hardness Testing of Electronics, ASTM International, West Conshohocken, PA, 2014.
2. ASTM E1855-10, Standard Test Method for Use of 2N2222A Silicon Bipolar Transistors as Neutron Spectrum Sensors and Displacement Damage Monitors, , ASTM International, West Conshohocken, PA, 2014.
3. Detailed Description of the Derivation of the Silicon Damage Response Function, P.J. Griffin, report SAND2016-2269 (rev. 1), Sandia National Laboratories, Albuquerque, NM, March, 2016.
4. G.H. Kinchin, R.S. Pease, "The Displacement of Atoms in Solids by Radiation", Reports on Progress in Physics, Vol. 18, 1955.
5. M.J. Norgett, M.T. Robinson, I.M. Torrens, "A Proposed Method of Calculating Displacement Dose Rates," Nuclear Engineering and Design, Vol. 33, pp. 50-54, 1975.
6. The NJOY Nuclear Data Processing System, Version, R.E. MacFarlane, D.M. Muir, R.M. Boicourt, A.C. Kahler, report LA-UR-12-27079, Los Alamos National Laboratory, Los Alamos, NM, Dec. 20, 2012.
7. J. Lindhard, M. Scharff, H. Schiott, "Range Concepts and Heavy Ion Ranges," Mat. Phys. Medd. Dan. Vld. Selsk, Vol. 33, pp. 1-40, 1963.
8. P. Sigmund, "A Note on Integral Equations of the Kinchin-Pease Type," Radiation Effects, Vol. 1, pp. 15-18, 1969.
9. A.J. Koning, D. Rochman, "Towards sustainable nuclear energy: Putting nuclear physics to work," *Annals of Nuclear Physics*, Volume 35, pp. 2024-2030, November 2008.
10. D. Rochman, A. Konig, S.C. van der Marck, A. Hogenbirk, D. van Veen, "Nuclear Data Uncertainty Propagation: Total Monte Carlo vs. Covariances," *Journal of Korean Physics*, Vol. 59, pp. 1236-1241, 2011.
11. M.T. Robinson, O.M. Torrens, "Computer Simulation of Atomic-Displacement Cascades in Solids in the Binary-Collision Approximation," *Physical Review B*, Vol. 9, pp. 5008-5024, June 1974.
12. A. Akkerman, J. Barak, "New Partition Factor Calculations for Evaluating the Damage of Low Energy Ions in Silicon," *IEEE Transactions on Nuclear Science*, Vol. 53, pp. 3667-3674, December 2006.
13. The Stopping and Range of Ions in Solids, J.F. Ziegler, J.P. Biersack and U. Littmark, Pergamon Press, Inc., New York, 1985.
14. M. T. Robinson: MARLOWE Binary Collision Cascade Simulation Program, Version 15b, A Guide for Users, December 5, 2002.
15. Numerical Linear Algebra for Applications in Statistics (Statistical Computing), J.E. Gentle, Springer-Verlag, Berlin, 1998.
16. Relationship between Metrics used to Represent Displacement Damage in Materials, P.J. Griffin, report SAND-2014-3341, Sandia National Laboratories, Albuquerque, NM, April, 2014.
17. J.G. Kelly, and P/J. Griffin, "Comparison of Measured Silicon Displacement Damage Ratios with ASTM E-722-87 and NJOY Calculated Damage," *Proceedings of the Seventh ASTM-EURATOM Symposium on Reactor Dosimetry*, Strasbourg, France, Aug. 1990, p. 711, Kluwer Academic Publishers, Boston, 1992.
18. P.J. Griffin, J.G. Kelly, T.F. Luera, A.L. Barry, and M.S. Lazo, "Neutron Damage Equivalence in GaAs," *IEEE Transactions on Nuclear Science*, NS-38, No. 6, 1991.
19. Primary radiation damage in materials - Review of Current Understanding and Proposed New Standard Displacement Damage Model to Incorporate In-Cascade Defect Production Efficiency and Mixing Effects, OECD/NEA Working Party on Multiscale Modelling of Fuels and Structural materials for Nuclear Systems, Expert Group on Primary Damage, NEA/NSC

Comparative study of Monte Carlo particle transport code PHITS and nuclear data processing code NJOY for PKA energy spectra and heating number under neutron irradiation,

Y. Iwamoto, T. Ogawa

Japan Atomic Energy Agency
Tokai, Ibaraki, Japan

1. Introduction

The modelling of the damage in materials irradiated by neutrons is needed for understanding the mechanism of radiation damage in fission and fusion reactor facilities. The molecular dynamics simulations of damage cascades with full atomic interactions require information about the energy distribution of the Primary Knock on Atoms (PKAs). The most common process to calculate PKA energy spectra under low-energy neutron irradiation is to use the nuclear data processing code NJOY2012 [1]. It calculates group-to-group recoil cross section matrices using nuclear data libraries in ENDF data format, which is energy and angular recoil distributions for many reactions. After the NJOY2012 process, SPKA6C [2] is employed to produce PKA energy spectra combining recoil cross section matrices with an incident neutron energy spectrum. However, intercomparison with different processes and nuclear data libraries has not been studied yet. Especially, the higher energy (~5 MeV) of the incident neutrons, compared to fission, leads to many reaction channels, which produces a complex distribution of PKAs in energy and type.

Recently, we have developed the event generator mode (EGM) [3,4] in the Particle and Heavy Ion Transport code System PHITS [5] for neutron incident reactions in the energy region below 20 MeV. The main feature of EGM is to produce PKA with keeping energy and momentum conservation in a reaction. It is used for event-by-event analysis in application fields such as soft error analysis in semiconductors, micro dosimetry in human body, and estimation of Displacement per Atoms (DPA) value in metals [6] and so on.

The purpose of this work is to specify differences of PKA spectra and heating number related with kerma between different calculation method using PHITS-EGM and NJOY2012+SPKA6C with different libraries TENDL-2015 [7], ENDF/B-VII.1 [8] and JENDL-4.0 [9] for fusion relevant materials.

2. PKA energy spectra calculated by PHITS-EGM with different libraries

The PHITS-EGM can calculate particle energy and emission angle with keeping energy and momentum conservation in event-by-event under low-energy neutron irradiation (< 20 MeV). **Figure 1** shows overview of PHITS-EGM. At first, reactions are sampled with Monte Carlo method from the reaction channel cross sections such as elastic, (n, γ), (n,n'), (n,2-4n), (n,p), (n,d), (n,t), (n, α), (n,np), (n,nd), (n,nt), (n,n α) in libraries with ACE format. The neutron incident reaction with the specific energy is sampled by the Monte Carlo method with the channel cross sections in the evaluated nuclear data library. When a neutron emission channel or elastic scattering is selected, the double differential cross sections of outgoing neutrons in the evaluated nuclear data library in ACE format are used to determine the energy, momentum and the scattering angle of emitted neutrons and momentum of recoils is determined accordingly. When the capture reaction or charged particle emission is selected, the excitation energy and momentum of residual nucleus are determined uniquely from the incident energy of neutron and target nucleus. For the decay process of this excited nuclei, the special statistical decay plus gamma de-excitation model, ENSDF [10] Based Isomeric Transition and isomEr production Model (EBITEM) [11], is applied to emit particles except for neutrons. Then all information of ejectiles such as charged particles, photon and residual nucleus can be determined. By these processes, a low energy neutron collision is treated as an "event", which means the energy and momentum are conserved in an event.

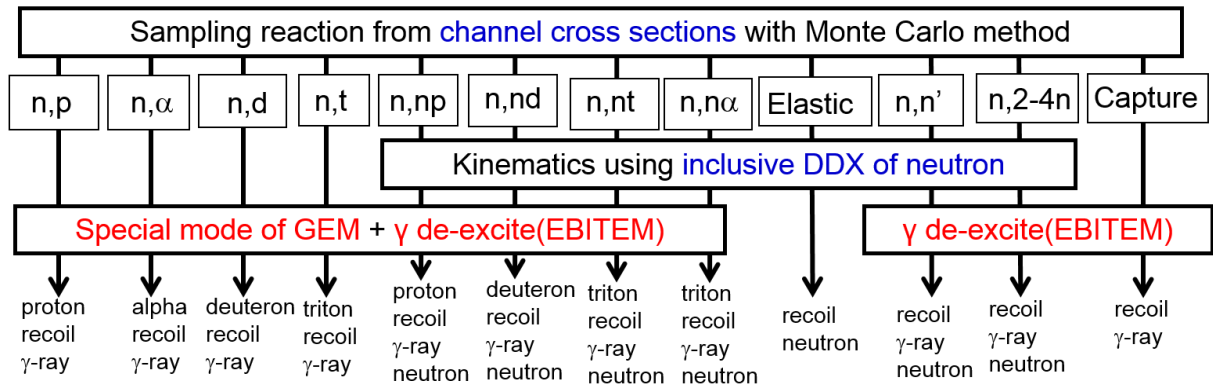


Fig. 1. Overview of the PHITS-EGM.

Table 1 indicates incident energies of neutrons and target elements related with fusion materials. Incident neutron energies are 5 and 14.5 MeV. The 22 target elements listed in the IAEA-CRP website (<https://www-nds.iaea.org/CRPdpa/>) were selected for this work. The PHITS-EGM used the reaction channel cross sections and double differential neutron production cross section of neutrons in nuclear data libraries such as TENDL-2015 in Ref. [7], ENDF/B-VII.1 in MCNP6, and JENDL-4.0 in PHITS2.82 with ACE format.

Table 1. Incident neutron energies and target materials in this study.

Neutron energy (MeV)	22 target elements
5.0, 14.5	^{56}Fe , ^{184}W , ^{28}Si , ^{58}Ni , ^{90}Zr , ^{12}C , ^{63}Cu , ^{55}Mn , ^9Be , ^{52}Cr , ^{27}Al , ^7Li , ^{208}Pb , ^{48}Ti , ^{16}O , ^{89}Y , ^{109}Ag , ^{106}Pd , ^{72}Ge , ^{69}Ga , ^{75}As , ^{238}U

Figures 2 shows total recoil spectra for interactions of neutrons with ^{63}Cu at the incident neutron energies of 5 and 14.5 MeV calculated by PHITS-EGM using TENDL-2015, ENDF/B-VII.1 and JENDL-4.0. Agreements between different libraries are good because the reaction channel cross sections in each library are almost same. The agreements are good for not only ^{63}Cu , but also other elements except for ^{55}Mn , ^{90}Zr and ^{184}W .

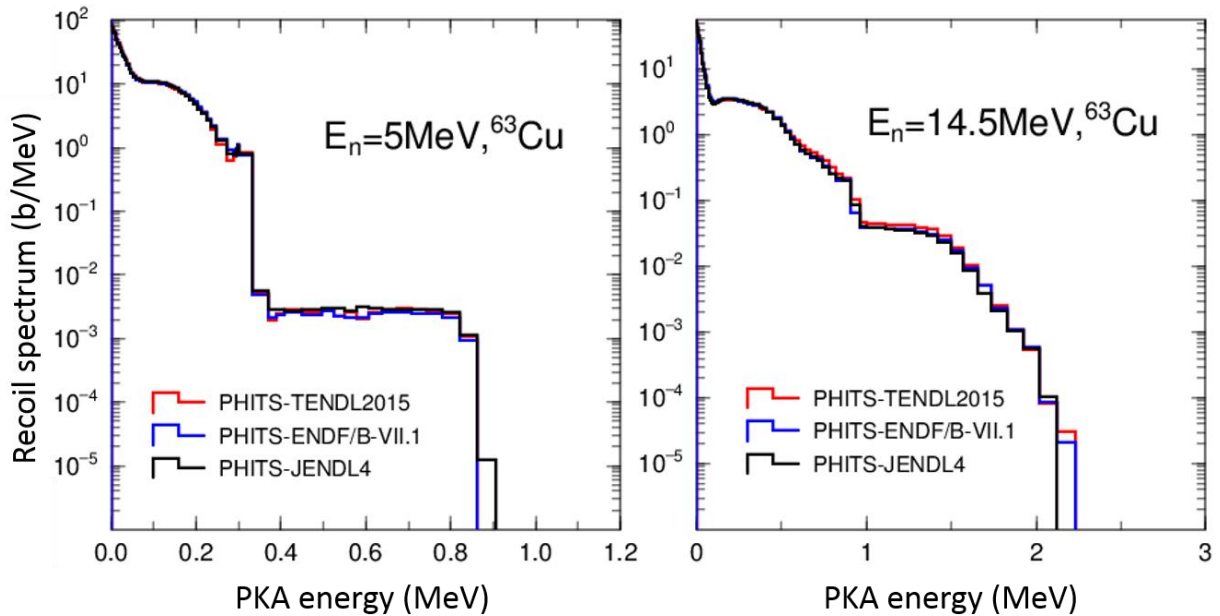


Fig. 2. Total recoil energy distributions for interactions of neutrons with ^{63}Cu at the incident neutron energies of 5 and 14.5 MeV calculated using PHITS-EGM with different libraries.

Figure 3 shows total recoil spectra for interactions of neutrons with ^{55}Mn , ^{90}Zr , ^{184}W at the incident neutron energies of 14.5 MeV. Whereas results for PHITS-TENDL2015 are almost same with those for PHITS-JENDL4, results for PHITS-ENDF/B-VII.1 are smaller than others in recoil produced by the (n, α) reaction. This discrepancy results from lack of the (n, α) cross section in ENDF/B-VII.1 at 14.5 MeV.

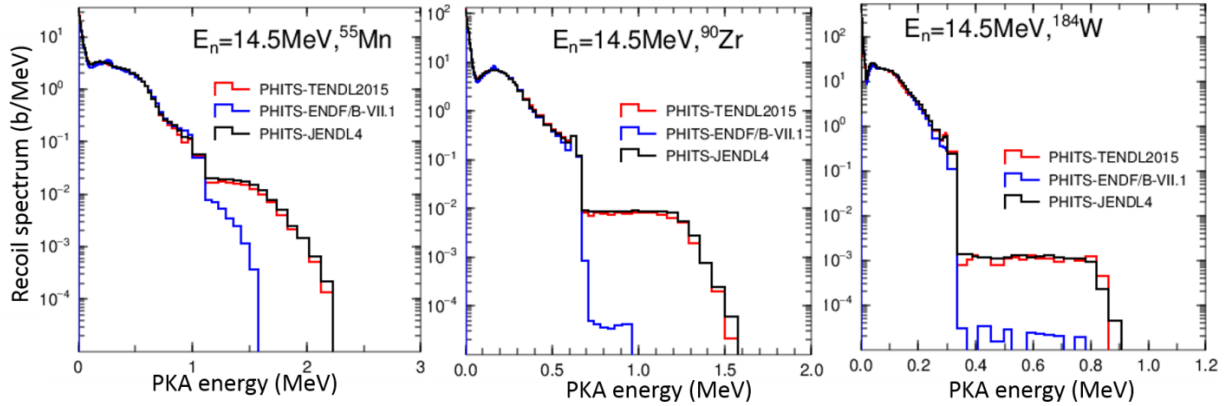


Fig. 3. Total recoil energy distributions for interactions of neutrons with ^{55}Mn , ^{90}Zr , ^{184}W at the incident neutron energies of 14.5 MeV calculated using PHITS-EGM with different libraries.

3. PKA spectra extracted from major libraries using NJOY2012-SPKA6C and comparison with PHITS-EGM-TENDL2015 results

Figure 4 shows total recoil spectra for interactions of neutrons with ^{28}Si and ^{56}Fe at the incident neutron energies of 5 and 14.5 MeV calculated by PHITS-EGM-TENDL2015 and extracted from different libraries such as TENDL-2015, ENDF/B-VII.1 and JEFF-3.2 [11] using NJOY2012+SPKA6C. JENDL-4.0 was not used for the NJOY2012+SPKA6C extraction due to lack of data libraries for energy and angular recoil distributions for many reactions. In general, agreements of PKA spectra between PHITS-EGM-TENDL2015 (red solid line) and NJOY2012+SPKA6C (other dashed lines) are good. It indicates that physics processes in PHITS-EGM are similar with the evaluation method of energy and angular recoil distributions in nuclear data libraries. Good agreements of PHITS-EGM and NJOY2012+SPKA6C were observed for ^{56}Fe , ^{184}W , ^{28}Si , ^{58}Ni , ^{90}Zr , ^{63}Cu , ^{55}Mn , ^{52}Cr , ^{27}Al , ^{208}Pb , ^{48}Ti , ^{16}O , ^{89}Y , ^{109}Ag , ^{106}Pd , ^{72}Ge , ^{69}Ga , ^{75}As and ^{238}U in TENDL-2015, ^{56}Fe , ^{28}Si , ^{58}Ni , ^{63}Cu , ^{52}Cr , ^{27}Al , ^{208}Pb , ^{16}O , ^{106}Pd , ^{238}U in ENDF/B-VII.1, and ^{56}Fe , ^{28}Si , ^{58}Ni , ^{63}Cu , ^{52}Cr , ^{27}Al , ^{16}O in JEFF3.2. The small difference of PKA spectra extracted by NJOY2012+SPKA6C between different libraries results from the difference of energy and angular recoil distributions of the (n, α) reaction in nuclear data libraries.

Figure 5 shows total recoil spectra for interactions of neutrons with ^{72}Ge and ^{90}Zr at the incident neutron energies of 5 and 14.5 MeV calculated by PHITS-EGM-TENDL2015 and extracted from different libraries such as TENDL-2015, ENDF/B-VII.1 and JEFF-3.2 (^{90}Zr only) using NJOY2012+SPKA6C. Agreements between PHITS-EGM-TENDL2015 (red solid line) and TENDL-2015 using NJOY2012+SPKA6C (red dashed line) are good for ^{72}Ge and ^{90}Zr .

On the other hands, the shape of PKA spectra extracted using NJOY2012 is strange for ^{72}Ge in ENDF/B-VII.1 and ^{90}Zr in JEFF3.2. It means that energy and angular recoil distributions are not included in libraries correctly. Similar results were obtained for ^{75}As , ^{89}Y and ^{109}Ag in ENDF/B-VII.1 and for ^{55}Mn in JEFF-3.2.

For ^{90}Zr , PKA spectra obtained with NJOY2012+SPKA6C using ENDF/B-VII.1 (blue dashed line) are smaller than others due to lack of energy and angular recoil distributions of inelastic reactions such as (n,n') and (n, α). Same trends were observed for ^7Li , ^9Be , ^{nat}C , ^{48}Ti , ^{55}Mn , ^{69}Ga and ^{184}W in ENDF/B-VII.1, for ^7Li , ^9Be , ^{nat}C , and ^{184}W in JEFF-3.2 and for ^7Li , ^9Be in TENDL-2015.

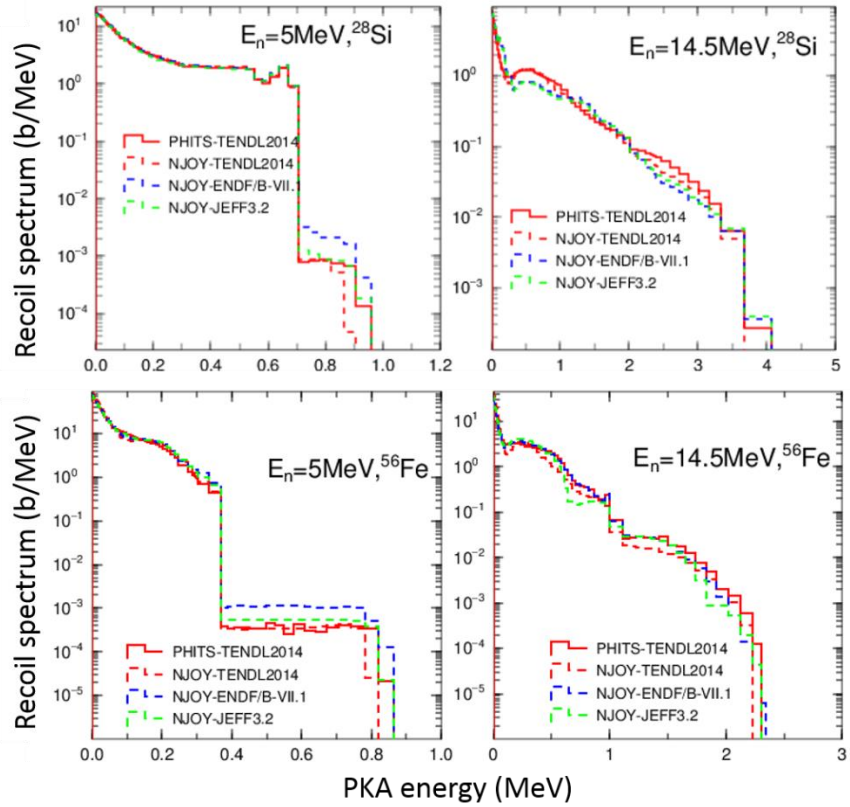


Fig. 4. Total recoil energy distributions for interactions of neutrons with ^{28}Si and ^{56}Fe at the incident neutron energies of 5 and 14.5 MeV calculated by PHITS-EGM-TENDL2015 and NJOY2012 with different libraries.

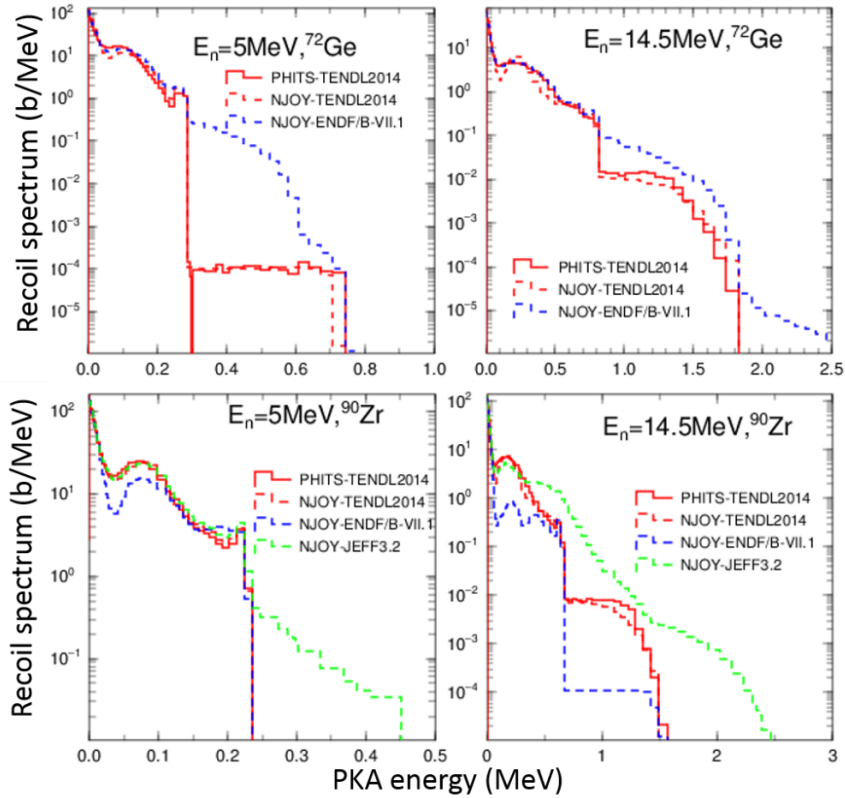


Fig. 5. Total recoil energy distributions for interactions of neutrons with ^{72}Ge and ^{90}Zr at the incident neutron energies of 5 and 14.5 MeV calculated by PHITS-EGM-TENDL2015 and NJOY2012 with different libraries.

4. Heating number calculated by PHITS-EGM with different libraries

PHITS-EGM can calculate heating number summed with kinetic energies of secondary charged particles produced by physics models as shown in **Fig. 1**. Neutron heating numbers were calculated by PHITS-EGM with TENDL-2015 listed in Ref. [7], ENDF/B-VII.1 in MCNP6 and JENDL-4.0 in PHITS2.82 to investigate dependency of nuclear data libraries to heating number. **Table 2** shows incident neutron energy range and target elements for calculations.

Table 2. Incident neutron energy range and target materials in this study.

Neutron energy (MeV)	5 target elements
10^{-11} - 20	^{56}Fe , ^{63}Cu , ^{184}W , ^{28}Si , $^{\text{nat}}\text{C}$

Figures 6 and 7 show neutron heating numbers calculated by PHITS-EGM with different libraries in ACE formats for ^{56}Fe , ^{63}Cu , ^{184}W and ^{28}Si . In the energy region below 5 MeV, agreements of heating number between different libraries are good because channel cross sections such as elastic scattering and capture are almost same within different libraries. On the other hands, differences of heating number are observed in high energy region over 5 MeV due to difference of inelastic channel cross sections such as (n,n') , (n,np) , (n,p) , (n,α) in different libraries.

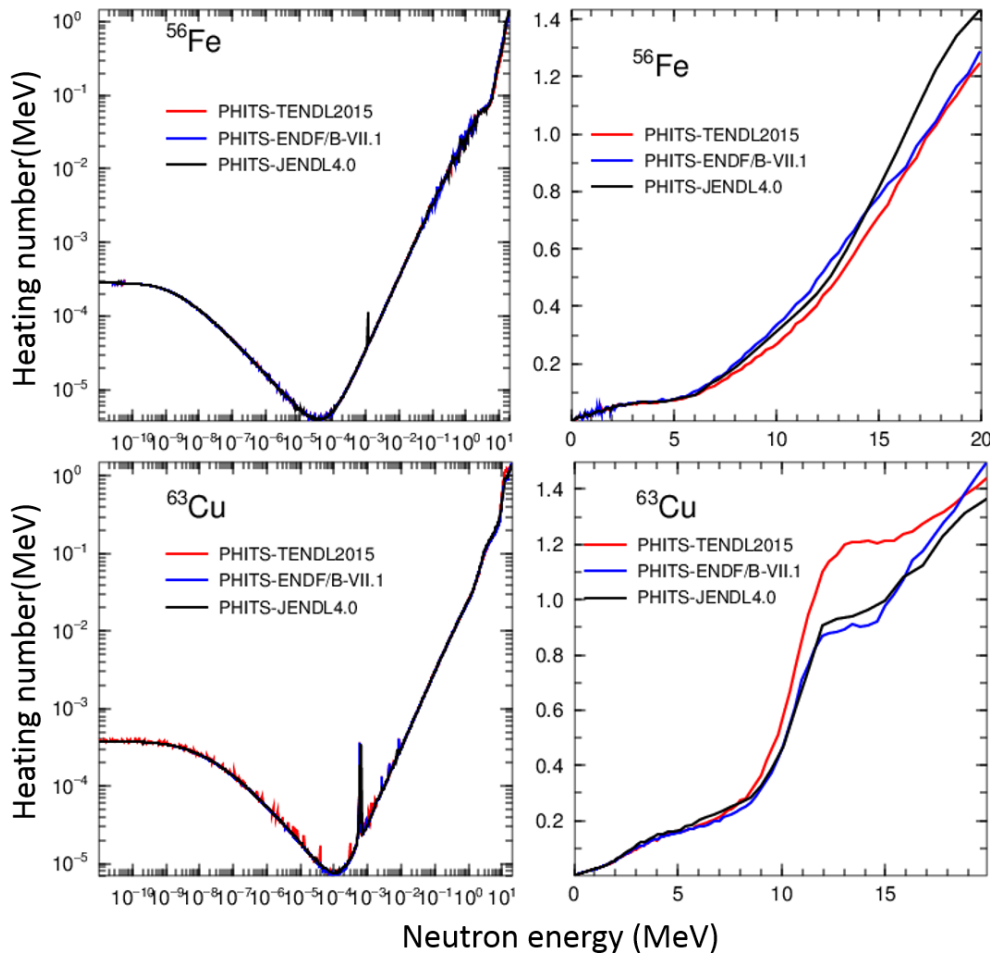


Fig. 6. Neutron heating number calculated by PHITS-EGM with different libraries in ACE formats for interactions of neutrons with ^{56}Fe and ^{63}Cu . Left side is log scale and right side is linear scale.

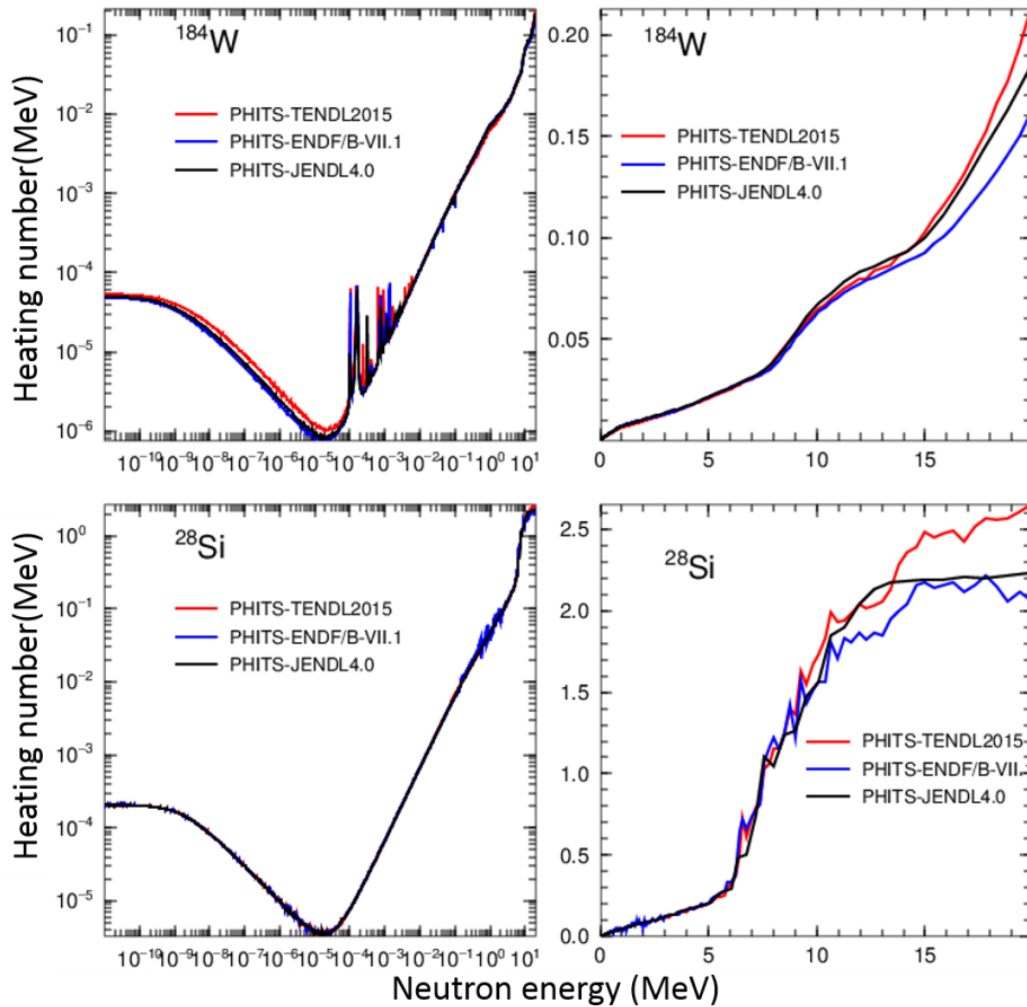


Fig. 7. Neutron heating number calculated by PHITS-EGM with different libraries in ACE formats for interactions of neutrons with ^{184}W and ^{28}Si . Left side is log scale and right side is linear scale.

5. Heating number extracted from major libraries in ACE format and comparison with PHITS-EGM-TENDL2015 results

Figures 8 and 9 show neutron heating numbers extracted from TENDL-2015, ENDF/B-VII.1 and JENDL-4.0 in ACE formats for ^{56}Fe , ^{63}Cu , ^{184}W and ^{28}Si . For ^{56}Fe and ^{63}Cu in Fig. 8, results calculated with PHITS-EGM-TENDL-2015 give good agreements with data extracted from ENDF/B-VII.1 and JENDL-4.0 in ACE format in energy region below 5 MeV. For ^{28}Si in Fig. 9, results calculated with PHITS-EGM-TENDL-2015 also give good agreements with data extracted from ENDF/B-VII.1 below 5 MeV. The other data extracted from libraries are smaller than results calculated by PHITS-EGM in neutron capture region (n,γ) below 10 eV. In particular, data extracted from TENDL2-015 are smaller than others for all elements. Heating numbers extracted ACE libraries were provided by the NJOY-HEATR process with nuclear data libraries [1]. It is known that the TENDL continuum gamma spectrum for the (n,γ) reaction has a very different average gamma energy – and results in a very different kerma due to how NJOY-HEATR treats the recoil for this reaction [12].

On the other hands, PHITS-EGM can calculate PKA and gamma energy spectra based on the EBITEM [4] in neutron capture region. In the model, reaction products after nucleon evaporation were de-excited by using theoretical calculations if the excitation energy was higher than 3000 keV and the mass number was greater than 40 amu. Otherwise, the nuclei were de-excited based on the scheme provided in the ENSDF [10]. The (n,γ) capture gammas are well represented by the prompt-gamma activation analysis (PGAA) library that is implemented within EBITEM.

Figure 10 shows the PKA and gamma energy spectra calculated by PHITS-EGM-TENDL2015 for ^{184}W at incident neutron energy range from 0.1 to 0.414 eV. PKA spectrum of ^{184}W results from elastic scattering and that of ^{185}W is recoil produced by gamma emissions based on EBITEM via de-excitation process after neutron capture reaction. Finally, heating number is obtained by sum of kinetic energies of ^{184}W and ^{185}W . The difference of heating number between PHITS-EGM and data extracted from ENDF/B-VII.1 and JENDL-4.0 in ACE format may come from data of gamma energy in data files. Further comparison about gamma emission will be needed in the next CRP task.

In high energy region above about 5 MeV, the small difference of heating number between PHITS-EGM-TENDL2015 (red solid line) and data extracted from TENDL-2015 in ACE file (red dashed line) is observed. It comes from the charged particle emission process via evaporation in PHITS-EGM. In PHITS-EGM calculations, although charged particles are emitted based on the channel cross sections in nuclear data libraries such as (n,p), (n,d), and (n, α), shapes of energy distributions of charged particles are determined by the evaporation models. Therefore, sum of kinetic energies of secondary charged particles may differ from heating number in the ACE files which determined by the different method, the energy balance method [1].

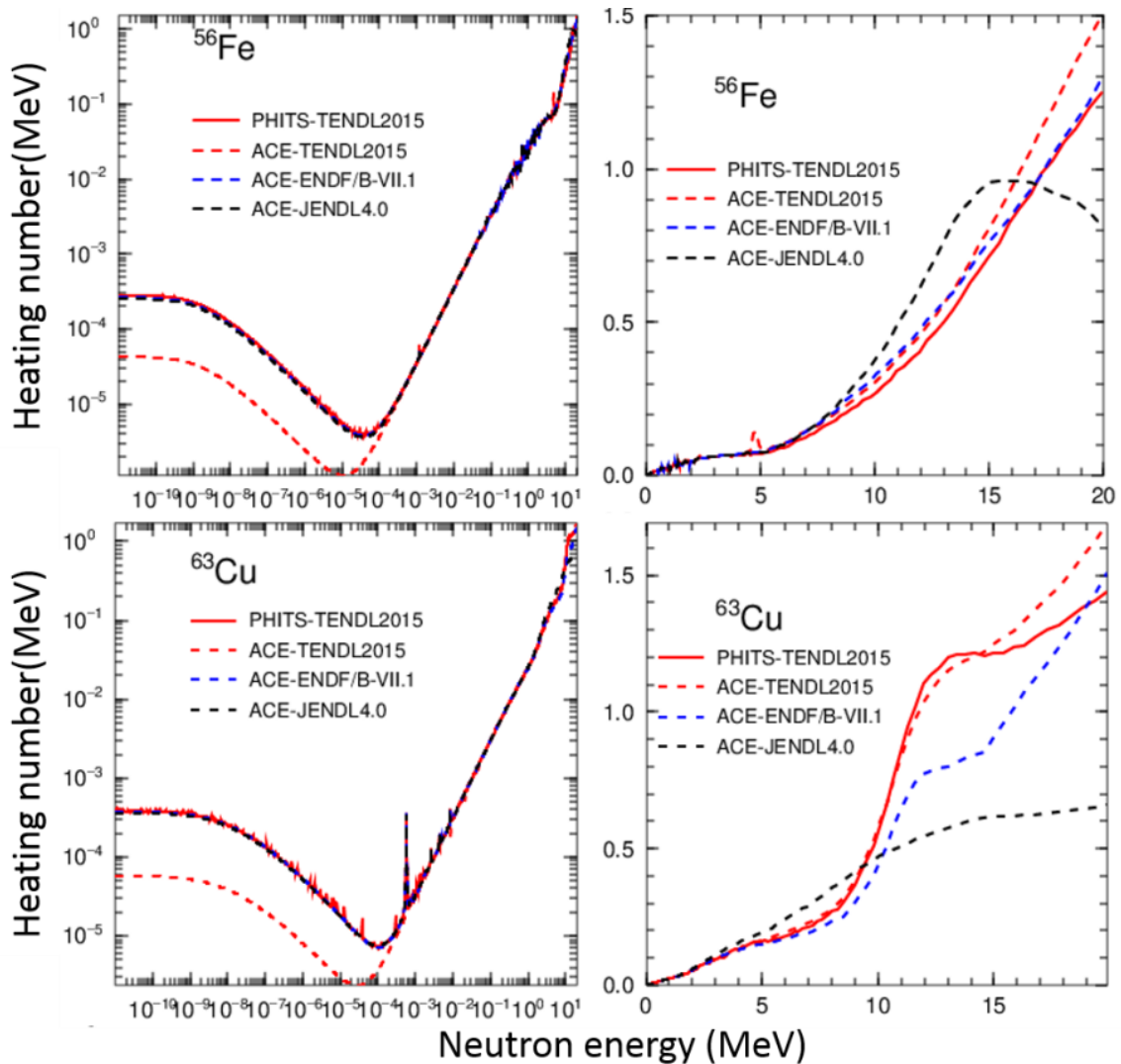


Fig. 8. Neutron heating numbers extracted from TENDL-2015, ENDF/B-VII.1 and JENDL-4.0 in ACE format and calculated by PHITS-EGM-TENDL2015 for ^{56}Fe and ^{63}Cu . Left side is log scale and right side is linear scale.

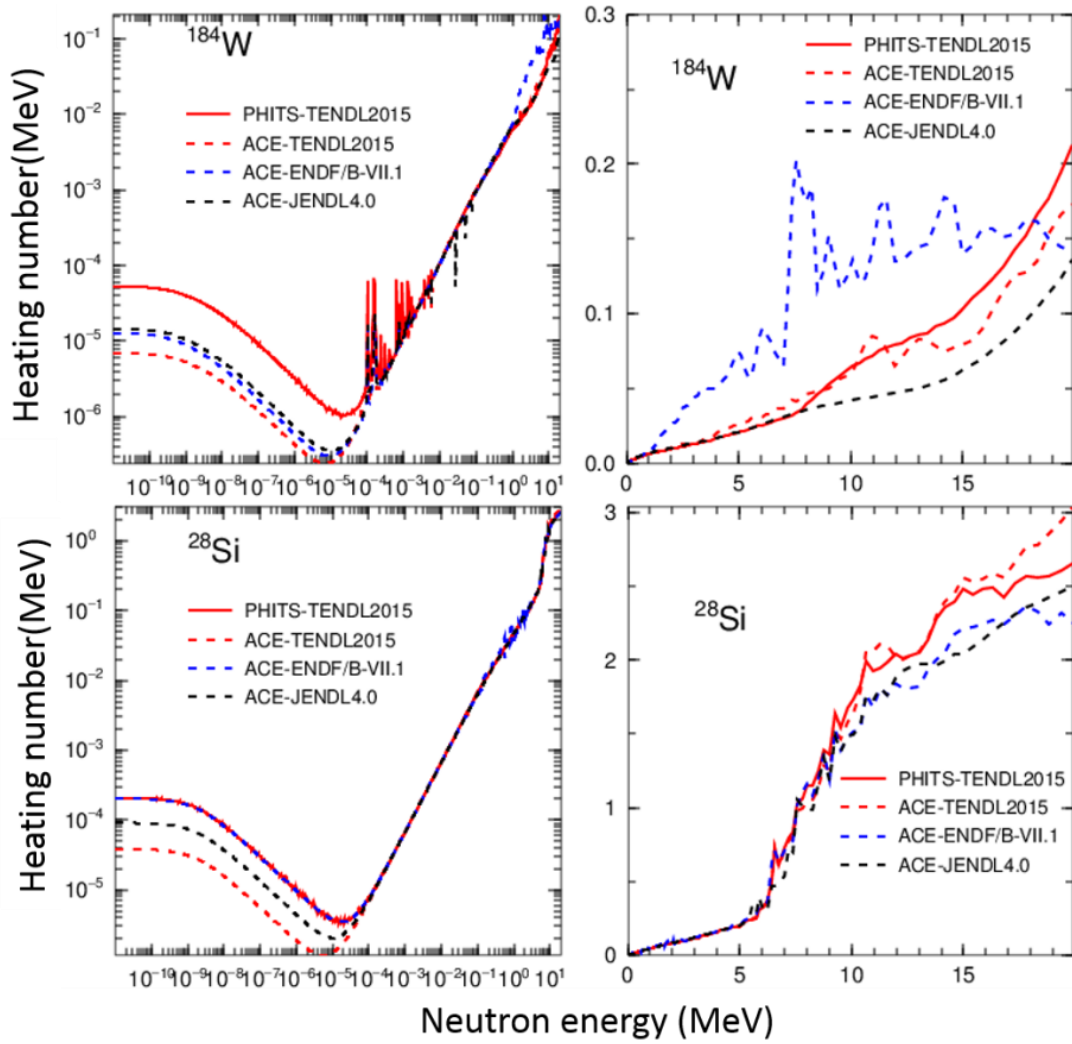


Fig. 9. Neutron heating number calculated by PHITS-EGM with different libraries in ACE formats for interactions of neutrons with ^{184}W and ^{28}Si . Left side is log scale and right side is linear scale.

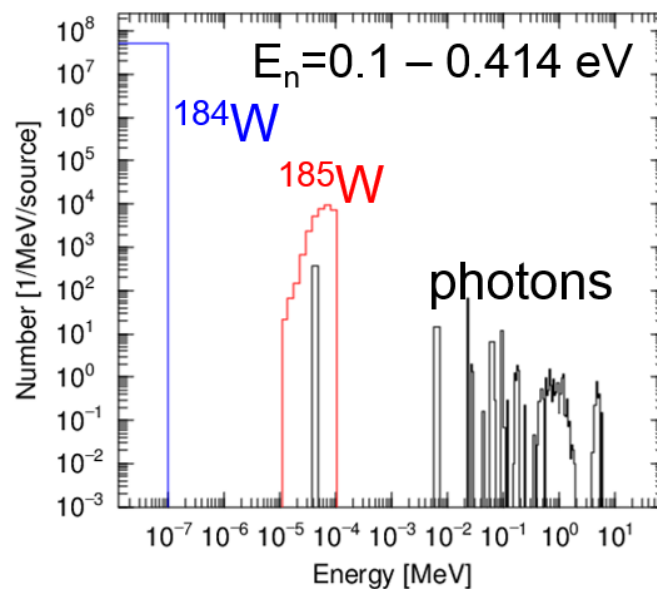


Fig. 10. PKA and gamma energy spectra calculated by PHITS-EGM-TENDL2015 for ^{184}W at incident neutron energies from 0.1 to 0.414 eV.

6. Summary and IAEA-CRP work plan 2016-2017

Energy spectra of PKA were calculated for fission and fusion relevant materials using PHITS-EGM and NJOY2012-SPKA6C with TENDL-2015, ENDF/B-VII.1 and JEFF3.2. Heating numbers were also calculated using PHITS-EGM and compared with data extracted from the ACE files of TENDL2015, ENDF/BVII.1 and JENDL4.0. In general, the difference of PKA spectra between PHITS-EGM-TENDL2015 and NJOY-SPKA6C-TENDL2015 was small. For analysis of PKA spectra extracted from NJOY2012+SPKA6C, we found that energy and angular recoil distributions were not included in libraries correctly for ^{72}Ge , ^{75}As , ^{89}Y and ^{109}Ag in ENDF/B-VII.1 and ^{90}Zr and ^{55}Mn in JEFF3.2. For analysis of heating number, we indicated that data extracted from ACE file of TENDL2015 for all elements in neutron capture region have problems due to incorrect data of secondary gamma energy. Supplementary data related to this report can be found at https://www-nds.iaea.org/CRPdpa/Iwamoto_comp-PKA-NJOY.pdf.

For the verification of NJOY processing code, PHITS-EGM was recognized as a useful verification path to PKA energy spectra and heating numbers in this TM. During next two years, we have plans to calculate PKA spectra, heating number, gas production cross sections and displacement cross sections for structural materials using PHITS-EGM, find the difference of results among methods and point out the problem. Development of a reaction ejectile sampling algorithm to recover kinematic correlations from inclusive cross-section data in Monte-Carlo particle transport simulations

References

- [1] R.E. MacFarlane, D.W. Muir, R.M. Boicourt, A.C. Kahler, The NJOY Nuclear data processing system, Los Alamos National Laboratory Report LA-UR-12-27079.
- [2] S.P. Simakov, SPKA code, FZK, 2007. Available from <https://www-nds.iaea.org/CRPdpa/>.
- [3] K. Niita, Y. Iwamoto, T. Sato, H. Iwase, N. Matsuda, Y. Sakamoto, H. Nakashima, A new treatment of radiation behaviour beyond one-body observables, in: International Conference on Nuclear Data for Science and Technology, ND2007, 2008, pp. 1167-1169.
- [4] T. Ogawa, T. Sato, S. Hashimoto, K. Niita, Development of a reaction ejectile sampling algorithm to recover kinematic correlations from inclusive cross-section data in Monte-Carlo particle transport simulations, Nucl. Instrum. Meth. A 763 (2014) 575-590.
- [5] T. Sato et al., Particle and heavy ion transport code system PHITS, version 2.52, J. Nucl. Sci. Technol. 50 (2013) 913-923.
- [6] Y. Iwamoto, K. Niita, T. Sawai, R.M. Ronningen, T. Baumann, Improvement of radiation damage calculation in PHITS and tests for copper and tungsten irradiated with protons and heavy-ions over a wide energy range, Nucl. Instrum. Meth. B 274 (2012) 57-64.
- [7] A.J. Koning, D. Rochman, J. Kopecky, et al., TENDL-2015: TALYS-based evaluated nuclear data library, https://tendl.web.psi.ch/tendl_2015/tendl2015.html .
- [8] M.B. Chadwick, M. Herman, P. Obložinský, et al., ENDF/B-VII.1: Nuclear Data for Science and Technology: Cross Sections, Covariances, Fission Product Yields and Decay Data, Nucl. Data Sheets 112 (2011) 2887 – 2996.
- [9] K. Shibata, O. Iwamoto, T. Nakagawa, et al., JENDL-4.0: A New Library for Nuclear Science and Engineering, J. Nucl. Sci. Technol. 48, (2011) 1-30.
- [10] Jagdish K. Tuli, Evaluated Nuclear Structure Data File, BNL-NCS, 51655-01/02-Rev, 2001.
- [11] T. Ogawa, S. Hashimoto, T. Sato, K. Niita, Development of gamma de-excitation model for prediction of prompt gamma-rays and isomer production based on energy-dependent level structure treatment, Nucl. Instrum. Meth. B 325 (2014) 35-42.
- [12] JEFF-3.2 evaluated data library - Neutron data, Available from https://www.oecd-neo.org/dbforms/data/eva/evatapes/jeff_32/.

Scoping of material damage with FISPACT-II and different nuclear data libraries: transmutation, activation, and PKAs, M.R. Gilbert and J.-Ch. Sublet

United Kingdom Atomic Energy Authority, Culham Science Centre, Abingdon, Oxfordshire, UK

The uncertainty associated with nuclear data, and the simulated predictions of transmutation, activation, and primary damage events derived from them, is not only that derived based on the quantified errors in a particular nuclear library. Uncertainty also manifests in comparisons between different libraries – if they do not produce the same results, then, since it is often impossible to know *a priori* which library is best, predicted results must be considered to have an uncertainty (at least) as much as the variation between libraries. Of course, this situation is further complicated by the fact that it is not always possible, or practical, to produce results with multi-libraries. There is thus a need, within the nuclear data community, to assess different libraries, and make recommendations about the best choice of library for particular applications, in this case material science.

The United Kingdom Atomic Energy Authority's contribution to the technical meeting on nuclear data and uncertainty quantification aimed to address this issue by making use of our advanced, modern, and flexible inventory simulation platform – FISPACT-II [1]. In particular, FISPACT-II is particularly suited to performing scoping calculations – covering multiple materials with multiple irradiation scenarios – enabling comparisons of activation, transmutation, and primary damage responses for different nuclear data libraries.

Our approach has been to perform an identical set of calculations – covering all naturally occurring elements from hydrogen to bismuth (by mass) – under fusion and typical fission irradiation conditions for the main international libraries that claim to be general purpose. The libraries considered, in identical fine 660-energy-group ENDF6 format, were:

- TENDL-2014 (calculations will be repeated for TENDL-2015 at a later date) [2];
- ENDF/B-VII.1 [3];
- JEFF-3.2 [4];
- JENDL-4.0 [5].

Activation response

We performed simulations of 2 full-power-year (fpy) irradiations of pure elements under DEMO first wall (FW), PWR, FBR, and HFR conditions, followed by years of cooling. Generally, good, order-of-magnitude agreement was observed for most elements between the four libraries. However, some notable differences were observed:

- In aluminium (see figure 1.), where JEFF-3.2 was found to under-predict (relative to the other libraries) the production of ^{26}Al via the (n,2n) reaction on ^{27}Al . At the same time, the JENDL-4.0 library used by FISPACT-II was found to be missing the key tritium production channels;
- In niobium (figure 2.), where only TENDL accounts for the necessary isomers and associated reaction channels to correctly predict the short-term activity associated with $^{92\text{m}}\text{Nb}$ and $^{94\text{m}}\text{Nb}$. This discrepancy (in the other libraries) has also been confirmed by experimental validation [6];
- Significant differences were also observed for Mo, Re, Os, Pb, Si, and Na.

As expected, the activation under fusion DEMO conditions was generally higher than for identical irradiation times under typical fission conditions (although there were some exceptions – for example, in Co and Ta).

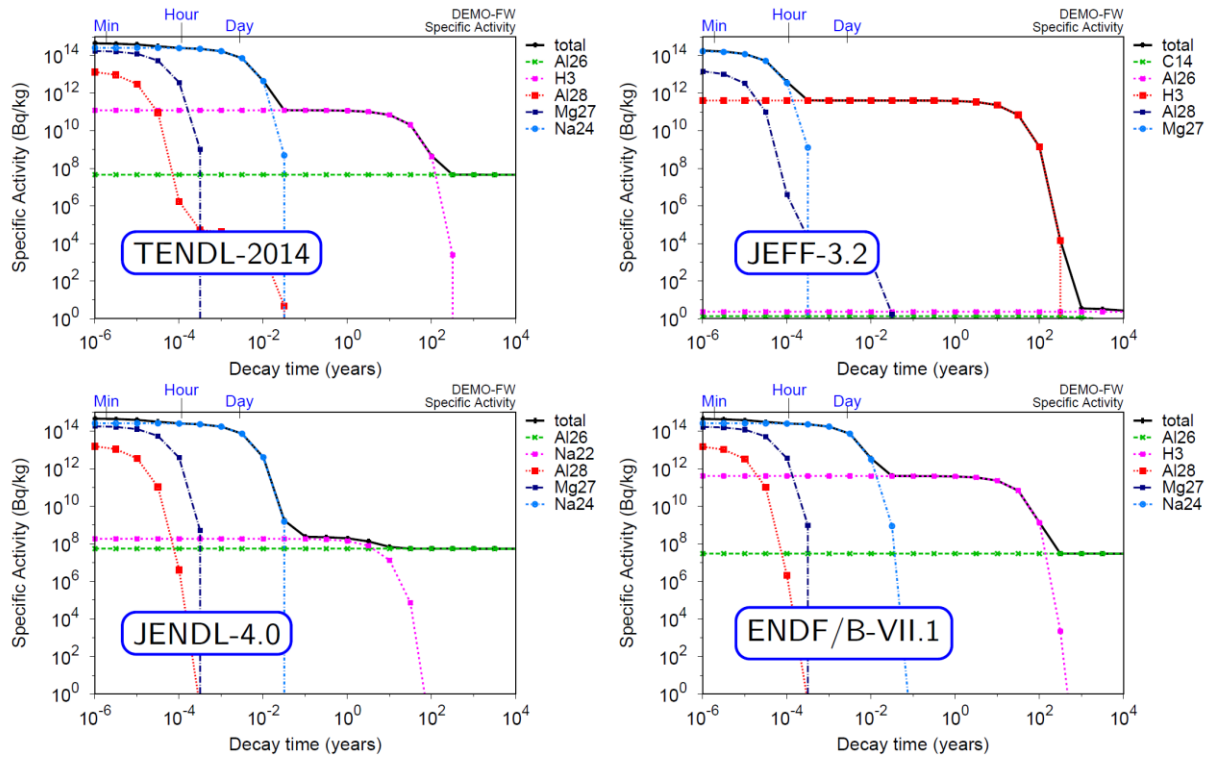


Fig. 1. Activation response of Al following a 2-fpy irradiation under DEMO-FW conditions with different nuclear data libraries. The missing ^3H production with JENDL-4.0, and under-prediction of ^{26}Al with JEFF-3.2 can be easily identified in these radionuclide contribution plots.

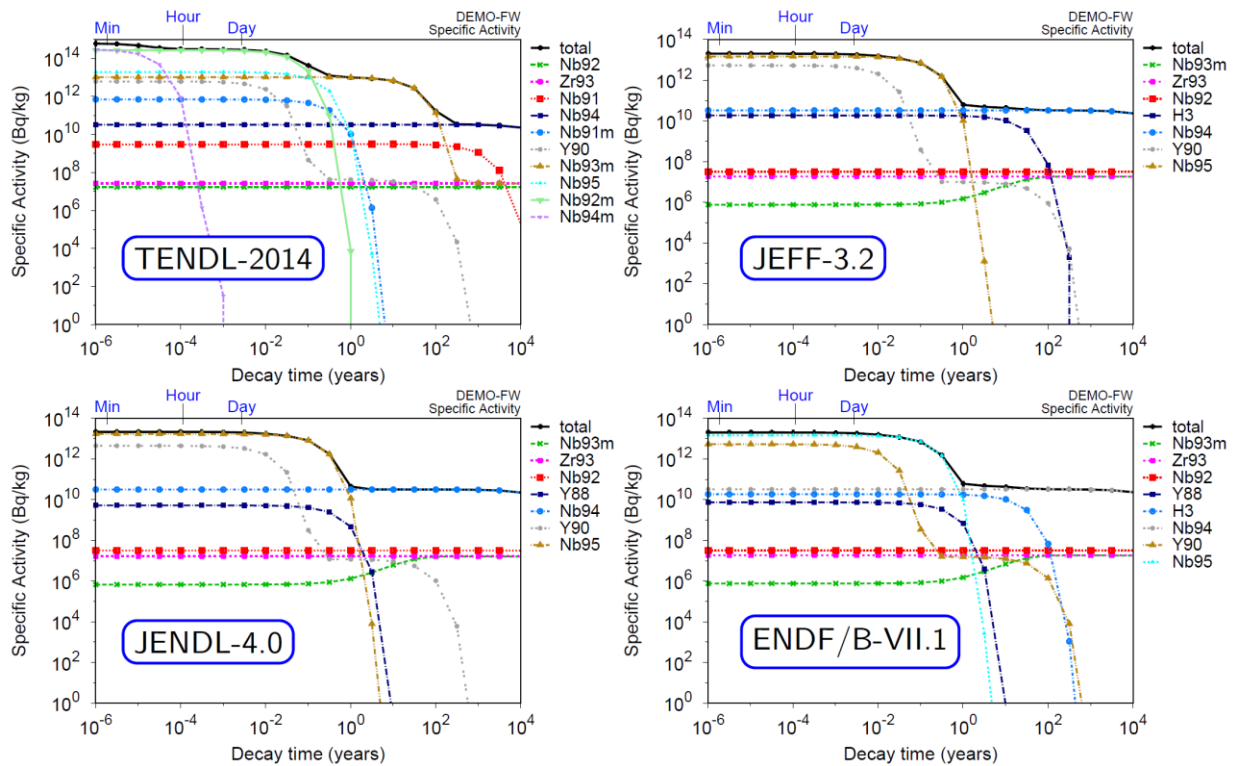


Fig. 2. Activation response of pure Nb following a 2 fpy irradiation under DEMO-FW conditions with different nuclear data libraries. The missing short-lived isomers ($^{92\text{m}}\text{Nb}$ and $^{94\text{m}}\text{Nb}$) with all libraries except TENDL, result in an under-prediction in activity at decay times of less than 1 year.

Transmutation

The transmutation of pure elements was found to be consistent with different libraries in most cases. For example, the % burn-up (the amount of the original element that is transformed/transmuted into a different element) per fpy under DEMO conditions for various nuclear relevant elements is shown in figure 3 and confirms order-of-magnitude agreement for the majority of elements. However, in agreement with the activation results, and demonstrating the importance of correct isomer coverage, for Nb there is significant disagreement, with TENDL predicting nearly a factor of 10 higher burn-up than the other libraries. There are also notable differences for C, Na, Bi, and Re, where in the latter case JENDL-4.0 has a significant problem with Re.

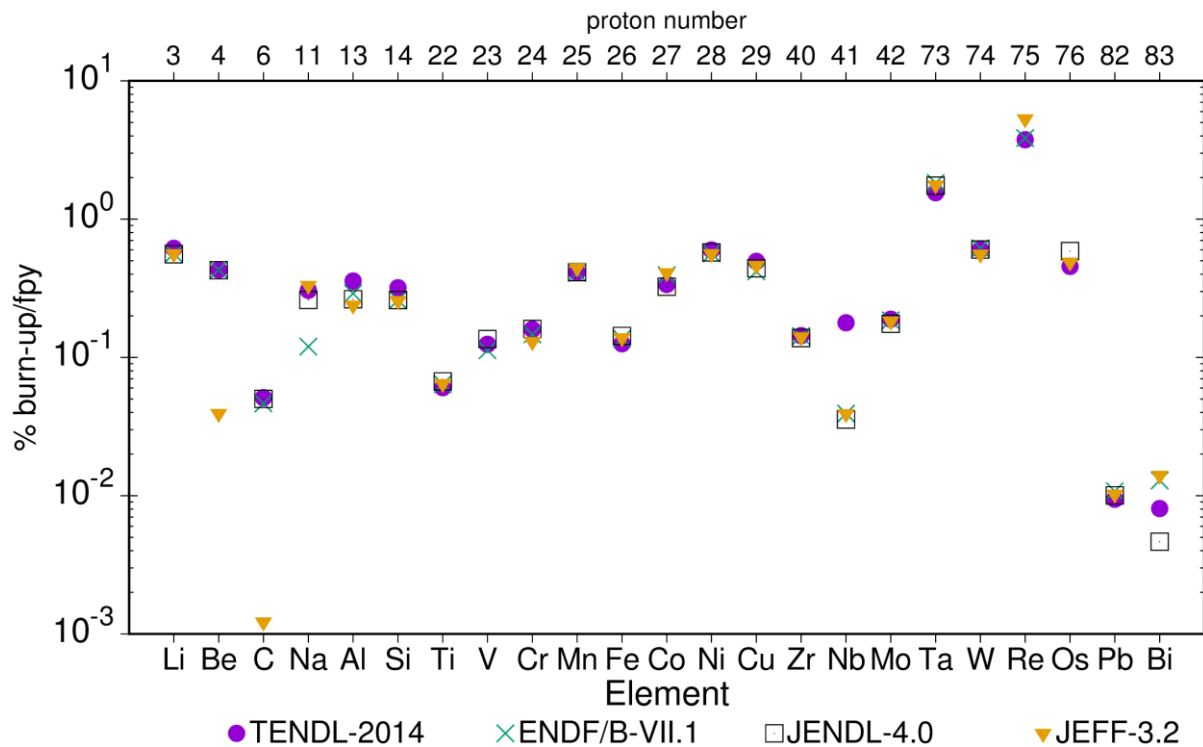


Fig. 3. % burn-up (transmutation) of pure elements in 1 fpy under DEMO conditions with different nuclear libraries.

The scoping studies also revealed that the HFR experimental reactor produces significantly higher transmutation rates than other scenarios due to its high fraction of thermal neutrons, which promotes neutron-capture-followed-by-decay chains to new elements. Conversely, DEMO-FW conditions lead to much higher (often several orders-of-magnitude in important elements) gas production rates (even when scaled by dpa rates) than any of the considered fission scenarios.

PKA spectra

The newly written SPECTRA-PKA code [7], whose computational methodology is explained in figure 4, has been used to evaluate the zero time (BOL Beginning-of-Life) snapshot of the PKA-rate energy-distributions for pure elements using the isotopic recoil matrices produced by NJOY [8] from the different nuclear data libraries.

In contrast to the transmutation-rate results, where HFR was the highest, it was found instead that the fast breeder reactor (FBR) conditions produced the highest PKA rates (with fusion DEMO second). As with the activation and transmutation results, there was generally a good order-of-magnitude agreement in the total PKA rates (summed over all heavy recoils, but excluding gas particles) between results with different libraries – see for example, figure 5, which shows the total PKA rates for nuclear relevant materials under DEMO FW conditions and for four different libraries. Some of the same discrepant materials (e.g. Re) are evident, but others, such as Nb, show much better agreement

between libraries than for the activation or transmutation results, demonstrating the dominance of the scattering channels for the PKA response, which are obviously well-known and reliable.

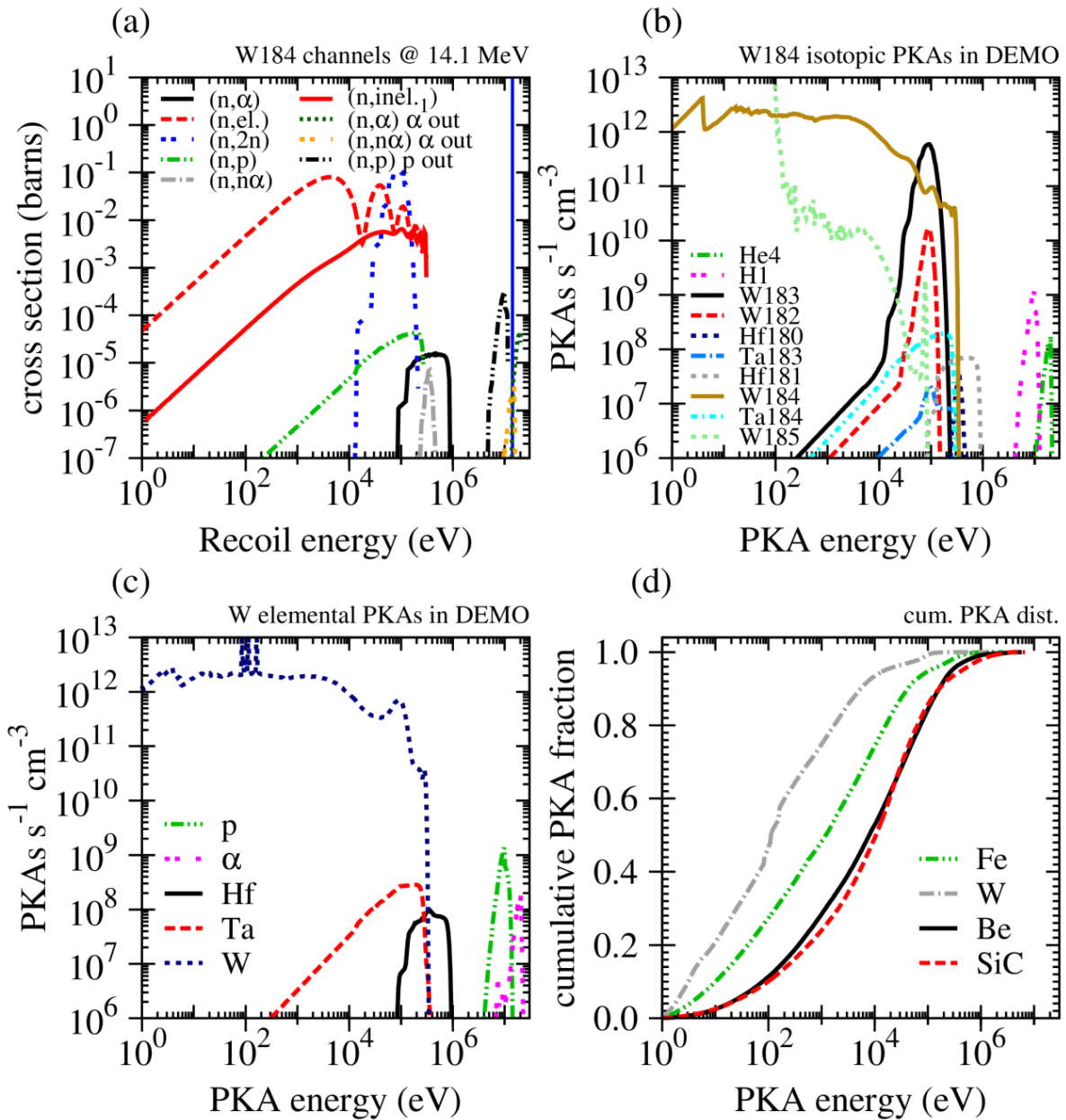


Fig. 4. Computational approach of SPECTRA-PKA. (a) an example snap-shot showing the recoil probability cross sections for various reaction channels due to a 14.1 MeV (the blue vertical line in the plot) neutron impinging on ^{184}W . (b) The PKA rates produced for different isotopes when the energy dependent recoil cross sections for ^{184}W are collapsed (merged) with a typical first wall (FW) neutron spectrum for a DEMONstration fusion power plant. (c) The PKA rates summed as a function of element for pure W (5 input target isotopes, including ^{184}W) under DEMO FW conditions. (d) Cumulative PKA distributions (summed over non-gas recoil elements) for Fe, W, Be, and SiC under DEMO FW conditions. Standard isotopic compositions, densities, and molar masses were used where necessary.

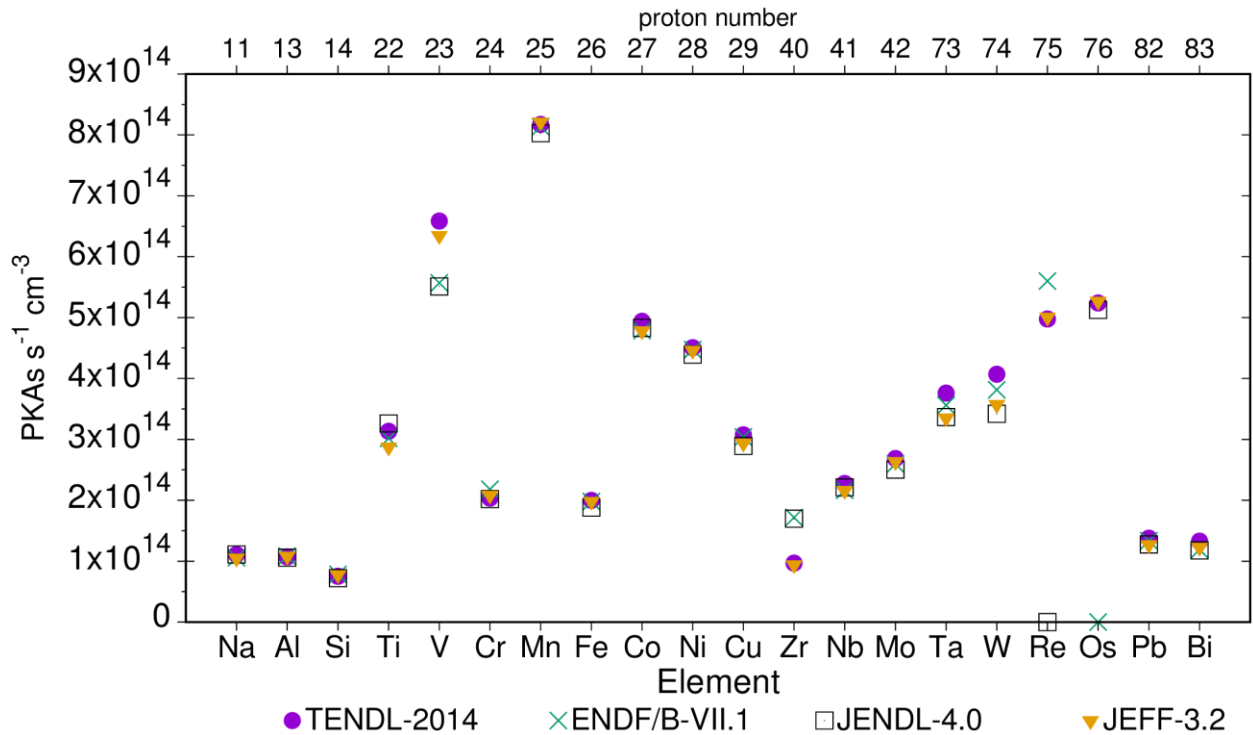


Fig. 5. Total PKA rates per unit volume (using standard elemental density conversion factors), for selected materials under DEMO FW conditions with four different NJOY-processed nuclear data libraries.

The latest modifications to SPECTRA-PKA allow the displacement energy, and hence NRT-dpa rates, to be evaluated on a per reaction channel basis. Preliminary results show the dominance of scattering in Fe, but show for W that scattering and (n,2n) contribute equally to dpa – see figure 6.

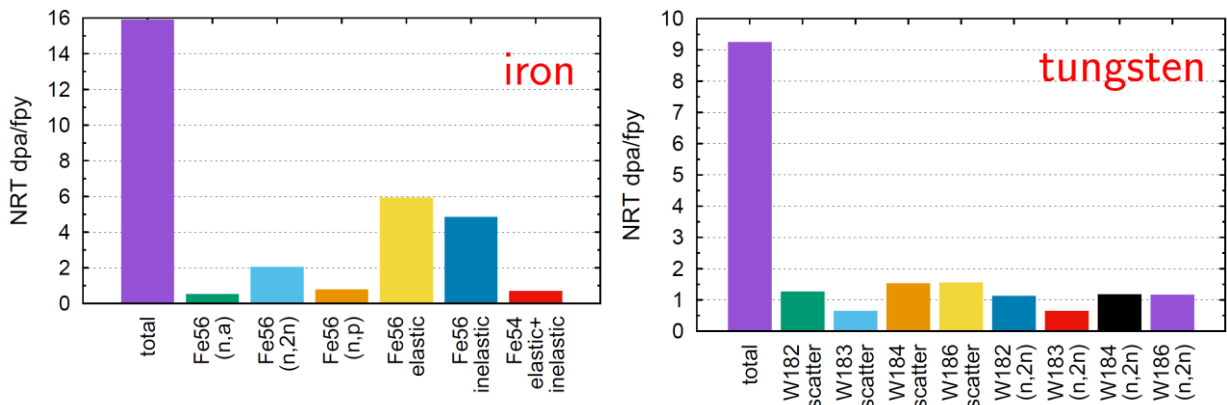


Fig. 6. Reaction channel breakdown of major contributions to dpa rate in pure (left) iron and (right) tungsten under DEMO FW conditions using TENDL-2014. For Fe, the elastic and inelastic scattering channels on ⁵⁶Fe dominate, but for W the (n,2n) channels on the constituent isotopes (182-4, 186) are as important as scatter (elastic+inelastic).

All of the results presented at the meeting are available in the suite of material response handbooks produced at UKAEA in the last 2 years – for each library four are available, considering the response under DEMO, PWR, FBR, and HFR conditions of all naturally occurring elements from H to Bi (see for example [8,9]).

References

- [1] J.-Ch. Sublet, J.W. Eastwood, J.G. Morgan, M. Fleming and M.R. Gilbert “The FISPACT-II User manual” CCFE-R(11)11 Issue 7 (2016), <http://www.ccf.ac.uk/fispact.aspx>
- [2] A.J. Koning, D. Rochman, S.C van der Marck, J. Kopecky, J. Ch. Sublet, S. Pomp, H. Sjostrand, R. Forrest, E. Bauge and H. Henriksson, “TENDL-2014; TALYS-based evaluated nuclear data library”, Available from <ftp://ftp.nrg.eu/pub/www/talys/tendl2014/tendl2014.html>
- [3] M.B. Chadwick et al., “ENDF/B-VII.1 Nuclear Data for Science and Technology: Cross Sections, Covariances, Fission Product Yields and Decay Data”, Nuclear Data Sheets Volume 112, Issue 12, December 2011, Pages 2887–2996.
- [4] The JEFF team, “JEFF-3.2: Evaluated nuclear data library.” <http://www.oecd-nea.org/dbdata/jeff>, 2014.
- [5] K. Shibata, O. Iwamoto, T. Nakagawa, N. Iwamoto, A. Ichihara, S. Kunieda, S. Chiba, K. Furutaka, N. Otuka, T. Ohsawa, T. Murata, H. Matsunobu, A. Zukeran, S. Kamada, and J. Katakura, “Jendl-4.0: A new library for nuclear science and engineering,” J. Nucl. Sci. Technol., vol. 48, pp. 1–30, 2011.
- [6] J.-Ch. Sublet and M.R. Gilbert, “Decay heat validation, FISPACT-II & TENDL-2014, JEFF-3.2, ENDF/B-VII.1 and JENDL-4.0 nuclear data libraries”, Technical report: CCFE-R(15)-25 (2015).
- [7] M.R. Gilbert, J. Marian, and J.-Ch. Sublet, “Energy spectra of primary knock-on atoms under neutron irradiation”, J. Nucl. Mater., vol. 467, pp. 121-134, 2015.
- [8] R.E. MacFarlane, D.W. Muir, R.M. Boicourt, and A.C. Kahler, The NJOY Nuclear data processing system – LA-UR-12-27079, <http://t2.lanl.gov/nis/publications/NJOY2012.pdf> (Version 2012-050+).
- [8] M.R. Gilbert, J.-Ch. Sublet and R.A. Forrest, “Handbook of activation, transmutation, and radiation damage properties of the elements simulated using FISPACT-II & TENDL-2014; Magnetic Fusion Plants” CCFE-R(15)26 (2015), http://www.ccf.ac.uk/fispact_handbooks.aspx
- [9] M.R. Gilbert, J.-Ch. Sublet and R.A. Forrest, “PKA distributions of the elements simulated using TENDL-2014; Magnetic Fusion Plants” CCFE-R(15)26-supplement (2015), http://www.ccf.ac.uk/fispact_handbooks.aspx

Differences among KERMA or DPA data calculated from JENDL-4.0, ENDF/B-VII.1, JEFF-3.2 and FENDL-3.1b with NJOY, C. Konno

Japan Atomic Energy Agency
Tokai-mura, Naka-gun, Ibaraki-ken, Japan

1. Introduction

The estimation of nuclear heating and material damage is one of the key nuclear analyses in nuclear reactor designs. Most nuclear reactor designers calculate the nuclear heating and material damage for their reactor designs by using the radiation transport code MCNP and ACE files. The ACE files are processed from a nuclear data library mostly with the NJOY code and include average heating numbers, which are KERMA (Kinetic Energy Release in Material) factors divided by total cross-section data, and damage energy production data related to DPA cross-sections.

KERMA factors can be calculated with two methods in NJOY. One is the “energy-balance method” and the other is the “kinematics method”. NJOY stores only the energy-balance KERMA factors to ACE files. It is known that KERMA factors of a lot of nuclei in the official ACE files are not always correct because of inconsistent energy-balance. In order to avoid this problem, not energy-balance

KERMA factors but kinematics KERMA factors are stored for nuclei of inconsistent energy-balance in the official ACE file of JENDL-4.0 and for all the nuclei in the official ACE file of FENDL-3.1b (the latest FENDL-3), by modifying the NJOY code.

It is known that KERMA and DPA data are different among JENDL-4.0, ENDF/B-VII.1, JEFF-3.2 and FENDL-3.1b even for nuclei with consistent energy-balance. Thus we compare KERMA factors or DPA cross-section data below 20 MeV in all the latest official ACE files calculated with NJOY from JENDL-4.0, ENDF/B-VII.1, JEFF-3.2 and FENDL-3.1b and try to specify reasons for differences of the KERMA or DPA data among the nuclear data libraries.

2. Method

For all the nuclei (497 nuclei) included in JENDL-4.0, ENDF/B-VII.1, JEFF-3.2 and FENDL-3.1b, we extracted the total cross-section data, average heating numbers and damage energy production data below 20 MeV from the latest official ACE files, converted the average heating numbers to KERMA (KERMA = average heating number x total cross-section) and the damage energy production data to DPA cross-section data and plotted the KERMA and DPA data for comparison:

- JENDL-4.0 : AceLibJ40 by JAEA (NJOY99.336+JAEA patch);
- ENDF/B-VII.1 : MCNP data by LANL (NJOY99.393);
- JEFF-3.2 : ACE file by OECD/NEA (NJOY99.393+ NEA patch);
- FENDL-3.1b : ACE file by IAEA (NJOY2012+IAEA patch).

Note that not an energy-balance KERMA but a kinematics KERMA is stored for nuclei of inconsistent energy-balance in the official ACE file of JENDL-4.0 and for all the nuclei in the official ACE file of FENDL-3.1b. We also extracted other cross-section data below 20 MeV, i.e., helium production cross-section data, from the ACE files and plotted them in order to investigate reasons for differences among KERMA or DPA data in the official ACE files. KERMA and DPA data were also calculated with the PHITS code (kinematics method) from reaction cross-section data in the ACE files in order to check if NJOY produces them adequately.

3. Results and discussion

The KERMA and DPA data of a lot of nuclei are different among JENDL-4.0, ENDF/B-VII.1, JEFF-3.2 and FENDL-3.1b. Reasons of almost all the differences in the KERMA or DPA data are successfully categorized as the followings. Note that this study is in progress.

1) Nuclear data

- Inconsistent energy-balance → Wrong energy-balance KERMA
✓ No secondary gamma data, mf12-15 mt3 data, etc.
- Cross-section difference of elastic scattering, helium production, fission, capture reactions, etc. → Wrong KERMA and DPA
- Wrong Q value → Wrong KERMA and DPA
- No secondary charged particle data → Wrong DPA

2) NJOY bug or unsupported issues

- ¹H problem (fixed in NJOY2012.43) → Wrong KERMA and DPA
- No secondary charged particle data → Wrong kinematics KERMA factors
- No secondary gamma data → Wrong kinematics KERMA and DPA
- mf12-15 mt3 data → Wrong kinematics KERMA and DPA
- mf6 mt102 data (also wrong secondary gamma spectra) → Wrong KERMA and DPA

3.1 Nuclear data issues

A lot of nuclei in ENDF/B-VII.1 and JEFF-3.2 have no secondary gamma data. Then energy-balance KERMA factors in the ACE files are not correct as shown in Fig. 1 (JEFF-3.2 is not correct because of no secondary gamma data).

JENDL-4.0 has a lot of nuclei with mf12-15 mt3 data, where it is difficult to keep energy-balance. Thus energy-balance KERMA factors are not correct. Fig. 2 is an example of this problem (energy-balance KERMA is not correct).

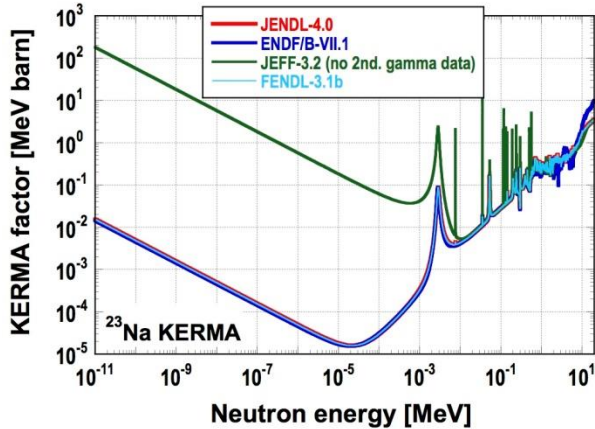


Fig. 1. KERMA factor of ^{23}Na .

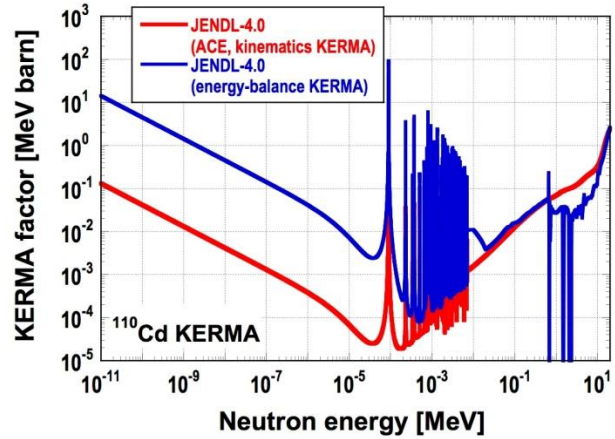


Fig. 2. KERMA factor of ^{110}Cd .

In some nuclei cross-section data of the elastic scattering, capture, helium production, fission reactions, etc. are different among the nuclear data libraries. Then KERMA and DPA data are also different. The typical example is shown in Fig. 3, where the difference of the DPA data comes from the difference of the helium production cross-section data shown in Fig. 4.

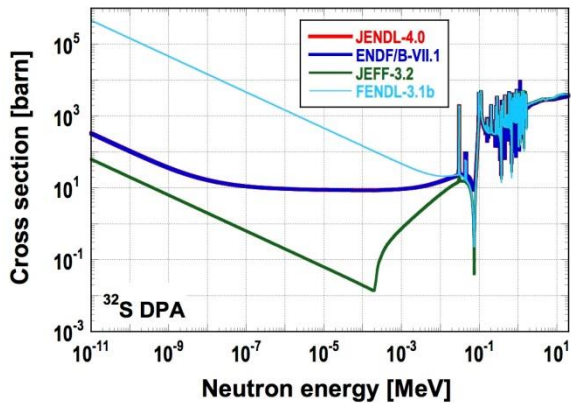


Fig. 3. DPA cross-section of ^{32}S .

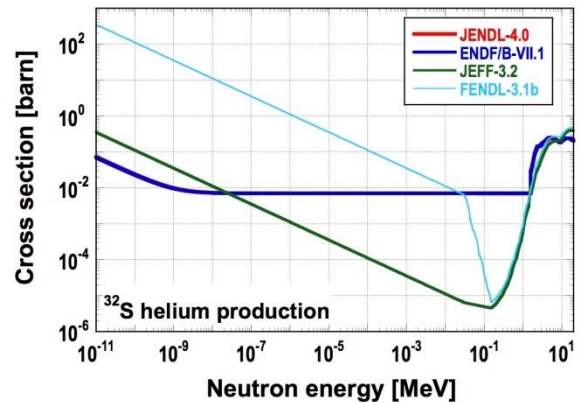


Fig. 4. Helium production cross-section of ^{32}S .

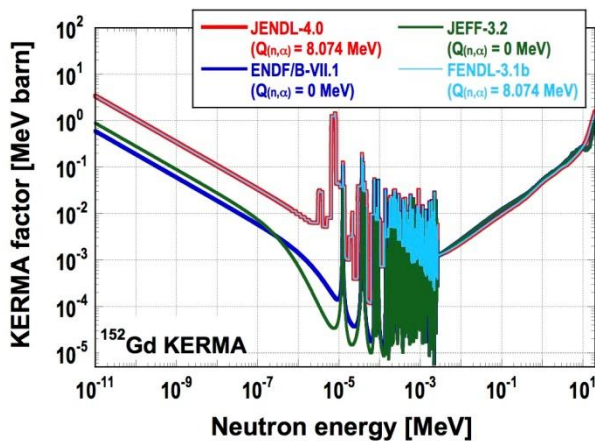


Fig. 5. KERMA factor of ^{152}Gd .

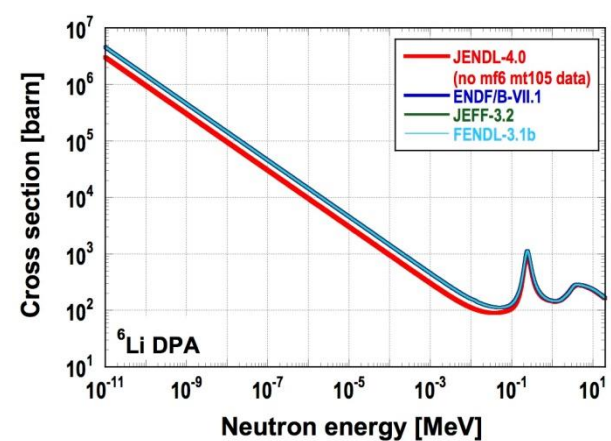


Fig. 6. DPA cross-section of ^6Li .

A Q value of the (n, α) reaction is wrong (Q value = 0.0 MeV) in several nuclei of ENDF/B-VII.1 and JEFF-3.2. This causes incorrect KERMA and DPA data as shown in Fig. 5 (ENDF/B-VII.1 and JEFF-3.2 in Fig. 5 are not correct.).

Non-existent secondary charged particle data cause smaller DPA data as shown in Fig. 6 (JENDL-4.0 in Fig. 6 is not correct.). This does not affect KERMA factors.

3.2 NJOY issues

NJOY had a bug in processing the mf6 mt102 data of ^1H in ENDF/B-VII.1 up to NJOY2012.43 as shown in Fig. 7 (ENDF/B-VII.1 and JEFF-3.2 in Fig. 7 are not correct.). JAEA corrected this bug for the ACE file of JENDL-4.0 unofficially. The ACE file of FENDL-3.1b has no problem because it was processed with NJOY2012.50. It is recommended that the ACE files of ^1H in ENDF/B-VII.1 and JEFF-3.2 should be revised with NJOY2012.50.

The KERMA factors of a lot of nuclei with inconsistent energy-balance in the JENDL-4.0 ACE file are already replaced with the kinematics KERMA factors, but it is found out that this is not always correct for nuclei without secondary charged particle data. Figure 8 shows an example of this issue (kinematic KERMA in Fig. 8 is not correct.). It seems that this is also a defect of NJOY.

Kinematic KERMA and DPA data are not correct in the case of nuclei without secondary gamma data (JENDL-4.0 in Fig. 9 is not correct.). Probably this is also due to a NJOY defect.

JENDL-4.0 adopted mt12-15 mt3 data including the capture reaction for a lot of nuclei, where the kinematics KERMA and DPA data have the same problem as that in nuclei without secondary gamma data (JENDL-4.0 and FENDL-3.1b in Fig. 10 are not correct. The difference between ENDF/B-VII.1 and JEFF-3.2 comes from the difference of the capture reaction cross-section data). It seems that NJOY cannot treat mt12-15 mt3 data adequately.

KERMA and DPA data of nuclei with gamma data of the capture reaction in mf6 are different from those of nuclei with gamma data of the capture reaction in mf12-15 (only JENDL-4.0 in Fig. 11 is correct.). NJOY outputs the following message only in the former case. It seems that NJOY cannot also treat mf6 mt102 data adequately:

“mf6, mt102 does not give recoil za=xxxx
photon momentum recoil used.”

Additionally I compare the KERMA and DPA data of ^{56}Fe including TENDL-2015 in Fig. 12. The secondary gamma data of the capture reaction in ^{56}Fe of JEFF-3.2 and TENDL-2015 are in mf6 mt102. Thus these KERMA and DPA data are not correct, but why are they different? It was found out that the secondary gamma data are very different, which causes the differences between the KERMA or DPA data of ^{56}Fe in JEFF-3.2 and TENDL-2015. This difference is one of nuclear data issues, not NJOY issues.

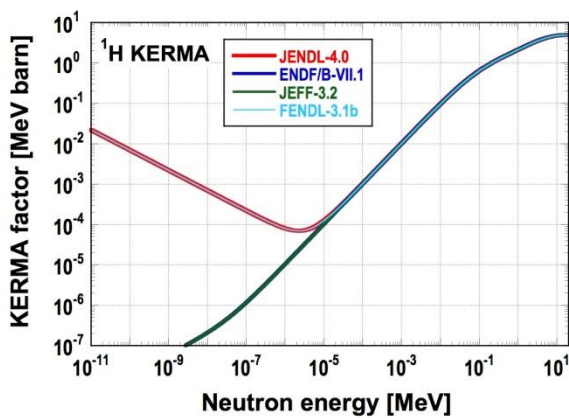


Fig. 7. KERMA factor of ^1H .

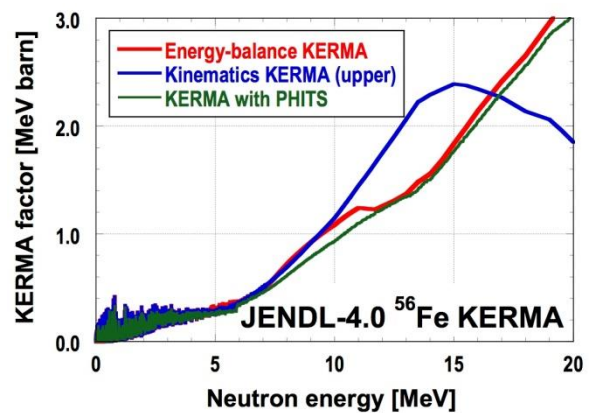


Fig. 8. KERMA factor of ^{56}Fe in JENDL-4.0.

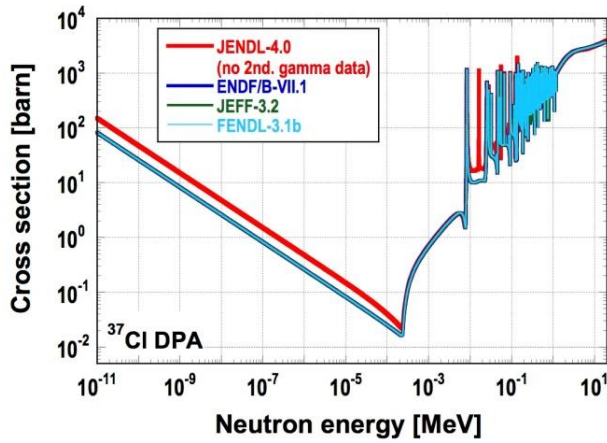


Fig. 9. DPA cross-section of ^{37}Cl .

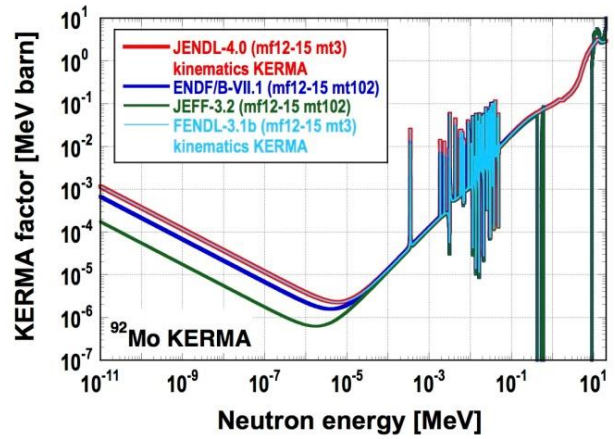


Fig. 10. KERMA factor of ^{92}Mo .

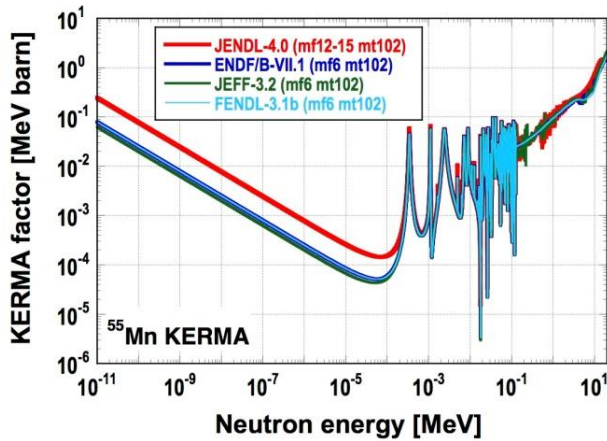


Fig. 11. KERMA factor of ^{55}Mn .

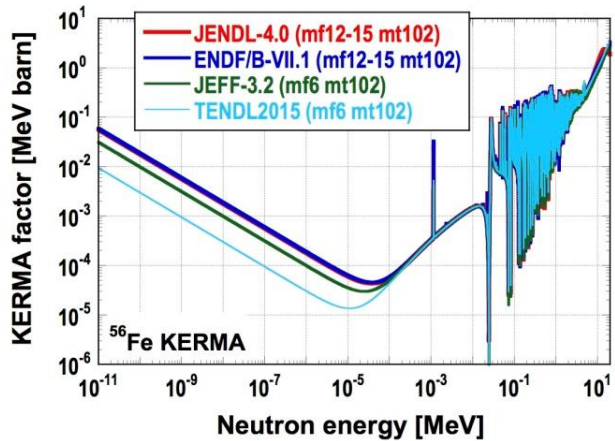


Fig. 12. KERMA factor of ^{56}Fe .

4. Summary

KERMA factors and DPA cross-section data below 20 MeV in the official ACE files of JENDL-4.0, ENDF/B-VII.1, JEFF-3.2 and FENDL-3.1b were compared in detail. As a result, it was found out that the KERMA and DPA data of a lot of nuclei were different among the nuclear data libraries. Reasons of most of the differences were successfully categorized to the nuclear data and NJOY issues. The KERMA factors and DPA cross-section data in the ACE files with the problems should be revised.

**ROSFOND based heating-damage cross sections sub-library:
preliminary uncertainty assessment,
V.V. Sinitsa**

National Research Centre “Kurchatov Institute”
Moscow, Russian Federation

1. Introduction

The accuracy of radiation damage calculations for the most important LWR component, the reactor pressure vessel (RPV), directly linked with the RPV End-of-Life (EoL) prediction which is in its turn connected with fundamental nuclear safety aspects and relevant economic impacts. In this connection, for nearly ten years the ENEA-Bologna Nuclear Data Group conducts the nuclear data processing and validation activities addressed to update the specialized broad-group coupled neutron/photon working cross section libraries for shielding and radiation damage calculations through NJOY [1, 2] and Bologna revised version of SCAMPI [3, 4] data processing systems.

A number of working group-wise data libraries has been prepared and transferred to the ENEA Data Bank for dissemination [5-11].

Several years ago the NRC “Kurchatov Institute” has reset the GRUCON project, originally designed to provide group constants for fast nuclear reactor calculations [12], with aim to expand its application area and to use in the WWER safety tasks, in particular, in the RPV radiation damage analyses. By means of updated GRUCON and NJOY-99 processing codes, and calculation procedure, developed in the NDG of ENEA Bologna, a sample of kerma&damage energy point-wise data sub-libraries from different evaluated data libraries has been generated. On the base of this sample, the quantitative assessment of kerma/dpa data precision in the RPV calculations is obtained.

2. Heating-damage cross sections sub-library

For the WWER component radiation damage analyses, the specialized kerma&damage energy point-wise cross sections for C, V, Cr, Mn, Fe, Ni, Zr and W from the ROSFOND evaluated data library have been generated through the GRUCON package (for cross sections linearization, reconstruction from resonance parameters and Doppler broadening) combined with the HEATR module of NJOY-99 [2] (for kerma factors and damage energy calculations). Interface between the GRUCON and NJOY modules was implemented through the binary PENDF file. The data types, included to the heating-damage sub-library, are given in the Table 1:

MT1	Total cross section(barn)
MT301	Kerma total (eV-barn)
MT302	Kerma elastic
MT303	Kerma non-elastic (all but MT2)
MT304	Kerma inelastic (MT51-91)
MT318	Kerma fission (MT18 or MT19-20-21-38)
MT401	Kerma absorption (MT102-120)
MT402	Kerma capture (MT102)
MT442	Total photon energy (eV-barn)
MT443	Total kinematic kerma (high limit)
MT444	Damage energy total (eV-barn)
MT445	Damage energy elastic (MT2)
MT446	Damage energy inelastic (MT51-91)
MT447	Damage energy absorption (MT102 - 120)

The ROSFOND heating-damage sub-library is represented in the ENDF format that allows subsequent post-processing these data through GRUCON: group-averaging with self-shielding for different group structures and weighting functions, preparation of heating-damage numbers for compositions.

3. Precision assessment procedure

To assess the uncertainty of response function calculations from the ROSFOND heating-damage cross sections sub-library, the ENEA Bologna Nuclear Data Group experience of generation the VITAMIN-B6/BUGLE-96 type working libraries has been taken into account. Procedures of specialized libraries generation is described in details in the ORNL original report [13]. The carbon steel composition (Table 2) and neutron spectrum at the point 1/4 T PV (Fig. 1), involved in the procedure, were used in assessment.

Isotope	Nuclear Density	
	[nuclei/barn]	[%]
C-12	9.8100E-04	1.160
Cr-50	5.5180E-06	0.007
Cr-52	1.0640E-04	0.126
Cr-53	1.2070E-05	0.014
Cr-54	3.0040E-06	0.004
Mn-55	1.1200E-03	1.324
Fe-54	4.7500E-03	5.617
Fe-56	7.5180E-02	88.899
Fe-57	1.7200E-03	2.034
Fe-58	2.4570E-04	0.291
Ni-58	3.0310E-04	0.358
Ni-60	1.1590E-04	0.137
Ni-61	5.0170E-06	0.006
Ni-62	1.5940E-05	0.019
Ni-64	4.0400E-06	0.005

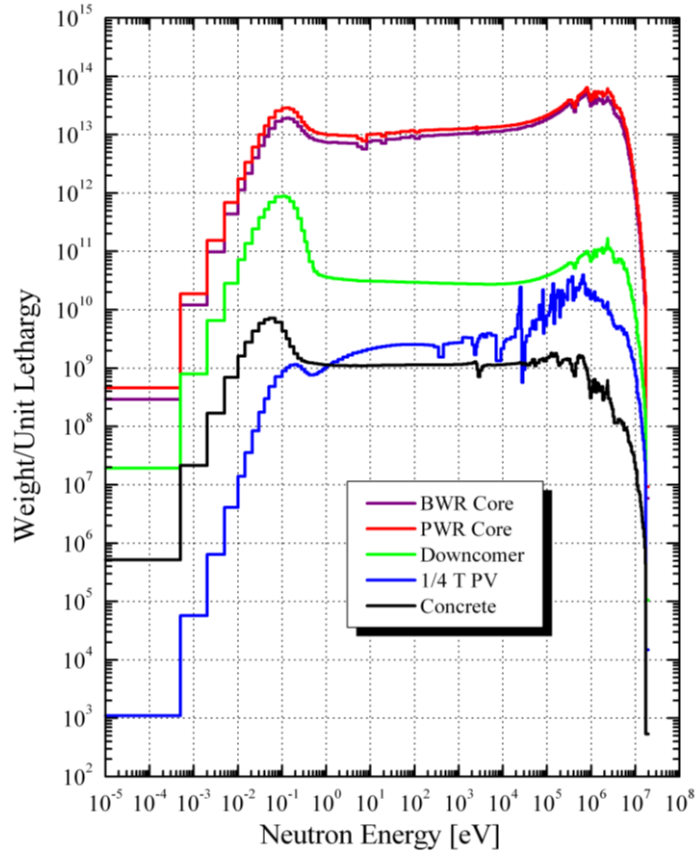


Fig.1. Weighting functions used in the BUGLE-96 library generation procedure [9].

The kerma factors and damage energies, prepared from the ENDF/B-VII.1, JEFF-3.2, JENDL-4.0, CENDL-3.1 and TENDL-2015 data files, supplemented by CIELO evaluation of Fe-56, are shown in Fig. 2. The essential differences among the heating and damage detailed data can be seen in Figure. The question is how they affect the integral values used in reactor applications, in particular, the RPV dpa calculation results.

The differences in the total kerma and dpa values for carbon steel (CS) components, weighted with the 1/4T PV neutron spectrum, are shown in Figs. 3 and 4.

Here:

$$\langle x \rangle = \frac{1}{N_{lib}} \sum_{i=1}^{N_{lib}} x_i \quad \text{-- kerma and dpa values, averaged over libraries sample,}$$

$$s = \sqrt{\frac{1}{N_{lib}-1} \sum_{i=1}^{N_{lib}} (x_i - \langle x \rangle)^2} \quad \text{-- standard deviations, obtained on the libraries sample,}$$

$$Eps = 3 \sum_{n=1}^{N_{comp}} \frac{s_n}{\langle x_n \rangle}$$

– dispersions, summarized over material components.

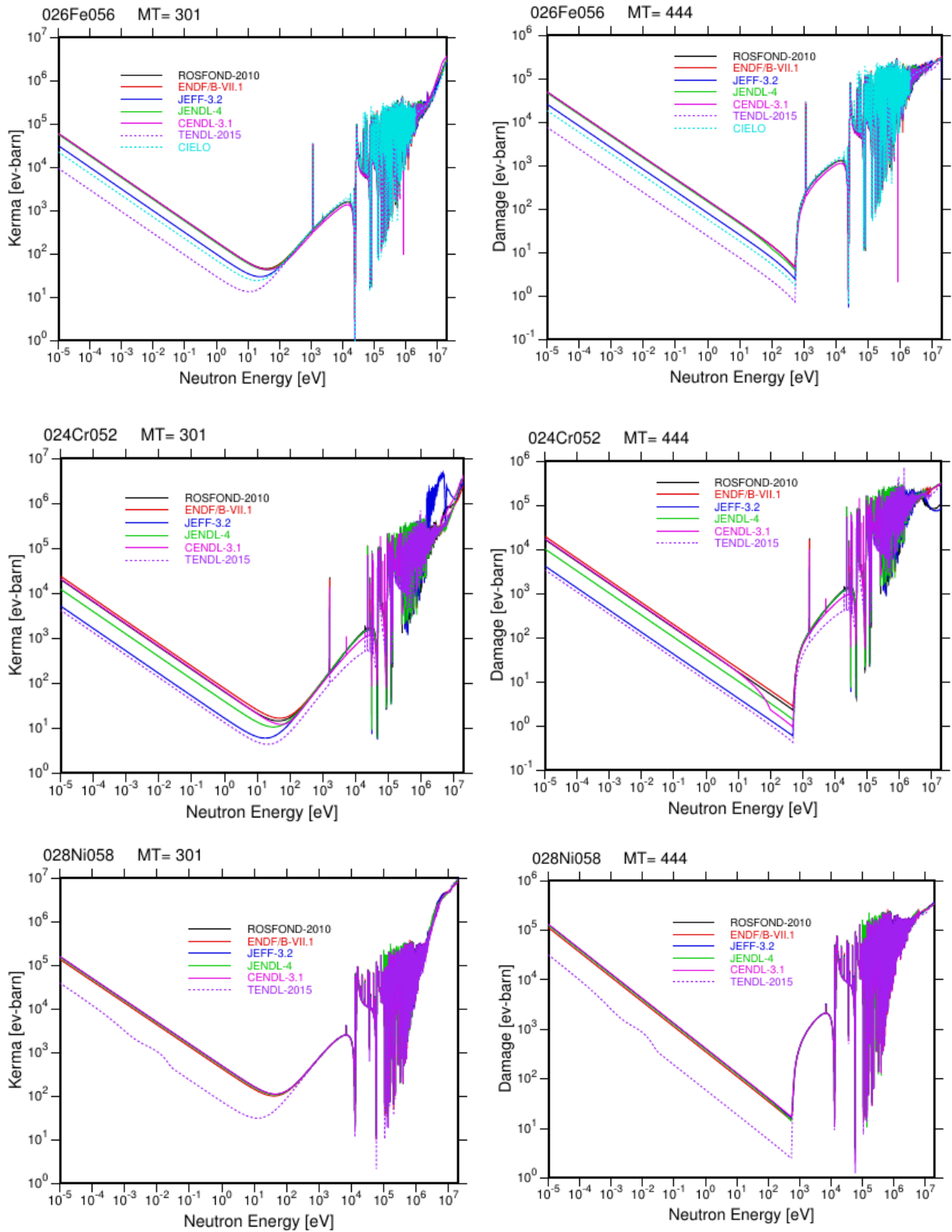


Fig. 2. Kerma factors and damage energies calculated from ROSFOND-2010, ENDF/B-VII.1, JEFF-3.2, JENDL-4.0, CENDL-3.1, TENDL-2015 and CIELO (Fe-56) evaluated data.

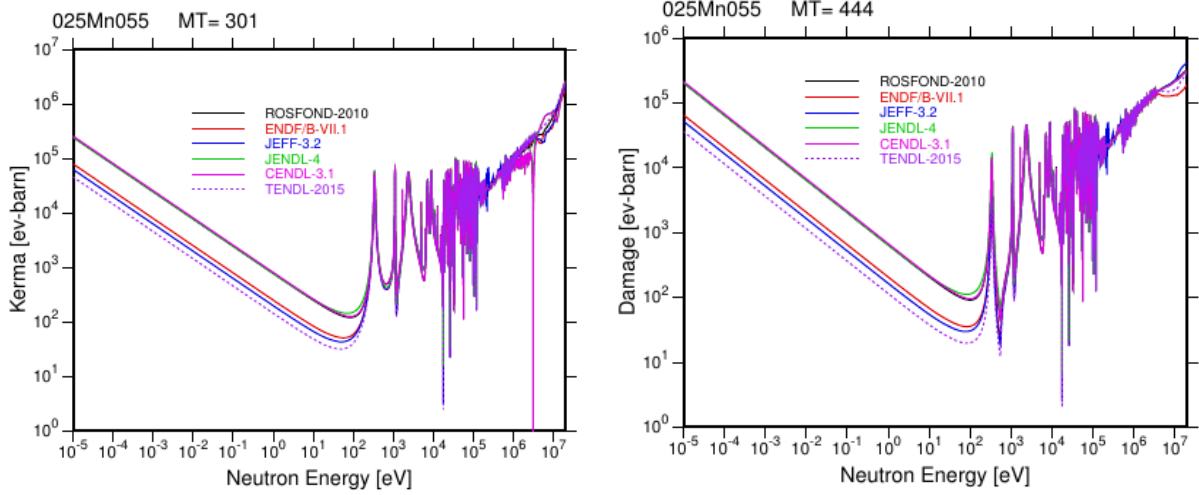


Fig. 2. (cont.) Kerma factors and damage energies calculated from ROSFOND-2010, ENDF/B-VII.1, JEFF-3.2, JENDL-4.0, CENDL-3.1, TENDL-2015 and CIELO (Fe-56) evaluated data.

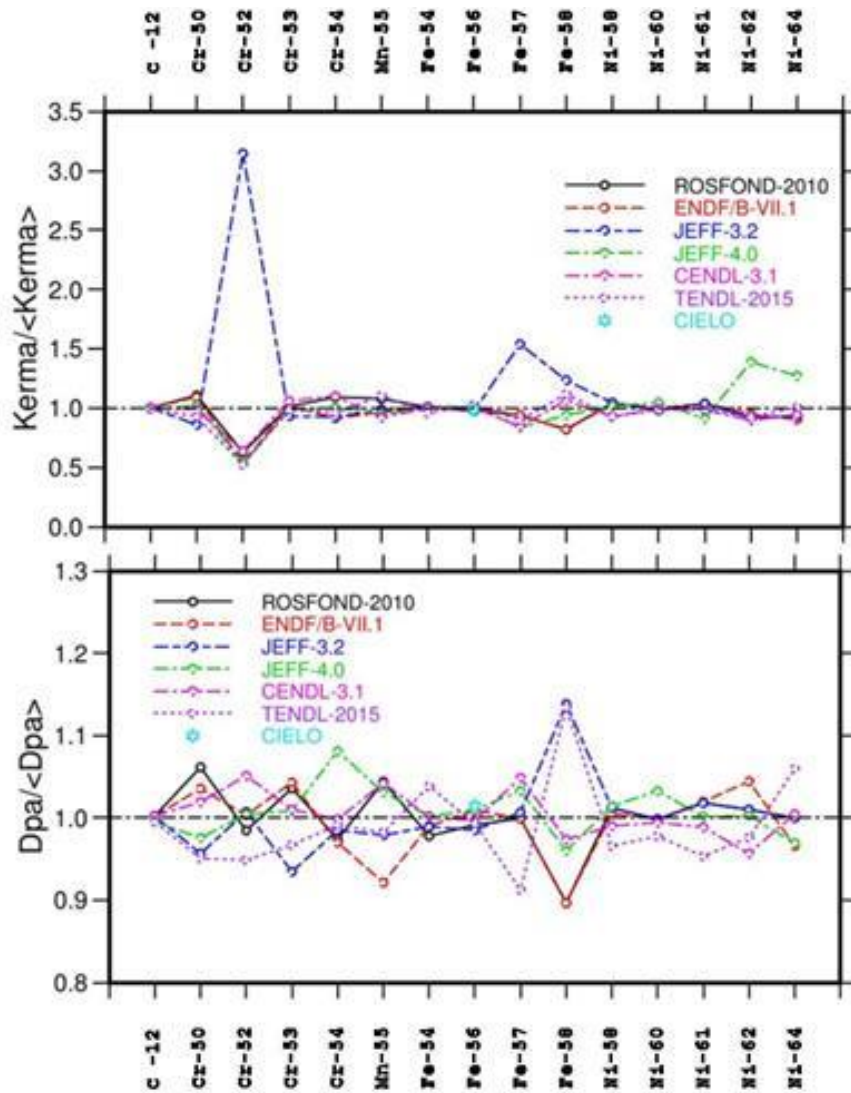


Fig. 3. Total kerma and dpa ratios to average values for carbon steel components.

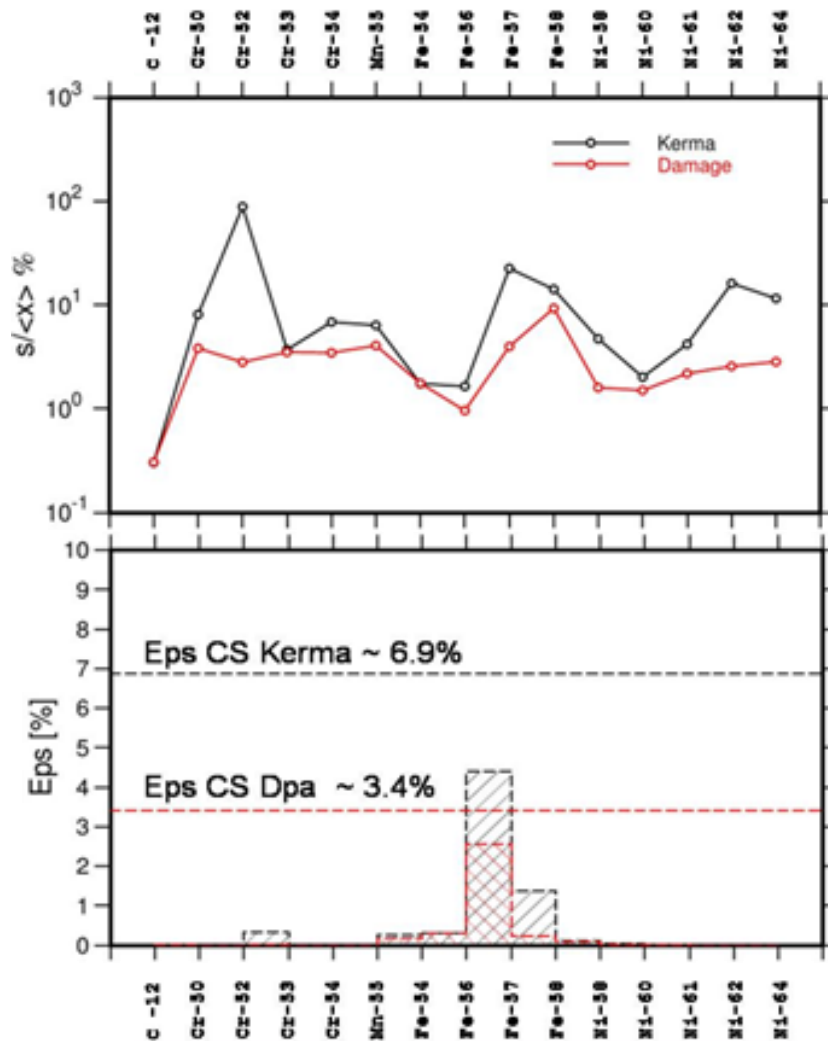


Fig. 4. Sample standard deviations and dispersion for carbon steel components.

Conclusion

Presently achieved precision of the WWER RPV heating and damage calculations on the base of ROSFOND evaluated data can be assessed as:

- dispersion (Eps) for Cross Section Kerma ~ 6.9%,
- dispersion (Eps) for Cross Section Dpa ~ 3.4%.

To decrease the data ambiguity and processing uncertainty, it should be desirable:

- to separate the heating-damage cross-sections to a specialized sub-library with point-wise representation,
- to implement to the GRUCON processing code an independent algorithm of kerma/dpa calculations.

References

1. R.E. MacFarlane, D.W. Muir, The NJOY Nuclear Data Processing System, Version 94.66, Los Alamos National Laboratory, December 19, 1996
2. R.E. MacFarlane, D.W. Muir, The NJOY Nuclear Data Processing System, Version 99, LA1270, LANL (2002)
3. SCAMPI: Collection of Codes for Manipulating Multigroup Cross Section Libraries in AMPX Format, Oak Ridge National Laboratory, RSIC Peripheral Shielding Routine Collection PSR-352, September 1995. Available from OECD/NEA Data Bank as PSR-0352 SCAMPI

4. V. Sinita, M. Pescarini, ENEA-Bologna 2007 Revision of the SCAMPI (ORNL) Nuclear Data Processing System, ENEA FPN-P9H6-006, September 13, 2007
5. [ZZ-VITJEF22.BOLIB, JEF-2.2 Multigr Coupled \(199n + 42gamma\) X-Section Lib. in AMPX Fmt for Nuclear Fission Applications](#)
6. [ZZ VITJEFF31.BOLIB,JEFF-3.1 Multigr Coupled \(199n + 42gamma\) X-Section Lib. in AMPX Fmt for Nuclear Fission Applications .](#)
7. [ZZ-VITJEFF32.BOLIB, JEFF-3.2 Multi-Grp Coupled \(199n+ 42gamma\) X-Sec. Lib. in AMPX Fmt for Nuclear Fission Applications](#)
8. [ZZ-VITENDF70.BOLIB, ENDF/B-VII.0 Multi-Grp Coupled \(199n +42gamma\)X-Sec.Lib.in AMPX Fmt for Nuclear Fission Applications](#)
9. [ZZ BUGJEFF311.BOLIB, JEFF-3.1.1 Broad-Group Coupled X Sect Lib. for LWR Shielding and Pressure Vessel Dosimetry Applications](#)
10. [ZZ BUGENDF70.BOLIB, ENDF/B-VII.0 Broad-Group Coupled X Sect. Lib. for LWR Shielding Pressure Vessel Dosimetry Applications](#)
11. V.V. Sinita, L.P. Abagyan, N.O. Bazazyants et al., GRUKON – Library of Computer Programs for Calculation of the Group Constants. – Moscow: Atomizdat, Nuclear Physics Research in the USSR, Computer Program Descriptions, vol. 27, 1979 (in Russian)
12. J.E. White, D.T. Ingersoll, R.Q. Wright, H.T. Hunter, C.O. Slater, N.M. Greene, R.E. MacFarlane, R.W. Roussin, “Production and Testing of the Revised VITAMIN-B6 Fine-Group and the BUGLE-96 Broad-Group Neutron/Photon Cross-Section Libraries Derived from ENDF/B-VI.3 Nuclear Data”, Oak Ridge, ORNL Report ORNL-6795/R1, NUREG/CR-6214, Revision 1, January 1995

Some experiences of dpa assessments using MCNP and SPECTER codes, C.S. Gil, W. Park, J. Kwon

Korea Atomic Energy Research Institute
Yuseong, Republic of Korea

1. Introduction

The DPA (Displacement Per Atom) of a reactor pressure vessel (RPV) has been issued for the extension of nuclear reactor operation. KAERI tried to assess dpa of structural material in KALIMER (Korea Advanced LIquid METal Reactor) under development. The dpa assessments of SS316, which is considered as a structural material of the KALIMER, were carried out with MCNP and SPECTER codes [1,2]. MCNP code has many advantages such as elimination of geometric approximation and avoiding of self-shielding effects of nuclear cross sections for nuclear applications. However, the results tallying with meaningful fractional standard deviation in small energy groups are very difficult for the large system analysis. The SPECTER code has been used for neutron damage calculations in irradiated materials.

2. DPA assessments for a fast reactor

To confirm and/or compare the dpa results of MCNP and SPECTER, preliminary calculations were performed for the simple spherical models. The differences between the dpa results of MCNP and SPECTER are not large considering the different damage cross section data and weighting function used in the energy group collapsing process of SPECTER code. Figure 1 shows the radial and axial cross-sectional view of a fast reactor (KALIMER) under development in Korea. The dpa assessments of the core support barrel and upper grid plate of KALIMER were carried out. The core support barrel and grid plates of SS316 will be irradiated by the highest neutron fluxes [3].

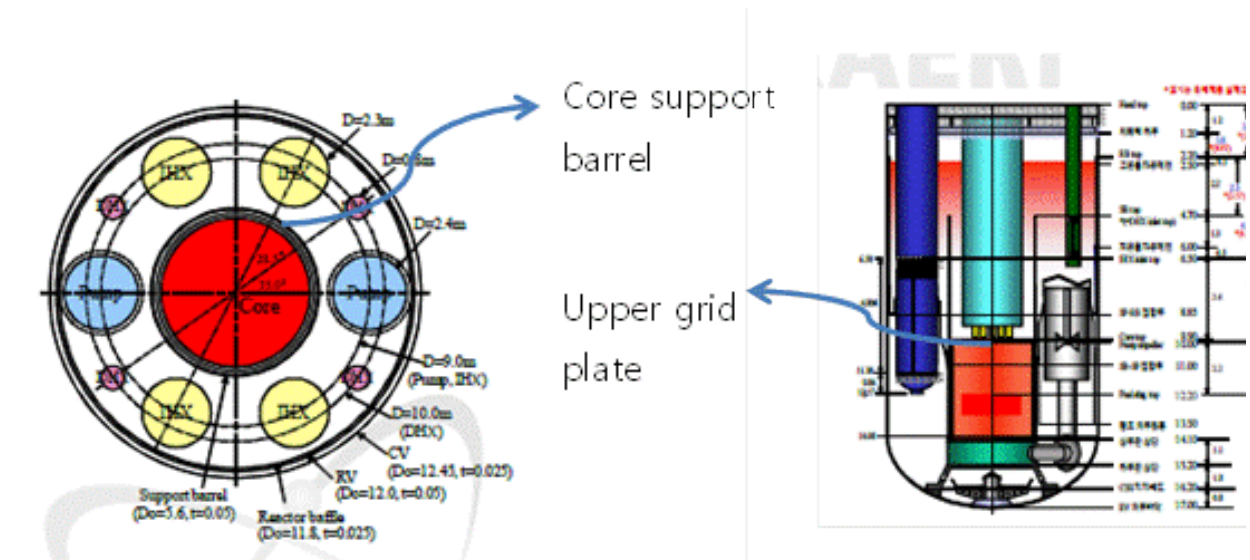


Fig.1 Radial and axial cross-sectional view of KALIMER.

3. Results and comments

Table 1 and Table 2 show predicted dpa results at the support barrel and upper grid plate of SS316 using MCNP with ENDF/B-VII.1. The 94% of SS316 consists of Fe, Cr and Ni and the neutron flux of KALIMER core is $1.11255E+20$ n/sec.

Table 1. Calculated dpa of SS316 at the center of support barrel with MCNP.

Isotopes	Fraction (%)	dpa/sec	dpa/year
Cr-52	18	8.397E-12	2.65E-04
Fe-56	65	2.175E-11	6.86E-04
Ni-58	7.62	7.622E-12	2.40E-04
SS316(Cr+Fe+Ni)	94	3.777E-11	1.19E-03

Table 2. Calculated dpa of SS316 at the center of upper grid plate with MCNP.

Isotopes	Fraction (%)	dpa/sec	dpa/year
Cr-52	18	1.840E-10	5.80E-03
Fe-56	65	4.663E-11	1.47E-02
Ni-58	7.62	1.940E-12	6.12E-03
SS316(Cr+Fe+Ni)	94	8.443E-11	2.66E-02

The largest dpa is occurred at the center of upper grid plate of SS316 and is $2.66E-02$ per a year. It takes about 150 years to reach the dpa limit considering ASME code criteria 4.1 dpa of SS316.

The damage cross section data of the NRT model were generated with NJOY for this MCNP calculation.[4] The CRP 'Primary Radiation Damage Cross Sections' suggests advanced models for the damage cross sections such as arc-dpa against NRT-dpa.

References

13. "MCNP5-A General Monte Carlo N-Particle Transport Code, Version 5," LANL, LA-UR-03-1987, April 2003.
14. Lawrence R. Greenwood and Robert K. Smither, "SPECTER: Neutron Damage Calculations for Materials Irradiations," Fusion Program, ANL (1985)
15. W. Park et al., "Radiation Damage Estimation for Sodium-cooled Fast Reactor using MCNP and SPECTER," KAERI/TR-4400/2011.
16. R.E. MacFarlane, D.W. Muir, "The NJOY Nuclear Data Processing System, Version 99," LA1270, LANL (2002)

Damage clustering in metals: importance, advances and challenges, K. Nordlund, A.E. Sand, F. Granberg, E. Levo, and F. Djurabekova

University of Helsinki
Helsinki, Finland

1. Introduction

The damage produced in metals has traditionally been primarily characterized in terms of the total damage production, which typically is first estimated with the dpa number. As discussed in previous meetings of this CRP, the dpa is not actually very well suited for typical dense metals, since the number it gives is typically about 3 times larger than the number of actual defects produced, and 30 times smaller than the actual number of defects produced. Hence we developed the improved arc-dpa and rpa standards, that give in a simple analytical form a defect number that does correspond well to MD and experimental data [1]. Section 2 summarizes the development of the arc-dpa and rpa standards. In sections 3 and 4 we discuss the role of damage clustering in damage production.

2. Status of arc-dpa and rpa development

The new functional forms for the "athermal recombination-corrected dpa" (arc-dpa) and "replacements-per-atom" (rpa) equations are:

$$N_d(E) = \left[\begin{array}{ll} 0 & \text{when } E < E_d \\ 1 & \text{when } E_d < E < 2E_d/0.8 \\ \frac{0.8E}{2E_d} \xi(E) & \text{when } 2E_d/0.8 < E < \infty \end{array} \right],$$

where the efficiency function $\xi(E)$ is for the arc-dpa:

$$\xi_{arc\,dpa}(E) = \frac{1 - c_{arc\,dpa}}{(2E_d/0.8)^{b_{arc\,dpa}}} E^{b_{arc\,dpa}} + c_{arc\,dpa}$$

and for the rpa:

$$\xi_{rpa}(E) = \left(\frac{b_{rpa}^{c_{rpa}}}{(2E_d/0.8)^{c_{rpa}}} + 1 \right) \frac{E^{c_{rpa}}}{b_{rpa}^{c_{rpa}} + E^{c_{rpa}}}$$

The original NRT-dpa damage efficiency is obtained with $\zeta_{NRT}(E) = 1$.

We emphasize that the arc-dpa and rpa equations are not intended to replace the NRT-dpa, which is still valid as a convenient energy deposition unit and can be used for e.g. comparing different kinds of irradiations. Rather, they are an alternative if one wishes to have a somewhat more accurate estimate of the actual damage production or number of replaced (mixed) atoms.

Within the IAEA CRP we have collected MD data on damage production and mixing for the metals in Fe, Ni, Cu, Ag, Au, Pd, Pt, W. We have fitted the data, including the uncertainty of the data if possible, using a least-squares Levenberg-Marquardt fitting algorithm for both the arc-dpa and rpa equations. The fits provide element-specific fitting parameters $b_{\text{arc-dpa}}$, $c_{\text{arc-dpa}}$, ... including their statistical uncertainties to the data. The fits will be done to composite data for several different interatomic potentials, and as such the uncertainties of the parameters will also include an estimate of the systematic error with respect to the variation of the potentials.

The fits to data on both damage and mixing, including an estimate of the upper energy limit for their validity, will be provided in the final report of the CRP group.

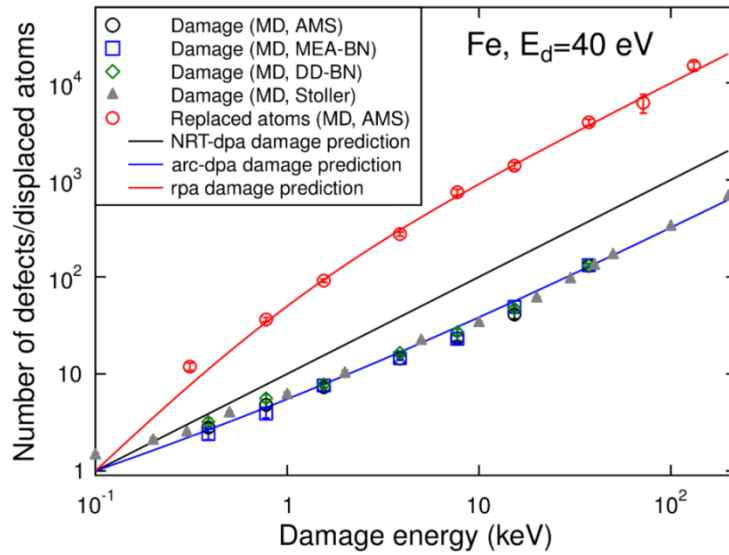


Fig. 1. Summary of fits of the arc-dpa and rpa functions to composite damage production and atom replacement (mixing) data in Fe.

3. Molecular dynamics modelling of cluster formation.

The arc-dpa data shows in some cases an increase in the damage production at the highest energies, which is due to formation of large dislocations loops in the cascades. This relates to the density of the material and the irradiation condition, as summarized qualitatively in Fig. 2. Even the primary damage state may contain a significant fraction of damage clustering.

Recently, we participated in a systematic study of damage clustering in W. Although damage production in W has already been studied for a long time, the fraction of damage in clusters has remained clear. Since the large damage clusters are likely to completely dominate the long-time scale evolution, knowing this fraction is crucial. Using in-situ transmission electron microscopy carried out by collaborators at CCFE, we directly observed nano-scale defects formed in ultra-high purity tungsten by low-dose high energy self-ion irradiation at 30K. At cryogenic temperature lattice defects have reduced mobility, so these microscope observations offer a window on the initial, primary damage caused by individual collision cascade events. Electron microscope images provide direct evidence for a power-law size distribution of nano-scale defects formed in high-energy cascades, with an upper size limit independent of the incident ion energy. Furthermore, the analysis of pair distribution functions of defects observed in the micrographs shows significant intra-cascade spatial

correlations consistent with strong elastic interaction between the defects. This study is the first ever direct determination of primary cluster sizes in experiments and simulations, and has attracted major interest in the international fusion community. The key result is shown in Fig. 3, which shows excellent agreement between simulations and experiments on damage clusters in W.

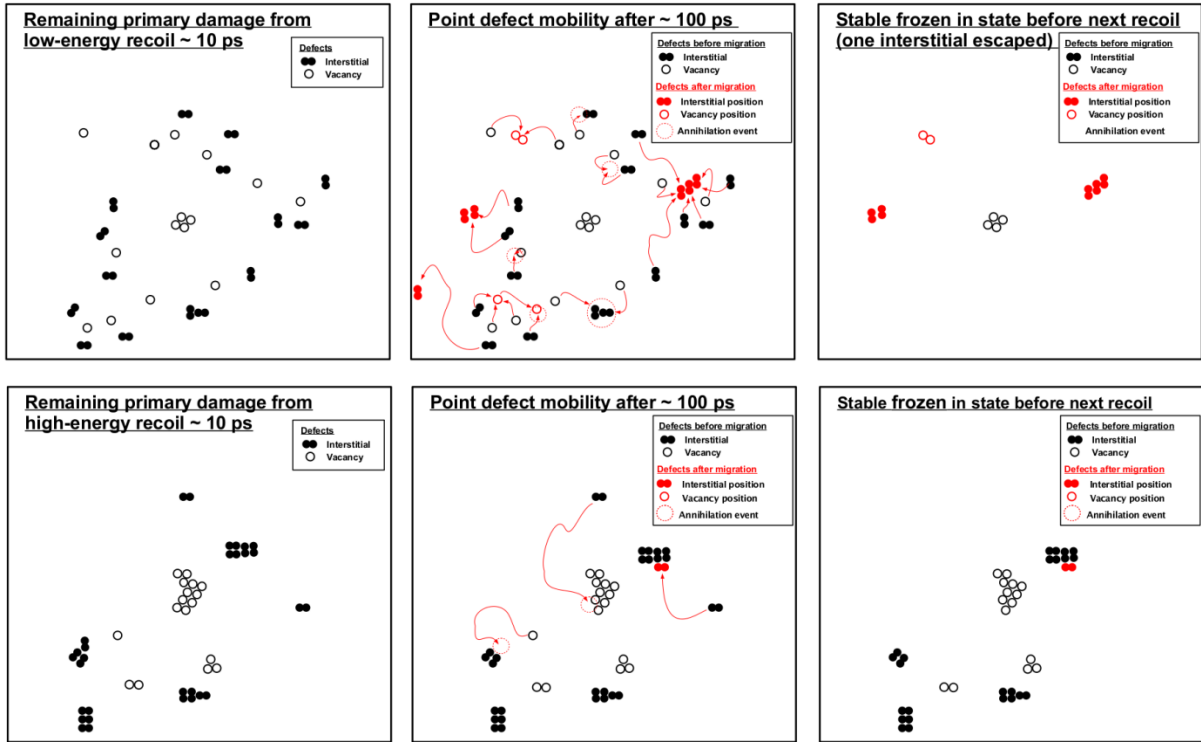


Fig. 2. Schematic illustration of damage production in collision cascades. Upper row: low-energy or light recoil. Lower row: high-energy, massive recoil. In both cases, damage clustering tends to occur, but in the case of heavy recoils in dense materials at high (> 10 keV) energies, they may dominate damage production already in the primary damage state.

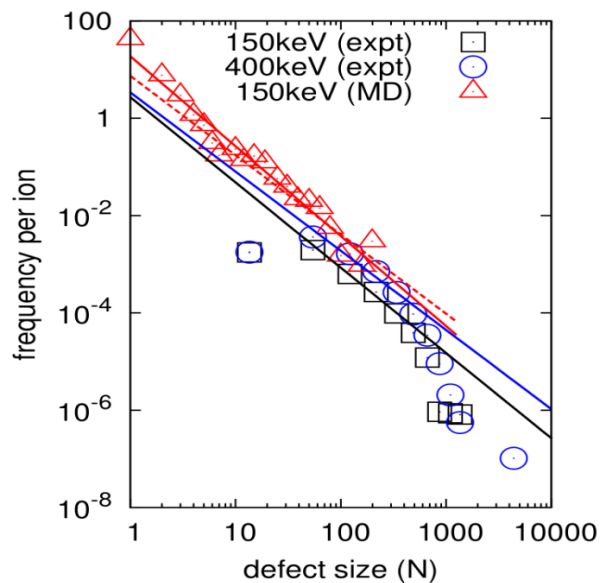


Fig. 3. Results on the size of damage clusters in W. From Ref. [2].

4. Reduced radiation damage in high-entropy alloys

The conventional metals we know from everyday life are based on one element forming a well-ordered crystal structure, with additional elements mixed in at small concentrations. A conceptually new way of making metals was thought out only recently, when it was found that one can mix numerous (three to seven) different types of metal atoms at completely random positions in equal concentrations, while still retaining a single good crystalline phase. In these, so called equiatomic or high-entropy alloys, the atoms are thus completely disordered in position.

We recently carried out, in collaboration with Oak Ridge National Laboratory, the first ever studies of radiation tolerance of high-entropy alloys [3]. The results of a combination of experimental and modeling efforts reveal that atom-level disorder in NiFe and NiCoCr alloys, compared to elemental Ni, indeed lead to a substantial reduction of damage accumulation under prolonged irradiation. The random arrangement of multiple elemental species lead to unique site-to-site lattice distortions, that slow down the motion of extended defects, known as dislocation formed by the irradiation. This in turn leads to slower growth of large dislocation loops, which are the dominant form of radiation damage in metals at high doses. Understanding of alloying effects on modified energy landscapes in such chemically disordered single-phase alloys will allow prediction of radiation-tolerance alloys for next-generation nuclear reactors and other high-radiation environments.

The analysis also revealed that alloying effects on significant reduction of dislocation mobility are generic, and not specific to the current choice of materials or number of elements in the system. The large improvement from NiFe to NiCoCr demonstrates that a reduction will depend on material choice, and suggests that there may be alloys with even larger damage reduction than the currently observed one – especially in more chemically disordered alloys with increasing number of principal elements at significant concentrations.

Overall, the work on both Ni and the alloys shows that under prolonged irradiation, damage production in dense metals is completely dominated by the evolution of defect clusters.

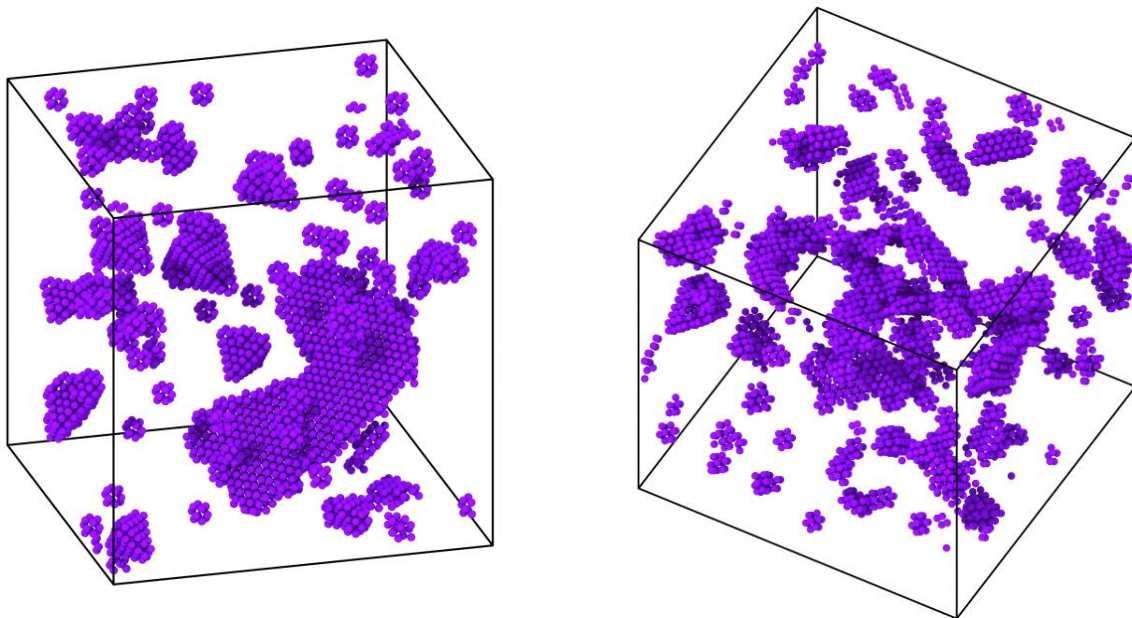


Fig. 4. Left: radiation damage in a conventional metal, Ni. Right: radiation damage for exactly the same dose in NiFe equiatomic alloys. Due to the random arrangement of atoms in NiFe, the defect structures are smaller in these alloys. Figure from Fredric Granberg (University of Helsinki).

References.

- [1] K. Nordlund, S. J. Zinkle, T. Suzudo, R. S. Averback, A. Meinander, F. Granberg, L. Malerba, R. Stoller, F. Banhart, B. Weber, F. Willaime, S. Dudarev, and D. Simeone, *Primary radiation damage in materials: Review of current understanding and proposed new standard displacement damage model to incorporate in-cascade mixing and defect production efficiency effects*, (OECD Nuclear Energy Agency, Paris, France, 2015), available online at <https://www.oecd-nea.org/science/docs/2015/nsc-doc2015-9.pdf>.
- [2] X. Yi, A.E. Sand, D.R. Mason, M.A. Kirk, S.G. Roberts, K. Nordlund, and S.L. Dudarev, *Direct observation of size scaling and elastic interaction between nano-scale defects in collision cascades*, EPL **110**, 36001 (2015).
- [3] F. Granberg, K. Nordlund, M.W. Ullah, Ke Jin, Chenyang Lu, Hongbin Bei, Lumin Wang, F. Djurabekova, W.J. Weber, and Y. Zhang, *Mechanism of radiation damage reduction in equiatomic multicomponent single phase alloys*, Phys. Rev. Lett. **116**, 135504 (2016) .

A methodology to assess dpa uncertainties from nuclear data covariances, L. Fiorito

Belgian Nuclear Research Centre SCK CEN
Mol, Belgium

Introduction

The motivation for this work was the characterization of damage metrics such as displacements per atom (dpa) for the MYRRHA reactor [1], which is a requested task for its design and licensing phase. MYRRHA is a multi-purpose irradiation facility conceived as an accelerator driven system (ADS) and currently in the design phase at SCK•CEN. Its core includes a MOX fuel cooled by liquid lead-bismuth (Pb-Bi) eutectic. MYRRHA is conceived to operate both in critical and subcritical conditions. In the second case, the linear accelerator provides high energy protons that are used in the spallation target to create neutrons and sustain the fission chain. The reactor configuration allows the production of neutron fluxes up to several hundreds of MeV.

Although the fast neutron source enhances the flexibility of the facility, the undergoing radiation damage has a major detrimental effect on the reactor components, such as material embrittlement. To quantify the damage metrics for the reactor's structural materials – e.g. beam window, fuel pin, cladding, core barrel – computer codes must be used with reliable evaluated nuclear data. Also uncertainty values should be provided for the damage metrics. Since MYRRHA's operational conditions cover neutron spectra much harder than those of traditional reactors (Fig. 1), several work packages of the FP7 project have been already dedicated to the development of adequate nuclear data and covariances for the MYRRHA reactor safety analyses [2].

The MYRRHA subcritical configuration also includes the possibility to irradiate material samples placed in the spallation target, where radiation damage levels comparable to fusion conditions can be reached.

In this work, dpa values for ^{56}Fe and ^{184}W subject to MYRRHA irradiation conditions were calculated using evaluated data from ENDF/B-VII.1 [2], JEFF-3.2 [3] and TENDL-2015 [4]. Then, a methodology was implemented to generate covariance matrices for energy-dependent damage metrics using NJOY [6] and the nuclear data sampling code SANDY [7]. These covariances were propagated and uncertainties for the dpa values were obtained.

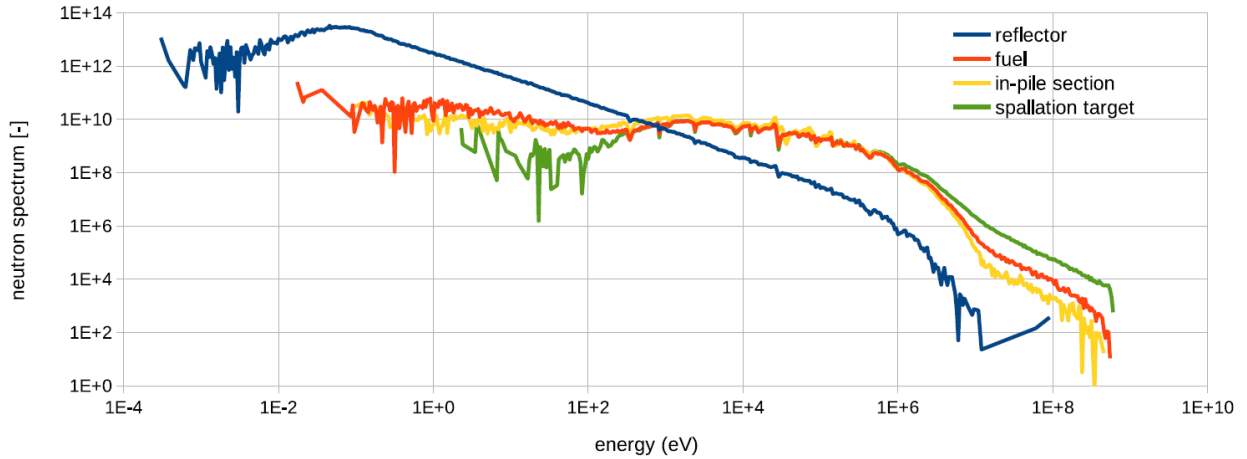


Fig. 1. Average nuclear spectra (in relative units) in four locations of the MYRRHA subcritical core.

Methodology

The SANDY code was used to propagate the cross sections and angular distributions covariances, respectively sections MF=33 and MF=34 of the ENDF-6 format [8]. SANDY, SAMpler of Nuclear Data and uncertainty, is a sampling tool applicable to SA and UQ problems. The code exploits the basic theory of stochastic Monte Carlo sampling to propagate nuclear data covariances and uncertainties through the nuclear model under study.

Random sets of nuclear parameters were sampled with SANDY according to a Normal multivariate PDF and the best estimates and variance-covariance matrices in the nuclear data files. Cross correlations between reactions were included, and summation cross sections were rebuilt according to the conservation equations. Eventually, the random nuclear data samples were written in perturbed copies of the original data files. Each perturbed file was processed with the NJOY code to produce perturbed energy-dependent displacement cross sections $\sigma_d(E)$ (MT=444 in ENDF-6 format). The covariance matrix between the perturbed $\sigma_d(E)$ functions were evaluated and processed in a multigroup energy structure (Fig. 22).

The derived covariance matrices were used to calculate uncertainty values for dpa according to the "NRT" formalism by Norgett, Robinson, and Torrens [9]

$$dpa = 0.8 \frac{E_a}{2E_d} ,$$

where 0.8 is the efficiency factor, E_d is the energy required to displace an atom from its lattice position (taken from the NJOY manual [6]) and E_a is the total available energy

$$E_a = \int_0^{\infty} \sigma_d(E)\varphi(E)dE$$

The method generates energy-dependent covariance matrices for damage metrics that reflect the level of uncertainty information currently available in the evaluated nuclear data files. However, several major sources of uncertainties are left out, such as uncertainties on PKA spectra, since they are not provided in the formatted files. Although the results obtained with our methodology are likely to underestimate the effective level of uncertainty of the damage metrics, they can be used to check the consistency of the uncertainty information currently available in the data files.

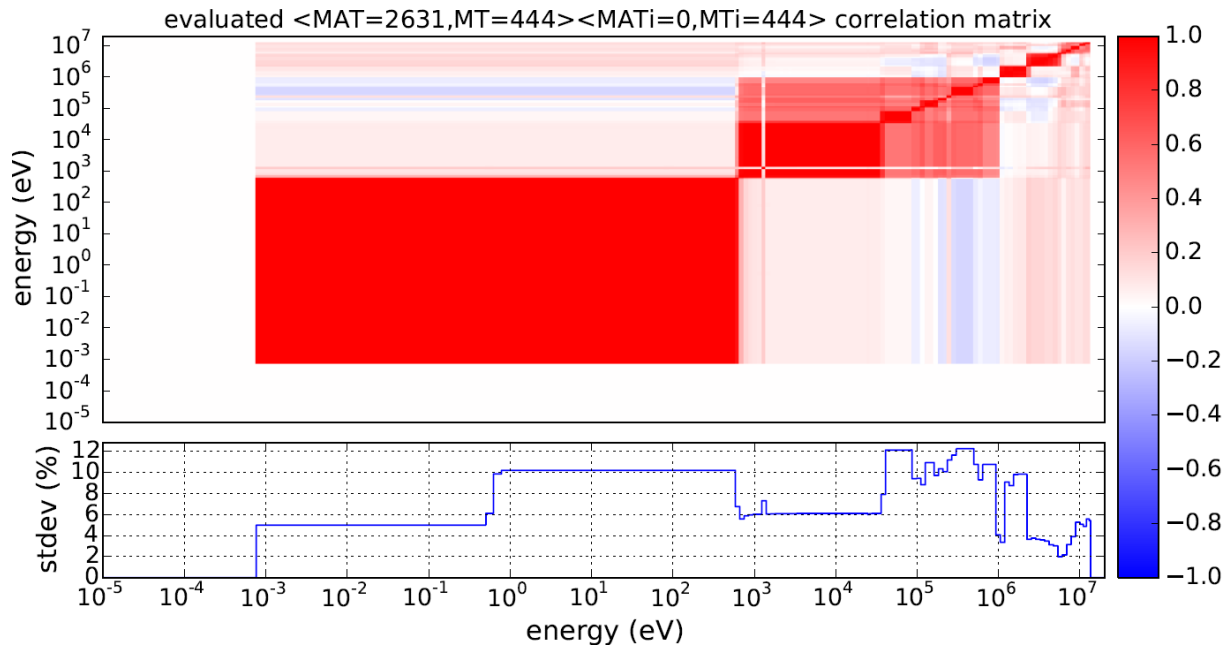


Fig. 2. Multigroup covariance matrix for the displacement cross section of ^{56}Fe averaged on the MYRRHA neutron spectrum in the reactor.

Results

Covariance matrices for the displacement cross sections were produced for ^{56}Fe and ^{184}W using the explained methodology. Then, the dpa per year values and uncertainties for ^{56}Fe were calculated in four regions of the MYRRHA core, i.e. spallation target, fuel, in-pile sections and reflector, and are reported in Table 1. The computational results for ^{184}W are reported in Table 2 for the irradiation conditions of the MYRRHA spallation target. These damage metrics are average values over the active part of the component. To obtain peak values it is sufficient to multiply the results by a factor of 1.37, which reflects the flux shape inside the assembly in radial and axial direction.

Table 1. Dpa and uncertainty values for ^{56}Fe subject to MYRRHA's irradiation conditions.

location	flux ($\text{n}/\text{cm}^2/\text{s}$)	dpa/y	uncert. (%)	dpa/y	uncert. (%)	dpa/y	uncert. (%)
reflector	1.37×10^{14}	0.16	5.77	0.17	2.53	0.17	0.04
in-pile section	2.28×10^{15}	18.96	4.85	19.70	2.61	20.01	3.21
Fuel	2.44×10^{15}	24.19	4.19	25.34	2.50	25.56	5.86
spallation target	2.98×10^{15}	38.54	3.13	42.29	2.19	41.70	7.15
fraction above 500 keV (%)		79.85	40.09	80.54	96.67	80.24	97.06
fraction above 20 MeV (%)		1.85	0.00	8.21	0.00	7.90	0.26

Table 2. Dpa and uncertainty values for ^{184}W subject to MYRRHA's irradiation conditions.

location	flux ($\text{n}/\text{cm}^2/\text{s}$)	dpa/y	uncert. (%)	dpa/y	uncert. (%)	dpa/y	uncert. (%)
spallation target	2.98×10^{15}	173.03	1.38	11.31	0.74	11.59	20.25
fraction above 500 keV (%)		98.64	19.23	80.63	15.82	81.63	16.21
fraction above 20 MeV (%)		93.54	0.02	16.94	0.10	15.96	0.00

Disagreement exists between dpa for ^{56}Fe calculated with different libraries (max 10%), which cannot be explained only by the calculated uncertainty level. The discrepancy is highlighted when the displacement cross sections are compared as in Fig. 3. The displacement cross sections in the fast energy region ($> 500\text{ keV}$) contribute to approximately 80% of the dpa in the spallation target. In the same energy region, the uncertainties on the displacement cross sections are very different between libraries, with ENDF/B and JEFF underestimating the evaluated uncertainty above 1 MeV. Because of the hard neutron fluxes achieved in MYRRHA, the contribution to dpa of the displacement cross sections above 20 MeV is still $\approx 10\%$. However, none of the libraries under study provide cross section uncertainties on ^{56}Fe at these neutron energies.

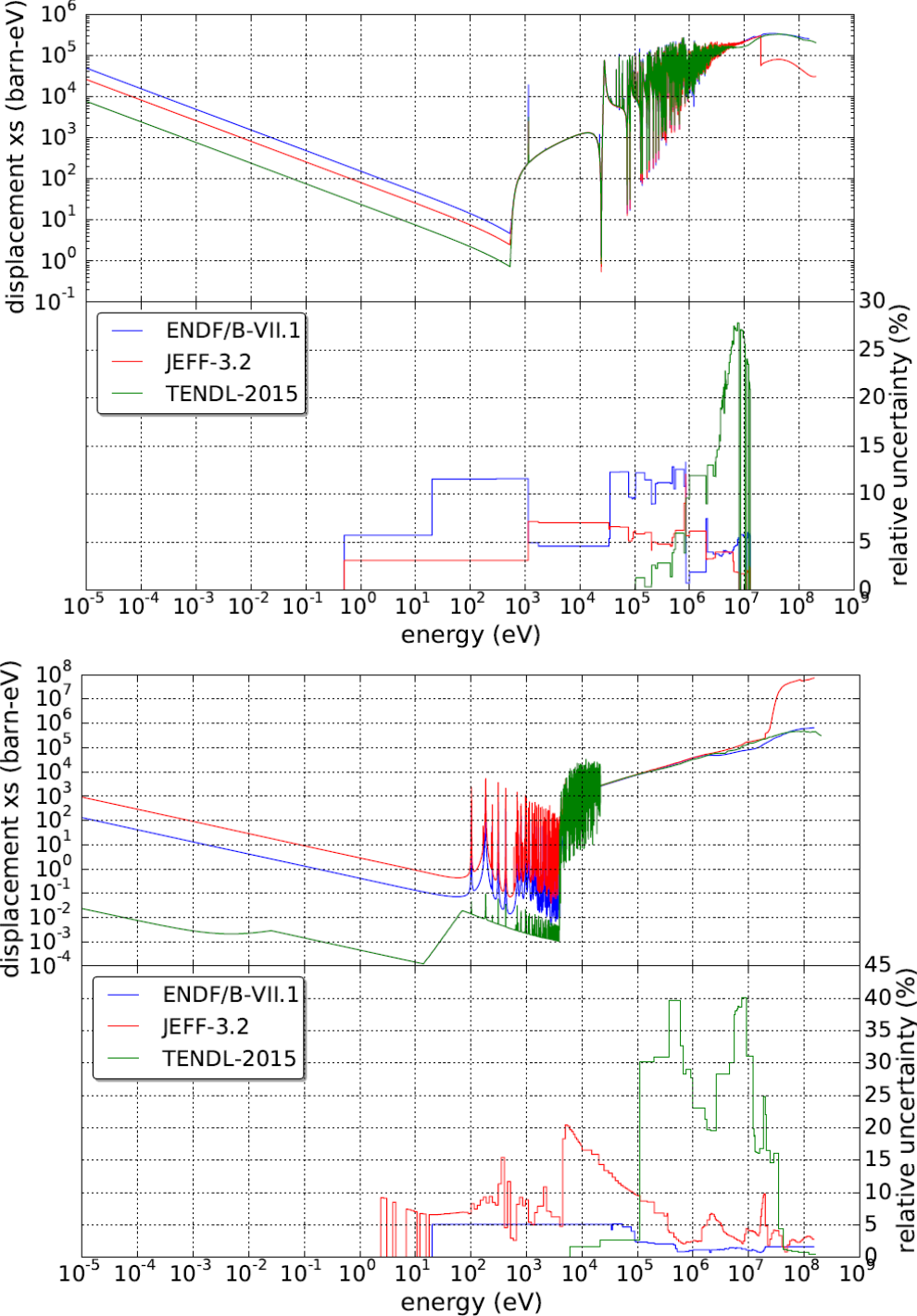


Fig. 3. Displacement cross sections and relative uncertainties of ^{56}Fe (top) and ^{184}W (bottom).

The dpa values for ^{184}W in the MYRRHA spallation target calculated with JEFF-3.2 is too large compared to the results of ENDF/B-VII.1 and JENDL-4.0. The discrepancy generates from the displacement cross section above 30 MeV (Fig. 3) and derives from a wrong estimation of the ^{182}Ta production yield. Other notable discrepancies for ^{184}W were observed between the TENDL-2015, ENDF/B-VII.1 and JEFF-3.2 evaluations in the energy range 0-5 keV (differences $\approx 100\%$) and 2 to 20 MeV (differences $\approx 30\%$). As for the case of ^{56}Fe , the displacement cross sections uncertainties of ^{184}W are underestimated by ENDF/B and JEFF at fast energies. Above 20 MeV the displacement cross sections uncertainties for the three libraries appear to be too low ($< 5\%$), although the contribution to the dpa values is still larger than 15%.

Conclusions

Dpa and associated uncertainties were calculated for ^{56}Fe and ^{184}W simulating MYRRHA's irradiating conditions. Discrepancies were identified between the results of the three libraries, JEFF-3.2, ENDF/B-VII.1 and TENDL-2015. A sampling-based methodology is proposed to propagate the cross section and angular distribution uncertainties, respectively sections MF=33 and MF=34 of the ENDF-6 format, to displacement cross sections. The uncertainty comparison shows a major disagreement between the three libraries and a lack or underestimation of the uncertainty above 20 MeV, where the MYRRHA spectrum is still significant.

Bibliography

- [1] H. Abderrahim, P. Baeten, D. De Bruyn et R. Fernandez, «MYRRHA - a multi-purpose fast spectrum research reactor,» *Energy conversion and management*, pp. 4-10, 2012.
- [2] CSEWG, «ENDF-6 formats manual. Data formats and procedures for the evaluated nuclear data files ENDF/B-VI and ENDF/B-VII,» Upton, 2013.
- [3] M. Chadwick et al., «ENDF/B-VII.1 nuclear data for science and technology: cross sections, covariances, fission product yields and decay data,» *Nuclear Data Sheets*, pp. 2887-2996, 2011.
- [4] L. Fiorito, G. Zerovnik, A. Stankovskiy, G. Van den Eynde et P. Labeau, «Nuclear data uncertainty propagation to integral responses using SANDY,» *Submitted to Annals of Nuclear Energy*, 2016.
- [5] A. Koning et D. Rochman, «Modern nuclear data evaluation with the TALYS code system,» *Nuclear Data Sheets*, pp. 2841-2934, 2012.
- [6] R. MacFarlane, D. Muir, R. Boicourt et A. Kahler, «The NJOY nuclear data processing system, version 2012,» LANL, 2012.
- [7] M. Norgett, M. Robinson et I. Torrens, «A proposed method of calculating displacement dose rates,» *Nuclear Engineering and Design*, pp. 50-54, 1975.
- [8] A. Santamarina et al., «The JEFF-3.1.1 nuclear data library,» OECD/NEA Data Bank, 2009.
- [9] P. Romojaro, C. Diez, N. Garcia-Herranz, F. Alvarez-Velarde, I. Kodeli, G. Zerovnik, A. Stankovskiy et G. Van den Eynde, «Report on sensitivity analysis of MYRRHA with list of key reactions,» 2015.

Links with NEA activities: Nuclear Data services and WPs, O. Cabellos

OECD/NEA/Data Bank
Paris, France

During the last three years a significant number of international activities have been undertaken on Primary Radiation Damage (PRD): the Expert Group on Primary Radiation Damage belonging to the Working Party on Multi-scale Modelling of Fuels and Structural Materials for Nuclear Systems (WPMM- OECD/NEA/NSC) [1], Coordinated Research Project (CRP) on “Primary Radiation Damage Cross Sections” (IAEA/NDS) [2] and the activities of the European Consortium on Nuclear Data Development and Analysis for Fusion within the Fusion for Energy (F4E) Program [3].

NEA activities related to fuels and structural materials are coordinated by the Working Party on Multi-scale Modelling of Fuels and Structural Materials for Nuclear Systems, WPMM. In May 2015, the Expert Group on “Primary Radiation Damage” reviewed the limitation of the NRT-dpa standard, and recommended a new improved standard of primary damage characteristics, the arc-dpa [4]. Recently, the new Expert Group on Structural Materials Modelling (SMM) has been created to enhance efforts on the multiscale modelling approach applied to structural materials, in order to investigate phenomena that can not be studied experimentally, predicting how the nanostructure and the microchemistry changes under irradiation.

Regarding “*Nuclear Reaction Data for Radiation Damage*”, NEA activities can be summarized as follows:

- The development of JANIS (JAVa-base Nuclear Data Information Software) designed to facilitate the visualization of nuclear data: *JANIS contains damage energy and gas production cross-sections for the main evaluated data files* [5].
- The compilation of experimental nuclear data for EXFOR database. *Unfortunately, an important amount of KERMA measurements data is still missed.*
- The Joint Evaluated Fission and Fusion (JEFF) Nuclear Data Library Project working in the evaluated nuclear data JEFF. *Recent activities are carried out in different Working Groups to improve the processing and evaluation of radiation damage cross-sections* [6,7,8,9].
- NEA data Bank has launched a new project (NDEC [5] – Nuclear Data Evaluation Cycle) which aims at streamlining a “QA” process for the selection of well validated, well documented Nuclear Data Files and Libraries. NDEC centralizes a series of tools (scripts & codes) for nuclear data processing, verification and benchmarking.
- NEA/DB also supports a repository and mailing list for NJOY users.

Finally, these issues are also assessed in the Working Party on International Nuclear Data Evaluation Co-operation (NEA/NSC/WPEC) established to promote cooperation between the evaluation projects. WPEC has carried out co-operative activities between the participating projects such as SG38 [10] (“A modern nuclear data structure beyond the ENDF format”) needed to define the basic requirements of the new data structure and SG40/CIELO [11] (“Pilot project of a Collaborative International Evaluated Library Organization”) proposed to foster evaluated nuclear data advances, ⁵⁶Fe is one of the six important isotopes initially selected in the CIELO project.

References

1. <https://www.oecd-nea.org/science/wpmm/>, Working Party on Multi-scale Modelling of Fuels and Structural Materials for Nuclear Systems (WPMM)
2. <https://www.nds.iaea.org/CRPdpa/>, Coordinated Research Project (CRP) on “Primary Radiation Damage Cross Sections”.
3. The Activities of the European Consortium on Nuclear Data Development and Analysis for Fusion, U. Fischer et al., Nuclear Data Sheets, Volume 120, June 2014, Pages 226-229
4. “Primary Radiation Damage in Materials”, NEA/NSC/DOC(2015)9

5. "Handling Nuclear Data at NEA: Overview of NEA Nuclear Data tools and NDEC". O.Cabellos, JEF/DOC-1719, Nov 2015
6. "Uncertainties of atomic displacement cross-sections for iron irradiated with neutrons up to 150 MeV energy". A.Yu. Konobeyev, U. Fischer, P.E. Pereslavytsev. EFF/DOC-1291, April 2016.
7. "Generation of a complete dpa cross section library up to 150 MeV based on JEFF-3.1.2 and suitable approximations". O. Cabellos, F4E-GRT-168.01, Task-4.1. November 2013
8. "Generation of a complete dpa cross section library up to 150 MeV based on JEFF-3.2". P. Sauvan, J. Sanz, F. Ogando. EFF/DOC-1292, April 2016.
9. "JEFF-3.3T1 UKAEA's processing steps and processed forms". J-Ch. Sublet, M. Fleming and M. Gilbert. JEF/DOC-1749, April 2016
10. <https://www.oecd-nea.org/science/wpec/sg38/>
11. <https://www.oecd-nea.org/science/wpec/sg40-cielo/>

Preliminary study on DPA cross-section of ^{184}W in JEFF-3.2, C. Konno

Japan Atomic Energy Agency
Tokai-mura, Naka-gun, Ibaraki-ken, Japan

1. Introduction

Dr. Fiorito reported in this meeting that the DPA cross-section data of JEFF-3.2 ^{184}W was too large above 30 MeV as shown in Fig. 1. I investigate this issue.

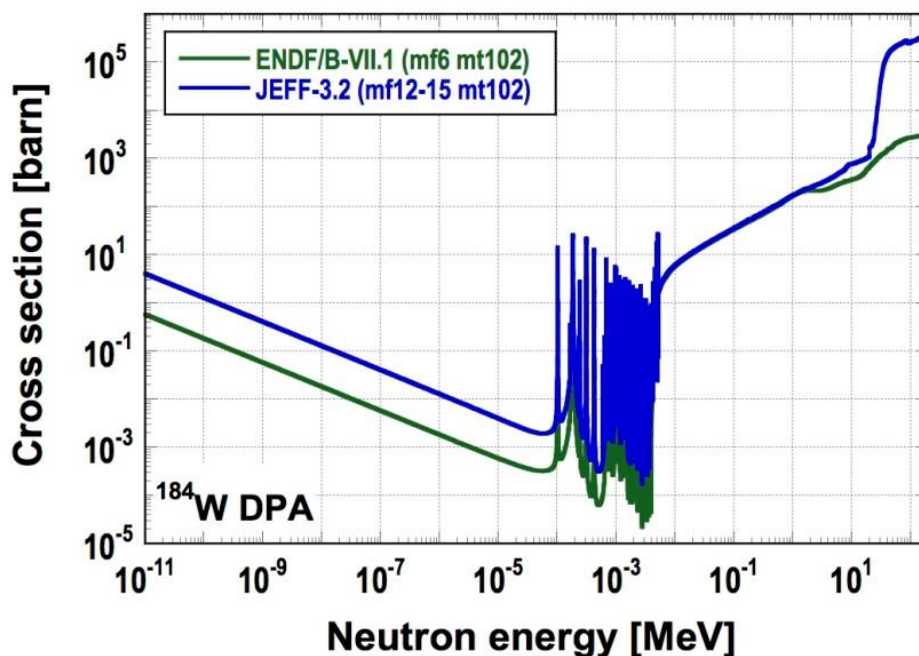


Fig. 1. DPA cross-section of ^{184}W .

2. Method

I processed JEFF-3.2 ^{184}W with NJOY2012.50 and checked the NJOY output file.

3. Results and discussion

I found out that the damage energy production of ^{182}Ta was too large in the NJOY heatr output. Then I examined the JEFF-3.2 ^{184}W original data and picked out that the production yield of ^{182}Ta in mf6 mt5 (Fig. 2) was too large compared other ones (around 0.01) and those (Fig. 3) in the TENDL-2015 ^{184}W data. Note that the ENDF/B-VII.1 ^{184}W data have no the production yield of ^{182}Ta in mf6 mt5. Then I replaced the production yield of ^{182}Ta in mf6 mt5 in JEFF-3.2 ^{184}W with that in TENDL-2015 ^{184}W . This modified file was processed with NJOY2012.50. As a result, the DPA cross-section data above 30 MeV of JEFF-3.2 decreases drastically as shown in Fig. 4. It is necessary to re-check all the production yields in mf6 mt5 of ^{184}W in JEFF-3.2. Additionally note that the difference between the DPA data of JEFF-3.2 and ENDF/B-VII.1 below ~ 100 eV are due to the format difference in the secondary gamma data which is described in this meeting by me.

The same issue also occurs in ^{182}W , ^{183}W and ^{186}W (^{182}W : ^{180}Ta production yield, ^{183}W : ^{181}Ta production yield, ^{186}W : ^{184}Ta production yield) as shown in Figs. 5 - 7. The reason for too small DPA of ^{186}W below 5 keV in Fig. 7 is under study.

7.318200+4	1.803871+2	0	1	1	277437	6	514826
	27	2			7437	6	514827
1.000000-5	2.600888-4	2.000000+7	2.600888-4	2.000001+7	2.600888-4	7437	6
2.200000+7	1.934007-2	2.400000+7	3.109512-1	2.600000+7	1.848131+0	7437	6
2.800000+7	5.566499+0	3.000000+7	1.190984+1	3.500000+7	3.424891+1	7437	6
4.000000+7	4.984054+1	4.500000+7	5.800758+1	5.000000+7	6.158442+1	7437	6
5.500000+7	6.396176+1	6.000000+7	6.506155+1	6.500000+7	6.583254+1	7437	6
7.000000+7	6.692767+1	7.500000+7	6.675690+1	8.000000+7	6.867207+1	7437	6
8.500000+7	7.027934+1	9.000000+7	7.002707+1	9.500000+7	6.980555+1	7437	6
1.000000+8	7.041330+1	1.100000+8	7.339577+1	1.200000+8	7.234447+1	7437	6
1.300000+8	7.564253+1	1.400000+8	7.592526+1	1.500000+8	7.735744+1	7437	6
1.000000+8	7.041330+1	1.100000+8	7.339577+1	1.200000+8	7.234447+1	7437	6
1.300000+8	7.564253+1	1.400000+8	7.592526+1	1.500000+8	7.735744+1	7437	6

Fig. 2. Production yield of ^{182}Ta in JEFF-3.2 ^{184}W .

7.318200+4	1.803871+2	0	1	1	277437	6	514826
	27	2			7437	6	514827
1.000000-5	4.280413-3	2.000000+7	4.280413-3	2.000001+7	4.280413-3	7437	6
2.200000+7	4.280413-3	2.400000+7	4.280413-3	2.600000+7	4.280413-3	7437	6
2.800000+7	4.280413-3	3.000000+7	4.280413-3	3.500000+7	7.436907-3	7437	6
4.000000+7	9.277380-3	4.500000+7	1.027915-2	5.000000+7	1.107062-2	7437	6
5.500000+7	1.107062-2	6.000000+7	1.127186-2	6.500000+7	1.164643-2	7437	6
7.000000+7	1.141378-2	7.500000+7	1.182715-2	8.000000+7	1.164182-2	7437	6
8.500000+7	1.182629-2	9.000000+7	1.201076-2	9.500000+7	1.192962-2	7437	6
1.000000+8	1.184848-2	1.100000+8	1.148347-2	1.200000+8	1.157130-2	7437	6

Fig. 3. Production yield of ^{182}Ta in TENDL-2015 ^{184}W .

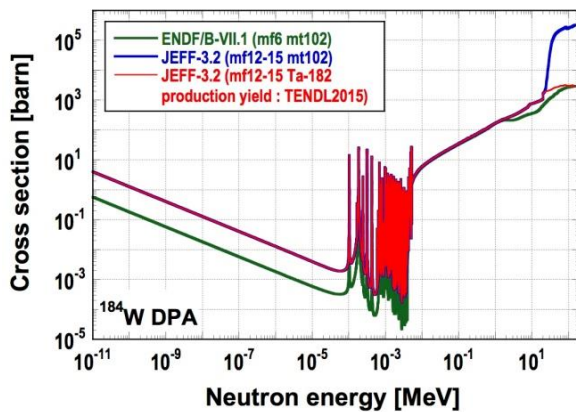


Fig. 4. DPA cross-section of ^{184}W (modified).

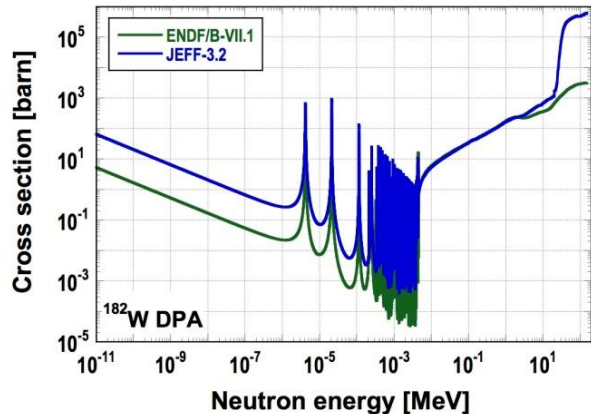


Fig. 5. DPA cross-section of ^{182}W .

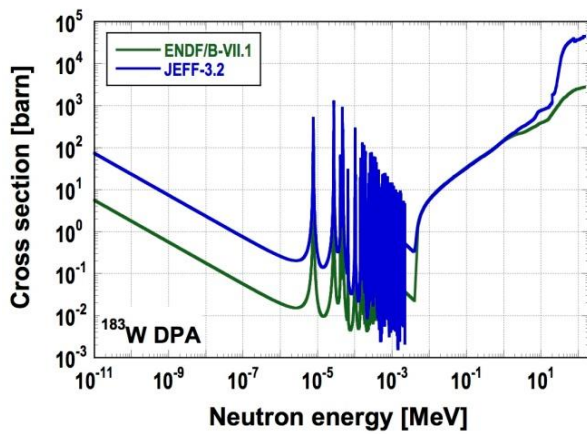


Fig. 6. DPA cross-section of ^{183}W .

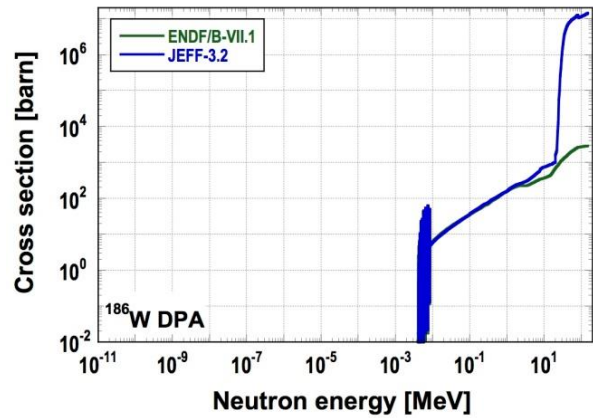


Fig. 7. DPA cross-section of ^{186}W .

4. Summary

I investigated reasons why the DPA cross-section data of JEFF-3.2 ^{184}W was too large above 30 MeV. As a result, I found out that the production yield of ^{182}Ta in mf6 mt5 in JEFF-3.2 ^{184}W was too large and demonstrated that the problem was solved if the production yield of ^{182}Ta was modified. I picked out that the same issue also occurred in ^{182}W , ^{183}W and ^{186}W . The production yield data of all the tungsten isotopes in JEFF-3.2 should be reconfirmed and revised if they have mistakes.

Appendix I: Agenda



Technical Meeting (TM)

“Nuclear Reaction Data and Uncertainties for Radiation Damage”

13 - 16 June 2016
IAEA Headquarters, Vienna, Austria
Meeting Room MOE05

Approved AGENDA

(presentations' time is approximate, it also includes questions and breaks)

Monday, 13 June

Opening (9:30 - 10:00)

Welcome address – A. Koning (NDS, Section Head)
Administrative announcements – A. Öchs (NDS)
Self-introductions and Election of Chairperson and Rapporteur - All
Approval of Agenda - All

Session 1: Individual Presentations

morning 10:00 - 12:00

D. Rochman, “TENDL-TMC for the dpa and pka Uncertainties”
S. Simakov, “Uncertainties and correlations for the ⁵⁶Fe damage cross sections and spectra averaged quantities based on TENDL-TMC”
A. Konobeev, “Estimation of uncertainties of displacement cross-sections for iron and tungsten at neutron irradiation energies above 0.1 MeV”

12:00 - 13:30 Lunch break + Administrative issues

evening 13:30 - 18:00

D. Bernard, “Estimation of Bias and Uncertainties for Radiation Damage calculation (Fission Reactors)”
P. Helgesson, “Justified and complete gas-production cross sections with uncertainties for Ni-59 and consequences for stainless steel in LWR spectra”
P. Griffin, “A Rigorous Treatment of Uncertainty Quantification for Silicon Damage Metrics”
Y. Iwamoto, “Comparative study of Monte Carlo particle transport code PHITS and nuclear data processing code NJOY for energy spectra of PKA and kerma under neutron irradiation”

Coffee breaks as needed

Tuesday, 14 June

<i>morning 9:00 - 13:00</i>	
M.R. Gilbert and J.-Ch. Sublet,	"Scoping of material damage with FISPACT-II and different nuclear data libraries: transmutation, activation, and PKAs"
C. Konno,	"Differences among KERMA or DPA data calculated from JENDL-4.0, ENDF/B-VII.1, JEFF-3.2 and FENDL-3.1b with NJOY"
V. Sinitisa,	"ROSFOND Based Heating-Damage Cross Sections Sub-Library: Preliminary Uncertainty Assessment"
C.S. Gil	"Some experiences of dpa assessments using MCNP and SPECTER codes"
<i>13:00 - 14:00 Lunch break</i>	
<i>evening 14:00 - 18:00</i>	
K. Nordlund,	"Damage clustering in metals: importance, advances, and challenges"
B. Braams	"Remarks for TM on <i>Nuclear Reaction Data and Uncertainties for Radiation Damage</i> "
L. Fiorito,	"A methodology to assess dpa uncertainties from nuclear data covariances"
<i>Coffee breaks as needed</i>	
Hospitality Event: 18:30 in Restaurant "Rembetiko" (http://www.rembetiko.at/) on rebuild Copa Cagrana	

Wednesday, 15 June

<i>morning 9:00 - 13:00</i>	
O. Cabellos,	"Links with NEA activities: Nuclear Data Services and WPs"
C. Konno,	"Preliminary study on DPA cross section of 184W in JEFF-3.2"
J.-C. Sublet,	"NJOY's processing steps and processed forms"
<i>13:00 - 14:00 Lunch break</i>	
Session 2: Joint Discussion, writing-up Summary and Recommendation for TM Report	
<i>evening 14:00 - 18:00</i>	
<i>Coffee breaks as needed</i>	

Thursday, 16 July

Session 3: Finalization of the Meeting Report Draft	
<i>morning 9:00 - 13:00</i>	
<i>13:00 - 14:00 Lunch break</i>	
<i>ending</i>	
<i>Coffee breaks as needed</i>	

Appendix II: List of Participants



Technical Meeting “Nuclear Reaction Data and Uncertainties for Radiation Damage”

13 – 16 June 2016

VIC Room M0E 05, Vienna, Austria

LIST OF PARTICIPANTS

<p>BELGIUM Mr Luca Fiorito Belgian Nuclear Research Centre Boeretang 200 Mol 2400 Tel.: E-mail: luca.fiorito@sckcen.be</p>	<p>FINLAND Mr Kai Nordlund Department of Physics University of Helsinki P.O. Box 43 Pietari Kalmink. 2 00014 Helsinki Tel.: +358 9 19150007 E-mail: kai.nordlund@helsinki.fi</p>
<p>FRANCE Mr David Bernard Centre d'Etudes Nucleaires de Cadarache Batiment 230 Bat 508 - B.P. No. 1 13108 Saint-Paul-lez-Durance Tel.: +33 442254913 E-mail: david.bernard@cea.fr</p>	<p>GERMANY Mr Alexandre Konobeev Institute for Neutron Physics and Reactor Technology Karlsruhe Institute of Technology Herman von Helmholtz Platz 1 76344 Eggenstein-Leopoldshafen Tel.: +49 721 608 23768 E-mail: alexander.konobeev@kit.edu</p>
<p>GERMANY Mr Stanislav Simakov Institute for Neutron Physics and Reactor Technology Karlsruhe Institute of Technology Herman von Helmholtz Platz 1 76344 Eggenstein-Leopoldshafen Tel.: +49 721 608 22537 E-mail: stanislav.simakov@kit.edu</p>	<p>JAPAN Mr Yosuke Iwamoto Japan Atomic Energy Agency 2-4 Shirakata, Tokai, Naka, Ibaraki 319-1195 Tel.: +81 29 282 5195 E-mail: iwamoto.yosuke@jaea.go.jp</p>

<p>KOREA Rep. Mr Choong-Sup Gil Nuclear Data Evaluation Laboratory Korea Atomic Energy Research Institute P.O. Box 105 Daedeok-Daero 989-111 Yuseong Tel.: + 82 42-868-8104 E-mail: csgil@kaeri.re.kr</p>	<p>OECD Mr Oscar Cabellos Nuclear Energy Agency (NEA) 46, quai Alphonse Le Gallo 92100 Boulogne Billancourt Paris Tel.: +33 1 45241084 E-mail: oscar.cabellos@oecd.org</p>
<p>SWEDEN Mr Petter Helgesson Division of Applied Nuclear Physics Department of Physics and Astronomy Uppsala University P.O. Box 516 75120 Uppsala Tel.: +46 18 4713329 E-mail: petter.helgesson@physics.uu.se</p>	<p>SWEDEN Mr Henrik Sjöstrand Department of Physics and Astronomy Division of Applied Nuclear Physics Uppsala University Box 516 751 20 Uppsala Tel.: +46 18 4713329 E-mail: Henrik.Sjostrand@physics.uu.se</p>
<p>SWITZERLAND Mr Dimitri Rochman Paul Scherrer Institut (PSI) Reactor Physics and Systems Behaviour Laboratory Villigen 5232 Tel.: +41 56 310 44 62 E-mail: dimitri-alexandre.rochman@psi.ch</p>	<p>UNITED KINGDOM Mr Mark Gilbert UK Atomic Energy Authority Culham Centre for Fusion Energy Abingdon Oxfordshire OX14 3DB Tel.: +44 1235 466569 E-mail: mark.gilbert@ccfe.ac.uk</p>
<p>UNITED KINGDOM Mr Jean-Christophe Sublet UK Atomic Energy Authority Culham Centre for Fusion Energy Abingdon Oxfordshire OX14 3DB Tel.: +44 1235 466400 E-mail: jean-christophe.sublet@ccfe.ac.uk</p>	<p>UNITED STATES OF AMERICA Mr Patrick Griffin Sandia National Laboratories P.O. Box 5820 Albuquerque NM 87185 Tel.: +1 505 845 9121 E-mail: pjgriff@sandia.gov</p>
<p>CONSULTANT Mr Chikara Konno Japan Atomic Energy Agency Nuclear Data and Reactor Engineering Division Research Group for Reactor Physics and Standard Nuclear Code System Shirakata-Shirane 2-4 Tokai-mura, Naka-gun, Ibaraki ken 319-195 Tel.: +81 29 282 6704 E-mail: konno.chikara@jaea.go.jp</p>	<p>CONSULTANT Mr Valentin Sinita Institute of Atomic Power Stations WWER Department National Research Centre - Kurchatov Institute Kurchatova Sq. 1 123182 Moscow Tel.: +7 499 190 5171 E-mail: sinita_vv@nrcki.ru</p>

<p>IAEA Mr Arjan Koning Scientific Secretary Nuclear Data Section Division of Physical and Chemical Sciences Tel.: +43 1 2600 21709 E-mail: a.koning@iaea.org</p>	<p>IAEA Mr Bastian Braams Atomic and Molecular Data Unit Nuclear Data Section Division of Physical and Chemical Sciences Tel.: +43 1 2600 21731 E-mail: b.j.braams@iaea.org</p>
<p>IAEA Mr Vivian (Paraskevi) Dimiriou Scientific Secretary Nuclear Data Development Unit Nuclear Data Section Division of Physical and Chemical Sciences Tel.: +43 1 2600 21708 E-mail: p.dimitriou@iaea.org</p>	<p>IAEA Mr Naohiko Otsuka Nuclear Data Services Unit Nuclear Data Section Division of Physical and Chemical Sciences Tel.: +43 1 2600 21715 E-mail: n.otsuka@iaea.org</p>
<p>IAEA Ms Valentina Semkova Nuclear Data Services Unit Nuclear Data Section Division of Physical and Chemical Sciences Tel.: +43 1 2600 21727 E-mail: v.semkova@iaea.org</p>	<p>IAEA Mr Andrej Trkov Nuclear Data Development Unit Nuclear Data Section Division of Physical and Chemical Sciences Tel.: +43 1 2600 21712 E-mail: a.trkov@iaea.org</p>
<p>IAEA Ms Ian Swenson Physics Section Division of Physical and Chemical Sciences Tel.: +43 1 2600 24215 E-mail: i.swainson@iaea.org</p>	

Nuclear Data Section
International Atomic Energy Agency
Vienna International Centre, P.O. Box 100
A-1400 Vienna, Austria

E-mail: nds.contact-point@iaea.org
Fax: (43-1) 26007
Telephone: (43-1) 2600 21725
Web: <http://www-nds.iaea.org>
